



**Deformation and Stress Analyses of the Ground During the Construction of
Multipurpose Road Tunnel Under Karnaphuli River**

A Thesis

By

Sultan Al Shafian

MASTER OF SCIENCE IN CIVIL ENGINEERING

DEPARTMENT OF CIVIL AND ENVIRONMENTAL ENGINEERING

ISLAMIC UNIVERSITY OF TECHNOLOGY

GAZIPUR, BANGLADESH

April, 2022

**Deformation and Stress Analyses of the Ground During the Construction of
Multipurpose Road Tunnel Under Karnaphuli River**

A Thesis

By

Sultan Al Shafian

Submitted to the Department of Civil and Environmental Engineering ,Islamic University
of Technology (IUT), Gazipur , in Partial fulfillment of the requirements of the Degree

of

MASTER OF SCIENCE IN CIVIL ENGINEERING

DEPARTMENT OF CIVIL AND ENVIRONMENTAL ENGINEERING

ISLAMIC UNIVERSITY OF TECHNOLOGY

GAZIPUR, BANGLADESH

April, 2022

Declaration of Candidate

It is hereby declared that this thesis has not been submitted elsewhere for the award of any Degree or Diploma.



Name of Supervisor:

Dr. Hossain Md. Shahin

Professor & Head

Department of Civil and Environmental Engineering

Islamic University of Technology

Board Bazar, Gazipur 1704.

Date: 25/04/2022



Name of Candidate:

Sultan Al Shafian

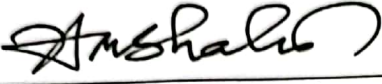

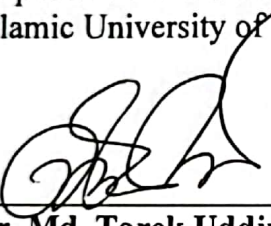


Student No.: 155610

Academic Year: 2015-2016

Date: 25/04/2022

Recommendation of the Board of Examiners

The thesis titled "Deformation and Stress Analyses of the Ground During the Construction of Multipurpose Road Tunnel Under Karnaphuli River " submitted by Sultan Al Shafian, Student ID 155610 of Academic Year 2015-2016 has been found as satisfactory and accepted as partial fulfillment of the requirement for the degree of Master of Science in Civil Engineering.

1. 
Dr. Hossain Md. Shahin(Supervisor)
Professor & Head
Department of Civil and Environmental Engineering (CEE)
Islamic University of Technology (IUT)
Chairman
and Ex-officio
2. 
Dr. Md. Rezaul Karim
Professor
Department of Civil and Environmental Engineering (CEE)
Islamic University of Technology (IUT)
Member
3. 
Dr. Md. Tarek Uddin, PEng.
Professor
Department of Civil and Environmental Engineering (CEE)
Islamic University of Technology (IUT)
Member
4. 
Dr. Shakil Mohammad Rifaat
Assistant Professor
Department of Civil and Environmental Engineering (CEE)
Islamic University of Technology (IUT)
Member
5. 
Dr. Mohammad Shariful Islam
Professor
Department of Civil Engineering
Bangladesh University of Engineering and Technology (BUET)
Member
(External)

Dedication

I dedicate this thesis to my family and all my teachers who brought me up to this moment

TABLE OF CONTENTS

RECOMMENDATION OF THE BOARD OF EXAMINERS.....	III
DECLARATION OF CANDIDATE.....	IV
DEDICATION.....	V
LIST OF TABLES.....	IX
LIST OF FIGURES	XII
ACKNOWLEDGEMENTS.....	XV
ABSTRACT.....	XVII
CHAPTER 1: INTRODUCTION.....	1
1.1 General.....	1
1.2 Background of the thesis.....	4
1.3 Objectives of the Study	7
1.4 Methodology	9
1.5 Layout of the Thesis.....	10
CHAPTER 2: LITERATURE REVIEW	11
2.1 Introduction.....	11
2.3 Tunnel Construction Techniques	11
2.3.1 Mechanized Shield Tunneling:.....	12
2.3.2 Closed Face Tunneling:.....	13
2.4 Tunnel Boring Machine	14
2.5 ITA Critical Cases.....	16
2.6 Numerical Method for Tunneling Analysis	17
2.6.1 Finite Element Method (FEM):.....	18
2.6.2 Constitutive Model:.....	22
2.7 Analysis of the Tunnel Section	26
2.7.1 Ground Behavior Analysis	26
2.7.2 Tunnel Lining Analysis.....	29
2.7.3 Research Gaps	35

CHAPTER 3: METHODOLOGY	37
3.1 General	37
3.2 Geometry of the Tunnel	37
3.3 Sub Soil Investigation and Laboratory Tests	38
3.4 Elementary Analysis for the Tunnel	40
3.4.1 Empirical Analysis for Predicting Settlement	40
3.4.2 Elastic Equation analysis for Tunnel lining	41
3.5 Finite Element Analysis of the Tunnel	44
3.5.1 Geotechnical and Other Material Parameters for analysis	44
3.5.2 General Layout of the Finite Element Model	48
3.5.3 Calculation Phases of the Finite Element Model	48
3.5.4 Forces in Plate Material	50
CHAPTER 4: RESULTS AND DISCUSSIONS	51
4.1 General	51
4.1.1 Ground Deformation Analysis	51
4.2 Ground deformation and Surface Settlement	51
4.2.1 Mohr-Coulomb Model	52
4.2.2 Hardening Soil Model	53
4.2.3 Subloading- t_{ij} Model	55
4.2.4 Settlement Data Comparison	56
4.3 Ground Stress and Strain Analysis During Tunnel Construction	58
4.3.1 Mohr Coulomb Model	58
4.3.2 Hardening Soil Model	63
4.3.3 Subloading- t_{ij} Soil Model	67
4.4 Tunnel Lining Analysis	71
4.4.1 Bending Moment Comparison	71
4.4.2 Shear Force Comparison	73
4.4.3 Axial Force Comparison	75

CHAPTER 5: CONCLUSIONS AND RECOMMENDATIONS	77
5.1 General.....	77
5.2 Conclusions.....	77
5.3 Recommendations for Future Work.....	78
REFERENCES	80
APPENDIX A : ANALYTICAL CALCULATION	84
APPENDIX B: SETTLEMENT MONITORING POINTS	85

List of Tables

Table 1.1 Technical Standards for the Karnaphuli Tunnel	6
Table 3.1. Tunnel Properties.....	38
Table 3.2. Laboratory test summary	39
Table 3.3. Typical k values.....	40
Table 3.4. Load classification according to JSCE	42
Table 3.5. Basic Soil Properties.....	44
Table 3.6. Mohr coulomb Model Properties.....	45
Table 3.7. Hardening Soil Model Properties	45
Table 3.8. Subloading- t_{ij} Model Properties.....	46
Table 3.9. Plate Material Properties.....	47
Table 4.1. Final Settlement(in mm) for 0.5% Volume loss	57

List of Figures

Figure 1.1 Tunnel collapse in Sao Paulo (Neto et al., 2002)	3
Figure 1.2 General layout of the tunnel project (China Communications Second Highway Survey, 2016.).....	5
Figure 1.3 Right-to-left alignment of Karnaphuli Tunnel	7
Figure 1.4 Research flow diagram	9
Figure 2.1 The famous Thames tunnel build under the principle of Brunel’s shield idea. (Mathewson et al, 2006)	12
Figure 2.2 Slurry Shield Tunneling workflow diagram (Smith, 2001).....	14
Figure 2.3 Types of tunnel boring machines (Yun, 2019).....	14
Figure 2.4 Single shield TBM (Kolymbas, 2008).....	15
Figure 2.5 Critical sections to be checked from ITA Guidelines(ITA ,2000)	17
Figure 2.6 FEM mesh example.....	20
Figure 2.7 Basic ideas of MC model: a) linear elastic perfectly plastic material behavior, b) yield surface in principal stress space with $c'=0$	23
Figure 2.8 Hardening Soil model- common definitions of different moduli on a typical strain-stress curve for soil (Schanz et al., 1999).....	24
Figure 2.9 Causes of settlement from a shield drive.....	26
Figure 2.10 Gaussian curve for transverse settlement trough and ground loss V_t (Möller, 2006)	28
Figure 2.11 Different types of segments.....	30
Figure 2.12 Segmental Lining Construction.....	31
Figure 2.13 Tunnel segment Joints	32
Figure 2.14 Load Distribution model as per JSCE	34

Figure 3.1. Geometry of the tunnel.....	37
Figure 3.2. Soil Sample Collection.....	38
Figure 4.1 Surface Settlement after the construction of first tunnel varying volume loss(Mohr-coulomb model)	52
Figure 4.2 Surface Settlement after the construction of second tunnel varying volume loss(Mohr-coulomb Model).....	53
Figure 4.3 Surface Settlement after the construction of second tunnel varying volume loss(Hardening Soil Model).....	54
Figure 4.4 Surface Settlement after the construction of second tunnel varying volume loss(Hardening Soil Model).....	54
Figure 4.5 Surface Settlement after the construction of second tunnel varying volume loss(Subloading t_{ij} model).....	55
Figure 4.6 Surface Settlement after the construction of second tunnel varying volume loss(Subloading- t_{ij} model).....	56
Figure 4.7 Surface Settlement after the construction of first tunnel for 0.5% volume loss	56
Figure 4.8 Surface Settlement after the construction of second tunnel for 0.5% volume loss	57
Figure 4.9 Ground Displacement during the construction phases of the tunnel.....	59
Figure 4.10. Ground Stress Analysis tunnel Construction(a,b)	60
Figure 4.11. Excess pore pressure during tunnel Construction(a,b,c)	61
Figure 4.12. Variation of ground strain during tunnel construction	62
Figure 4.13. Variation of ground strain during tunnel construction	63
Figure 4.14. Ground Stress Analysis tunnel Construction(a,b)	64
Figure 4.15. Excess pore pressure during tunnel Construction(a,b,c)	65
Figure 4.16. Total strains during the construction of the tunnel.....	66

Figure 4.17. Total strains during the construction of the tunnel.....	67
Figure 4.18. Effective stress during tunnel construction	68
Figure 4.19. Excess pore pressure during tunnel construction	69
Figure 4.20. Variation of strain during tunnel construction.....	70
Figure 4.21. Bending Moment Diagram For First Tunnel Lining	71
Figure 4.22. Bending Moment Diagram for Second Tunnel Lining.....	72
Figure 4.23. Shear forces comparison for First Tunnel Lining.....	73
Figure 4.24. Shear Force Comparison for Second Tunnel Lining.....	74
Figure 4.25. Axial forces for Mohr-colulomb model	75
Figure 4.26. Axial forces for Mohr-colulomb model	76

Acknowledgements

Glory and praise be to Allaah the Almighty for giving me the strength and courage to successfully complete my M.Sc. thesis. Verily there is no strength except with Allaah.

First of all, I would like to acknowledge the support and motivation of my thesis supervisor Prof. Dr. Md. Hossain Md. Shahin, to whom, I owe my sincere appreciation for guiding throughout the research works. He has been a true inspiration that led me into research field of Geotechnical Engineering. It is only through his concern, encouragement, and motivation that this work was completed. I am forever indebted.

A note of thanks is also extended to Prof. Dr. Md. Rezaul Karim, Dr. Md. Tarek Uddin, Dr. Shakil Mohammad Rifaat and Dr. Mohammad Shariful Islam, who served on my Master's Thesis Committee, for their time and thoughtful review.

I also acknowledge the financial support provided by the Islamic University of Technology to conduct this study. Also thankful for the the laboratory and other associated facilities provided by the Department of Civil and Environmental Engineering, Islamic University of Technology (IUT), Gazipur to carry out this study. I am thankful to CCCC for allowing me to use the soil investigation data for the study.

I want to thank my beloved iutian juniors specially Daud Nabi Hridoy, Fuad Bin Nazrul, Farhan Anjum Badhon, Md. Habibur Rahman Bejoy Khan , Mohammad Zunaied-Bin-Harun, Musaddik Hossain, Mozaher Ul Kabir Mahadi and Niaz Ahmed .Without their unconditional support , it would not be possible to finish it on time. My sincere gratitude to my senior Ijaj Mahmud Chowdhury and Dr.Tanvir Ahmed for providing me guidelines during my research assistantship days. I also want to thank my colleagues of SMEC-ACE for supporting me in the office. My batchmates, specially Saadi, Navid, Nafis, Digonto, Sajal, Zihan, Noman vai, thank you all. And how can I forget Md. Shaheduzzaman and Muntasir Ahmed, no words can describe your contributions in my life brothers. May Allah give barakah to these kind hearted people.

I want to remember my mother, who left this worldly life in 2019. Ammu, without your blessings and dua, I would not survive at all. I want to thank my elder brother who never stopped supporting me even if he is thousand kilometers away in Australia. I'm grateful to my father for letting me pursue my studies from IUT.

Finally, I want to thank my in laws, Mst. Tajkera Khatun and Md. Asaduzzaman. They actually adopted me after my mother's departure. Without their mental support during the hard times specially during of COVID-19, I would not be able to make it here. Tomal and Lamiya, you guys are my inspiration. And finally my wife, Dr. Afrina Tasneem. Bou, without your unconditional love and care, my journey would have been thousand times harder. Thank you for dealing with me every day.

Abstract

Underground tunneling is an excellent option to accommodate the increasing amount of traffic in the densely populated areas like Bangladesh. However, these tunneling constructions certainly induce ground movement to a certain scale. Even though developing new excavation technologies has opened the opportunity to construct tunnels in challenging ground conditions, the ground response due to these mechanized excavations is still attracts the attentions of the researchers. In particular for multilayered soft ground conditions like those found in Bangladesh, the ground surface movement brought on by such tunneling works is highly unpredictable. In order to gain a basic understanding of the ground's behavior, finite element analysis is a useful tool.

In the course of this study, a finite element analysis was performed by making use of the Plaxis 2D program in order to examine a particular stretch of the multi-lane road tunnel that was constructed underground in Chattogram, Bangladesh which is also the first underground tunnel in Bangladesh. The tunnel is located at the sea entrance of River Karnaphuli of Chattogram suburb and its west coast starting point is connected with costal road. The geological condition of the area is consisting of alternating layers of cohesive soil layer and sandy soil layer mostly. Even though the tunneling depths is variable along the route, however, to simulate the most critical situation of the construction, maximum soil overburden depth of 35 m for the twin tunnel has been chosen for this analysis.

To understand the soil structure interaction phenomena, the constitutive models that were utilized in the study are as follows : Subloading- t_{ij} model, Mohr –coulomb model(MC), & Hardening Soil model(HS). The finite element analysis has been conducted to investigate the following three scenarios, in the first place, the response of the ground before the tunnel was installed, in the second place, the response of the ground after the first tunnel was constructed, and in the third place, the response of the ground after the second tunnel was constructed. Mostly drained analysis is done for the excavation works. After that, each and every one of the finite element results are checked with the empirical and analytical findings. In addition to this, the failure mode of the tunnel lining structure has been studied, taking into account the load impacts of the soil in the surrounding area. When it came to

the case of loading, factors including hydrostatic pressure, soil pressure and the weight of the tunnel itself were taken into account. All the analysis were done in plastic condition.

The Subloading- t_{ij} results reveal that the settlements of the ground surface caused by tunnel construction are greatest for the ground surface directly above the tunnel crown and significantly reduces respectively on both sides of the tunnel. The MC and HS models both seem to have the same settlement troughs in their results. Volume loss for shield tunneling is considered from 0.5% to 1.0% which is applied as contraction in Plaxis 2D. The settlement results were further compared with the onsite settlement data. A comparative results graphs have been plotted to understand the effect of using different soil models for the excavation works.

Consolidation analysis has been conducted for all three models in Plaxis. It has been discovered that, after the construction of both tunnels is finished, consolidation period is takes 15-24 days to finish. The effect on tunnel lining has also been studied at the end of the research. As Subloading- t_{ij} and Mohr-colulomb soil models are generating maximum soil stress, the forces (the moment, axial and shear forces) are found higher in these two models than the hardening soil models.

Keywords: Tunneling, Excavation, Volume loss, Plaxis 2D, Settlement

CHAPTER 1: INTRODUCTION

1.1 General

Tunneling is often regarded as the most practicable approach to the building of subsurface structures for the goal of enhancing mobility and developing interconnections in all form of civil engineering projects. The development of metropolitan areas, subways, underground commercial complexes, drainage systems, power cables, network cables, gas conduits, underground parking facilities and many other varieties of infrastructures are only few of the many different multifunctional uses for tunneling.

The most typical urban activities, such as mass transit, community facilities (gas supply, residential and commercial water supply, energy, and wastewater) and safety (protection against flooding), works as the strong reason to use the underground space in a densely populated metropolitan area. In addition, establishing these common urban infrastructures under the ground will not only reduce the collisions but also cut down the amount of noise pollution and preserve the nature. Tunneling is the most practical and essential method of underground space utilization, as it frees one from the need to utilize digging techniques.

The process of excavating a tunnel will almost certainly result in soil deformation and may have an impact on neighboring existing buildings. This is not in the least bit debatable. The mismanagement of utility lines, poor quality soil conditions, successive intervention with the water table, and the insignificant overburden in relation to excavation diameter are the typical major risks that are found to be associated with underground tunnels in densely populated urban areas such as Bangladesh. These are the types of risks that are typically found to be associated with underground tunnels.

When building an underground tunnel, the following are the primary issues that need to be taken into consideration:

1. The placement of the alignment might be limited by common urban restrictions, which can result in numerous and often unavoidable interferences with housing at the surface, buried utilities, and other pre-existing underground constructions.
2. Basic site investigations might be limited for restricted access.
3. The subsurface at shallow depths often consists of loamy soils, alluvial deposits, or fills created by humans. This poor condition of the earth is one of the important variables that must be taken into consideration throughout the planning and control of the tunnel's construction.
4. Even under the most controlled conditions, urban tunneling at shallow depth often results in settlements at the surface. This is true even when the tunnel-driving activities are properly regulated.

In fact, now a days, it is conceivable to excavate tunnels without causing significant disturbances to the surface activities in an urban city area, even though there is a presence of loose ground, and or even under a water table. All of these are becoming possible for the prodigious developments in mechanized excavation technologies achieved in the last 30 years. But these uncertainties get reduced to much lower level when the tunneling is done in suburban area.

No doubt whether it's a suburb or urban area, underground space development for a long period is a great challenge for the Owners, Planners, Designers and Contractors, as they have to work in such a way that the construction works disturbs the daily surface activities as little as possible while ensuring the quality, safety, time and achieving targets of the development at the same time

To aim for a safe construction process, the contact between the above ground infrastructures and utilities with tunnel construction has to be evaluated with precise calculation .How tunnel induced settlements will affect the surface structures and how to handle it has to be analyzed appropriately. Without these preliminary studies, there is a great chance of facing unavoidable damages which can cause great loss for the infrastructure development.



Figure 1.1 Tunnel collapse in Sao Paulo (Neto et al., 2002)

That's why it's always advisable to prepare an extensive geotechnical, structural environmental monitoring plan.

Numerous researches had been performed to keep the settlements within allowable limits and suggest a proper economical way to construct the tunnel. The response of the nearby surface structures is the most important while conducting the studies. Finite element analysis is the most powerful, common and widespread tools for researchers and engineers worldwide to predict the surface settlement and earth pressure during the excavation process.

Recent advancement of finite element analysis in the field of geotechnical engineering can help the engineers various ways . According to Potts et. al. (2001), in short, finite element analysis can be useful to:

- Take into account the complicated terrain conditions.
- Simulate an accurate behavior of the soil;
- Take care of difficult hydraulic situations;
- Effect of ground treatment
- To model the short-term , medium and long-term condition;

In order to design the tunnel lining, the engineers have to precisely consider the surrounding soil loads, grouting pressure, jack forces from TBM, surcharge above ground etc. acting on the lining structure. But the most important of all is to simulate the earth pressure on the tunnel lining. Typically earth pressure in tunneling is estimated by using rigid plastic theory in which the deformation properties of soil and excavation sequence is not considered. In genuine site condition, the earth pressure depends on both properties of the ground and excavation sequences of the tunnel. Elastic analysis also cannot properly explain such dependence of earth pressures in tunneling. Hence more accurate rigid plastic deformation analyses are required to get realistic results of earth pressures. It is evident that meaningful numerical analysis can be made only if the stress distribution and density within the ground be predicted reliably. Therefore, some suitable constitutive models that the engineer can comprehend and apply easily when required. The constitutive model should consider typical soil behaviors including positive and negative dilatancy of soils, dependency of density and or confining pressure of soils and shear strength of soil (ϕ , C). Mohr-Columb model, Hardening soil, subloading t_{ij} model are the constitutive models - which can describe different important characteristics of soils and soil-structure relations.

This thesis considers the suburb area of Chattogram, Bangladesh where disturbance due to traffic and other underground utilities is almost zero. Main focus of the research is to analyze the settlements of the ground, understand the development effective stress due to tunnel excavation as well as the characteristics of the pore pressure in soil in different stages of the construction life using finite element analysis for a specific section of the Karnaphuli River Tunnel in most extreme condition (for overburden stress) .

1.2 Background of the thesis

The Karnaphuli River serves as a natural boundary between the two halves of the Chattogram Region. The city and the seaport are included within one portion, while the region of heavy industry comprises the remaining portion. The current two bridges are not adequate to support the large traffic volume that is both present and expected to increase. Because of the physical characteristics of the river, siltation on the bed of the Karnaphuli

River is a significant issue that poses the greatest risk to the efficient operation of the Chattogram Port. Instead of building yet another bridge across the Karnaphuli River, the government of Bangladesh intends to construct a tunnel that would travel under the waterway. This decision was made in order to combat the issue of siltation. The Bangladesh Bridge Authority (BBA) was given the responsibility of putting the project into action. (Bangladesh Bridge Authority, 2013)

The proposed tunnel is located in Chattogram, Chattogram District, Bangladesh. It will connect the east bank with the west bank of Karnaphuli River at the estuary. The Project connects with the Coastal Road under planning at its starting point (at the west bank), then it goes east along the existing Sea Beach Road, and then it crosses gate of Naval Academy and Karnaphuli till the east bank of Chattogram underground. The planned route is 9,265.971 m long in total.

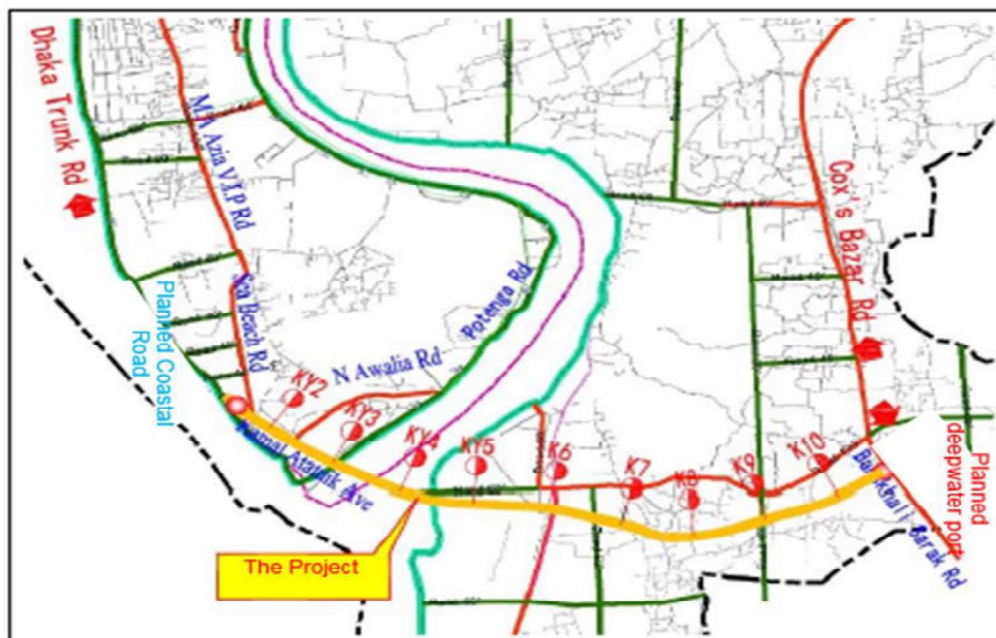


Figure 1.2 General layout of the tunnel project (China Communications Second Highway Survey, 2016.)

The main parts (tunnel and bridge) of the Project are designed and constructed as expressway standards and the connection roads as urban trunk highway (access control in parts), with the design speed of 80 km/h.

A preliminary design of the tunnel is made following the international standards and codes:

- Dual two-lane tunnel design without non-motorized vehicle lane and sidewalk
- Cross section type of twin-tube dual two-lane.
- Through comprehensive comparison among the various tunnel construction methods suitable for this project, shield-driven method is recommended for tunnel construction
- The segment for shield tunnel is 10.8m in diameter, 0.5m in thickness and 2m in ring width. Common segment with taperness of 36mm is adopted. The segment separation adopts the pattern of 5+2+1, i.e. total 8 pieces, including 5 standard pieces, 2 adjacent pieces and 1 capping piece. Both ring and longitudinal joints of segments adopt inclined bolt connections.

Technical Standards considered for the design of the Kanaphuli Tunnel are as followings:

Table 1.1 Technical Standards for the Karnaphuli Tunnel

Serial No	Criteria	Characteristics
1	Design speed	80 km/h
2	Number of lane expressway	Two-way four-lane expressway
3	Lane Widths	2×3.65 m
4	Lane height	4.9 m
5	Minimum radius of horizontal curve at shield section	2,550 m
6	Maximum longitudinal gradient	4%
7	Least radius of vertical curves	convex 7,050 m, concave 6,000 m

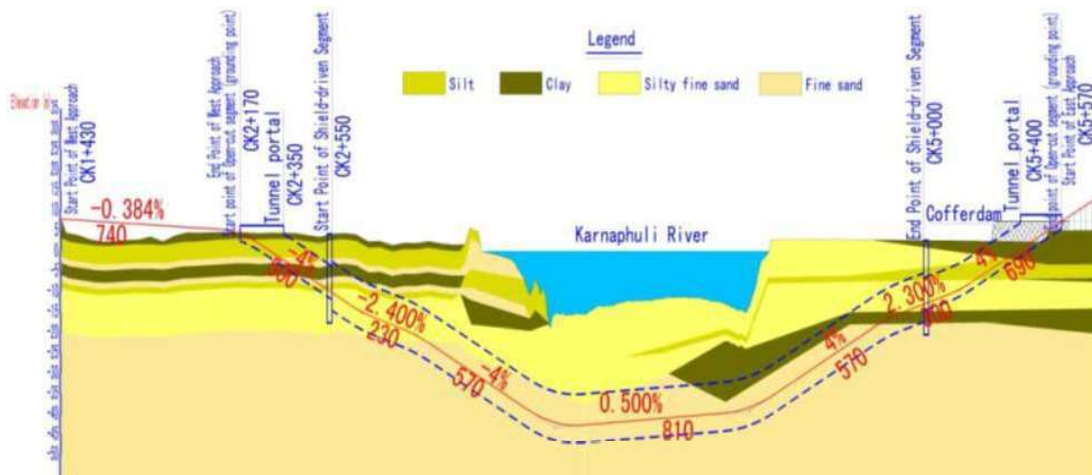


Figure 1.3 Right-to-left alignment of Karnaphuli Tunnel

Fig. 1.3 shows the vertical alignment of the Karnaphuli Tunnel. The depth of the tunnel crown from the bottom of the river bed varies from approximately 20.0m to 40.0m along the alignment.

1.3 Objectives of the Study

The objectives of this study are as follows:

1. To create Finite Element model of Karnaphuli Shield Tunnel
2. To investigate the influence of soil cover on surface settlement and earth pressure due to tunnel excavation considering the ground as a greenfield.
3. To compare the findings from evaluating the surface settlement using three distinct kinds of constitutive models at various stages of tunnel construction.

4. To assess the ground stresses ,effective stresses and excess pore pressure developed throughout the course of the tunnel's construction.

1.4 Methodology

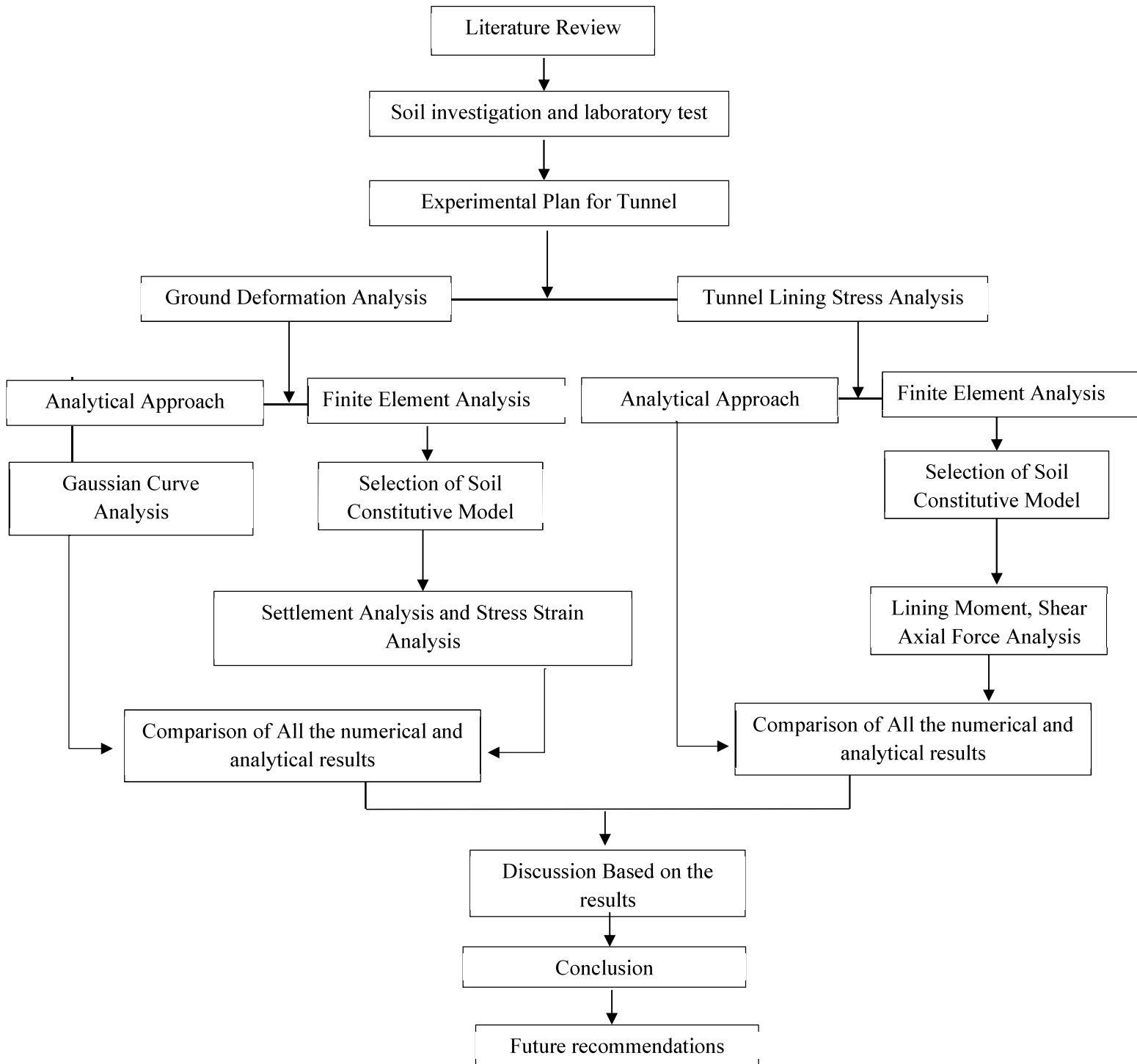


Figure 1.4 Research flow diagram

The steps followed to conduct this study have been shown in sequential order in **Fig. 1.4**. In this study, an experimental investigation was planned to carry out to investigate the soil deformation due to the excavation of tunnels (35m deep from surface) in Chattogram soil. Also, analytical studies will be performed at the same time to compare the results with numerical analysis. Afterwards, the behavior of the tunnel lining is analyzed. For better understanding, only the loads from the soil and water pressure have been considered. Prior to starting the experimental process, a detailed literature review was done to establish the scope of the work. After defining the scope of the work, an experimental plan was set up.

Based on the obtained results a number of conclusions have been drawn. Depending upon the limitations of present study, a guideline for conducting future studies has also been recommended.

1.5 Layout of the Thesis

Chapter 1 thoroughly discusses the background and objectives of this study. **Chapter 2** discusses the previous research works using different constitutive model and analytical approaches to analyze the tunnel lining behavior and surface deformation due to tunneling. **Chapter 3** presents the detailed procedure for the finite element analysis. In short, the multilayered ground condition is modelled at first and then the 1st tunnel has been excavated. With the presence of 1st tunnel, 2nd tunnel excavation is conducted. The analysis is done using 3 different constitutive model and other analytical approaches. The chapter concludes with information pertaining to the test methods and procedures followed in this study. **Chapter 4** presents the results of analysis for both tunnels. These results include settlements of the ground over the tunnel, stress strain curve and bending moment, axial and shear force diagram of the tunnel lining. **Chapter 5** presents the conclusions drawn from the results of this research and also suggests recommendations for future works.

CHAPTER 2: LITERATURE REVIEW

2.1 Introduction

Tunneling is a complex construction action and proper analysis of the ground can minimize the construction risks to a great extent. Understanding the effects due to tunneling specially for shield tunneling, has been studied by researchers for a long time. With advanced constitutive models, finite element analysis is a great way to understand the effects of tunneling work. In this study, a literature review has been done to discover what studies have been done in this area. In the short discussion, different ways of building tunnels are described, and the important factors that can go wrong during construction are investigated. Common tunneling construction techniques have been reviewed primarily for soft soil condition like Bangladesh. Then, finite element approaches for analyzing underground tunnels have been reviewed as well.

As the Karnaphuli tunnel is the first shield tunneling project in Bangladesh and there haven't been many studies done on the soft soils in this country, there is a lot of room to study how tunneling works affects the surface settlements. For this, literature review of the research has been divided into two parts: one is for performing the numerical analysis model for simulating the tunneling system and the other is for the analysis of surface settlement and tunnel lining considering the excavation in soft soil.

2.3 Tunnel Construction Techniques

At present, three common methods are adopted worldwide for tunnel construction. These popular methods are Cut and Cover method, New Austrian Tunneling Method (NATM) and Mechanized Shield Tunneling method. Considering the ground conditions, depth of excavation, underground water conditions, the length and diameter of the tunnel drive, the depth of the tunnel and many more important parameters, mechanized shield

tunneling was the best option for Karnaphuli tunnel. Because mechanized shield machines can provide support at the excavation face using slurry materials. Also, the tunnel alignment mostly passes through sand soil with high permeability. So, a mechanized shield tunneling machine with adequate slurry pressure and proper advance rate can ensure the safest construction work at site.

A brief discussion on the mechanized shield tunneling has been provided below:

2.3.1 Mechanized Shield Tunneling:

The history of shield tunneling is almost 200 years old which started with the revolutionary idea of shield tunneling by Marc Isambard Brunel. The famous Thames tunnel, which was constructed between 1823 and 1843, followed Brunel's marvelous shield tunneling idea. The historical picture of the Thames tunnel is provided in **Figure 2.1**.

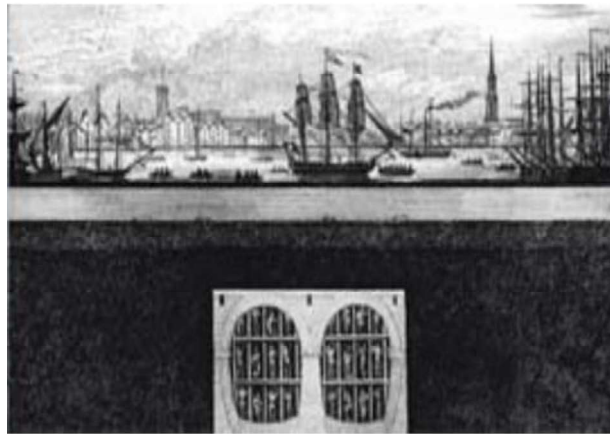


Figure 2.1 The famous Thames tunnel build under the principle of Brunel's shield idea. (Mathewson et al, 2006)

For a long period of time, all of the excavated materials were extracted by means of human labor. Finally, in the year 1876, an automated method was developed, which made it possible for tunnel project to make use of the shield as an industrialized operation. J.H. Greathead and J.J. Robins, two well-known engineers, are credited with developing the improved mechanized shield tunneling machine between the years 1887 and 1889, and we are thankful to both of them.

Shield Tunneling is mainly considered for tunneling in softer and weaker soils. During shield tunneling, continuous radial support has to be provided (Kolymbas, 2008).

The shield is actually a cylindrical steel tube which moves forward and does the excavation in the front while in the back it provides the facilities for erecting prefabricated segmental linings. In shield tunneling, two common tunneling techniques are followed, they are:

- i. Open face tunneling
- ii. Closed face tunneling.

In this research, we will investigate the settlement while considering the slurry shield tunneling techniques which falls in the category of closed face tunneling. Therefore, brief discussion is provided on closed face tunneling.

2.3.2 Closed Face Tunneling:

In the closed face tunneling techniques, a continuous ground support has to be provided while the TBM machine advances. This technique is famous for constructing a tunnel with minimum surface deformation but eventually leading an enormous load from ground on tunnel lining. For soft soil, slurry shield tunneling has more advantages than other techniques. For closed faced tunneling, one of the most common methods of tunneling is “Slurry Shield Tunneling”

The tunnel face was stabilized by Slurry Shields by the application of pressured bentonite slurry. This is one of the most popular soft grounds tunneling method. The excavated soil is typically mixed with the slurry during TBM operation and after excavating certain tunneling distance, the soil has been removed from the slurry in different treatment plant called Slurry Treatment Plant (STP). In order to exert control over the pressure of the slurry, a chamber that contains pressurized air is linked to the slurry. The Bentonite suspension, which provides the slurry pressure, can minimize the risks of blow outs and eventually, all the works can be done under normal atmospheric condition. The schematic diagram for the shield tunneling work flow has been shown in **Figure 2.2**.

During the time of maintenance, the air pressure from the air chamber replaced the slurry pressure. Sometimes, the soil ahead of the cutter head are frozen to balance the soil pressure during maintenance.

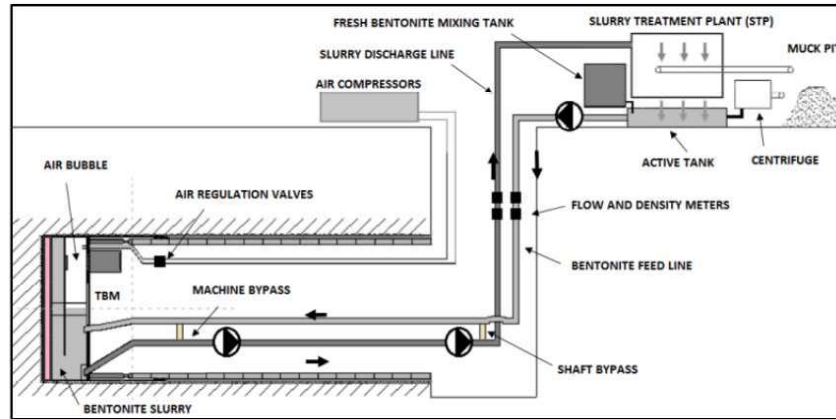


Figure 2.2 Slurry Shield Tunneling workflow diagram (Smith, 2001)

2.4 Tunnel Boring Machine

The construction industry has advanced with time and now there are some advanced (almost automated) boring machine which can continue the excavation process in the safest way possible. There are different types of Tunnel boring machines which are used for tunneling. Typically based on the soil characteristics, the classification of tunneling machines is provided in Fig . 2.3:

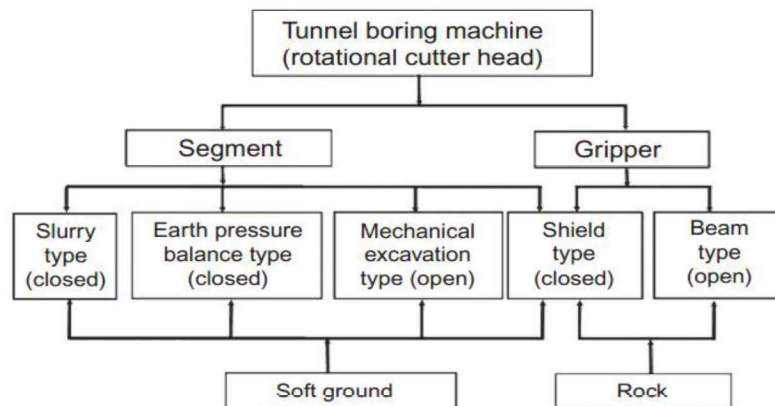


Figure 2.3 Types of tunnel boring machines (Yun, 2019)

As the research is conducted for soft ground tunneling, the working methodology of the shield tunneling technique is taken into account.

A shield tunnel has the following components which excavate the soft soil with minimum surface disturbances:

- a) Shield Heading: A circular steel tube with steel cutter ahead helps to excavate the soil
- b) Jacks: The jacks push the shield forward into the ground with a pressure up to 400 bar and can apply forces up to 3MN
- c) Cutterhead: The cutterhead at the front can be driven electrically or hydraulically, responsible for excavating the soil. It is normally comprising of disc cutters, chisels and scrapers
- d) Slurry Circuit: Conveys face support suspension to the excavation chamber and the mixture of excavated material and suspension back to the slurry treatment plant.
- e) Face Support Chamber: This chamber maintains the pressure in front of cutterhead with necessary bentonite pressure
- f) Segment erector: A segment erector at the end of shield is mechanically equipped to assemble the tunnel segment and form the tunnel lining.

A figure of single shield TBM is provided in **Fig. 2.4** for better understanding:

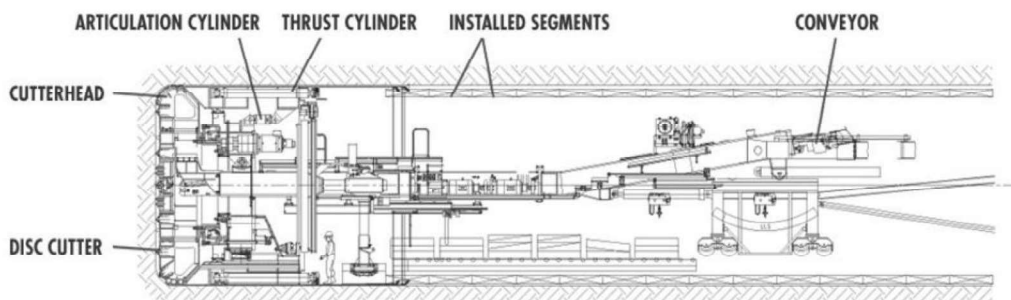


Figure D-5 Typical Diagram for Single Shield TBM (Robbins)

Figure 2.4 Single shield TBM (Kolymbas, 2008)

Typical advance rate of TBM is 0.8 to 2.0 m depending in the size of each segment. After the segmental lining has been erected, grout is used to fill the space that remains between the lining and the soil. A full cycle of shield tunneling includes the following steps:

- Excavating and provide temporary support at the front face
- Move forward as well as receiving support from the erected lining.
- Setting up segments in the permanent tunnel lining

2.5 ITA Critical Cases

Before analyzing a tunnel section, especially for the lining design, the ITA (International Tunneling Association) guidelines (ITA 2000) can be followed to understand the effect at the most critical sections. The **Fig. 2.5** depicts 8 (Eight) critical cases which should be considered as “critical section” during tunnel construction, they are:

- i. Section with the deepest overburden
- ii. Section with the shallowest overburden
- iii. Section with the highest groundwater table
- iv. Section with the lowest groundwater table
- v. Section with large surcharge
- vi. Section with eccentric loads
- vii. Section with unlevel surface
- viii. Section with adjacent tunnel at present or planned one in the future

Before pursuing the FEM analysis, the Karnaphuli tunnel alignment has been studied to identify the above-mentioned ITA cases for the analysis. After evaluation, Case i and Case viii have been considered to analyze the ground behavior and forces on the tunnel lining. Reasons for omitting the other cases are:

- Case ii, Case iii and Case iv has been omitted as the surface settlement data was not available for comparison with the FEM analysis.

- As the tunnel is constructed in greenfield condition, so case 5 has been omitted.

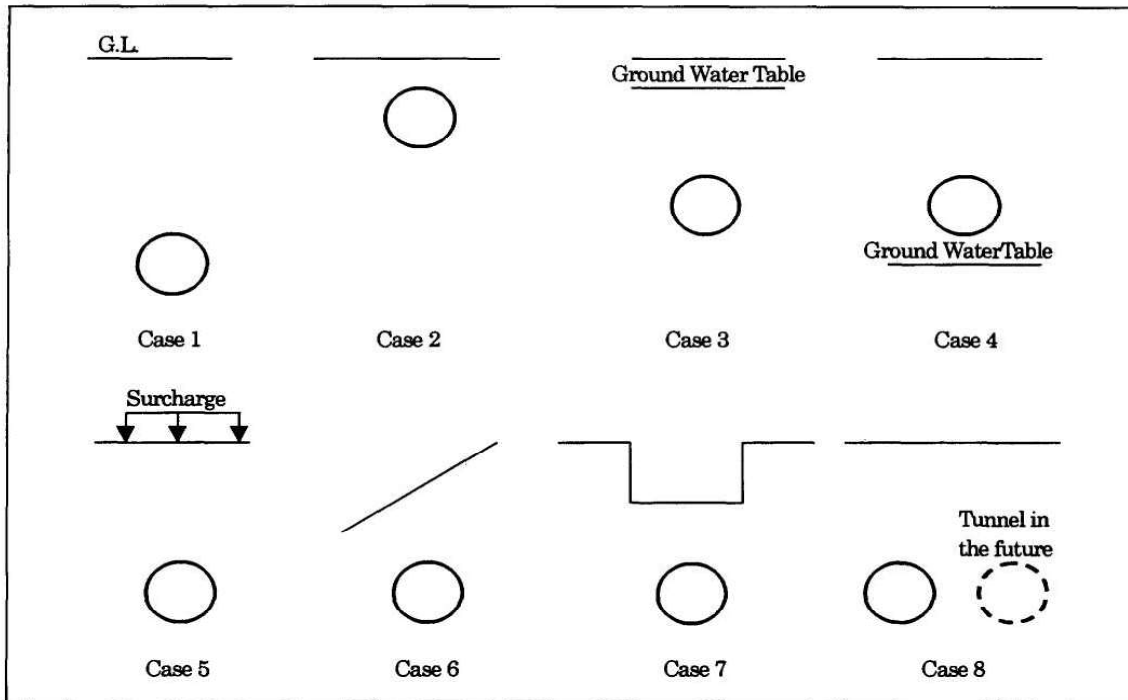


Figure 2.5 Critical sections to be checked from ITA Guidelines(ITA ,2000)

- Case vi and case vii are not applicable as per the project site location.

For this research, both selected case i (maximum overburden depth) and case viii (tunnel in future) are considered near the launching shaft of the project in West Bank of the Karnaphuli tunnel. The regular monitoring data has been collected and later compared for both of these cases.

2.6 Numerical Method for Tunneling Analysis

From 1960, the use of numerical modelling for tunneling has been widely developed and accepted by researchers worldwide. There are various numerical tools to analyze the tunneling problems for example: Finite element method, Finite difference

method, Boundary element method, discrete element method and so on. Automatic mesh calculation and attractive visual results are also encouraging engineers to carry on the research works in numerical analysis. Numerical analysis involves the study of approximation techniques for solving mathematical problems, taking into account the extent of possible errors. Though this analysis is an approximation, but results can be made as accurately as desired.

Numerical Analysis is widely used in geotechnical engineering for the following reasons:

- Analysis process is quick and easy to conduct the simulation.
- More reliable and realistic analysis.
- To understand and to determine the structural behavior practically.
- To view each structural behavioral steps of construction process, it is the best analytical approach.
- Solve for the roots of a non-linear equation.
- Solve for large systems of equations.
- Soil-structure interaction is accounted properly in this type of analysis.
- Soil-water interaction can be simulated accurately in this analysis.
- Settlement and deformation of the ground surface and structures can be determined accurately.

Among the numerical analysis, Finite element method is most widely used for solving the geotechnical problems. In this research, 2D FEM model has been created in Plaxis software using different constitutive soil models.

2.6.1 Finite Element Method (FEM):

The finite element technique, often known as the FEM method, is one of the numerical approaches that is used the most frequently in geomechanics. Although it is a continuum model, specific discontinuities may be modeled with it as well.. In finite element modeling (FEM), the hosting ground is divided up into a finite number of smaller components. These components are linked together at various nodal locations. Alterations

made to the initial subsurface conditions are the source of the stress, strain, and deformation that must be studied.. For instance, such change might be induced by tunneling process. The stressed and strains are generated in one element effects the interconnected elements and so forth.

Modeling the stress-strain connection of the components numerically requires the creation of a global stiffness matrix, which integrates the unknown numbers with the quantities that are already determined. Then, this matrix is solved using standard matrix reduction techniques and the results are obtained. The equation to be solved are highly complicated and as the number of the elements in the model increase, the calculation time and the storage capacity increase dramatically.

By means of FEM, complex underground conditions and tunnel characteristics can be analyzed. Furthermore, this method enables the simulation of complex constitutive laws, non-homogeneities and the impact of advance and time dependent characteristics of the construction methods.

On the contrary ,in order to use most FEM applications, one will need to have a higher level of program and computer understanding than other approaches. It is often problematic to evaluate the findings since the output of the analysis is complicated, making the study itself complex. However, the use of a post processor may be considered in order to get over this challenge..

2.6.1.1 General Steps in FEM:

The general steps in finite element method are described below:

- i. Preprocessing
- ii. Solution
- iii. Post Processing

These three (3) steps are being discussed below:

i. Preprocessing:

In a broad sense, it can be said that the preprocessing stage consists of model definition.. It consists of following steps:

- a) Meshing (or discretization): Mesh generation is the process of using finite elements to describe a physical region, and the resultant collection of elements is called the finite element mesh. The whole structure or geometry is divided into small pieces or nodes. In **Fig. 2.6** , typical mesh example has been provided.

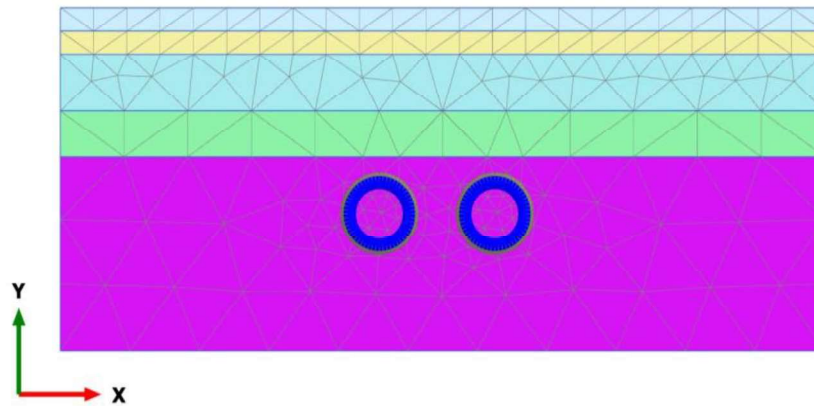


Figure 2.6 FEM mesh example

- b) Create a rough set of equations that describes the entire structure by connecting its parts at their nodes. (forming element matrices). Establishment of stiffness relations for each element. Material properties and equilibrium conditions for each element are used in this establishment. Enforcement of compatibility, i.e, the elements are corrected. Enforcement of equilibrium conditions for the whole structure, in the present case for the nodal joints. By means (ii) and (iii) steps, the system of equations is constructed for the whole structure, which is called assembling.
- c) The physical constraints (or Boundary Conditions) are defined.
- d) Material and geometrical characteristics (length, area etc.) of the element are defined in this stage

e) Finally, the loading condition is created in this stage.

ii. Solution:

In the solution phase, the finite element software compiles the governing algebraic equations into matrix form and then computes the unknown values of the main field variable (s). The values that have been calculated are subsequently used through back substitution in order to generate new, deduced variables. Some examples of these variables are forces, stresses, and so on.

In this solution phase, a proper constitutive model has to be defined. A brief discussion has been done in the experimental program chapter

iii. Post processing:

Postprocessing is a term that refers to the process of analyzing and evaluating the outcomes of the solution. The postprocessor software includes complex procedures that are put to use in the process of classifying, publishing, and graphing certain findings obtained from a finite element solution. The following types of possible tasks that may be carried out:

- ✓ Sequence pressures on elements by magnitude.
- ✓ Check equilibrium.
- ✓ Calculate FOS(factor of safety).
- ✓ Draw a distorted model of the structure.
- ✓ Simulate the actions of a dynamic model.
- ✓ Create temperature graphs using a color-coded system.

Finite element method requires the solution of the element analysis and the system analysis. The element analysis yields a relationship between nodal forces and nodal displacements from equilibrium conditions at nodes. This relationship is expressed in terms of a stiffness matrix for the element. To form the complete structure from the stiffness matrices one needs to assemble all individual elements. This results in a system of equilibrium equations. Finally, prescribed boundary conditions are to be applied to solve these equations. When the selected displacement patterns for the elements are able to

produce constant stress fields inside the elements, the method gives sufficiently accurate results. The number of division of elements of a body and connectivity among them are arbitrary. The choice will depend on simplicity, adaptability, and accuracy of results.

In the course of this investigation, both two- and three-dimensional finite element studies have been carried out. In order to conduct an analysis in two dimensions, the ground soil is segmented into a predetermined number of components with four nodes each. For simplicity, all four and eight-noded is treated as isoparametric elements. In two-dimensional analyses, both plane Strain and axisymmetric conditions have been applied according to the problems. In this chapter, we shall discuss some important features of finite element method. It will cover descriptions of shape functions, isoparametric elements, principle of virtual work and formulation of finite element method.

2.6.2 Constitutive Model:

Constitutive equations are the formulas that describe the relationship between stress and strain for a certain element. These equations are known as the constitutive equations for that material. A constitutive relation approximates the observed physical behavior of a material under specific conditions of interest. To summarize, constitutive relations are required for two reasons:

- (i) To include the material-dependent nature of the force-displacement connection.
- (ii) For the purpose of developing a force - deformation correlation, bridging the gap between the number of unknowns and the available formulas.

To define a proper constitutive model for a soil is very much necessary in FEM analysis. Some of the widely used soil models are: Linear elastic constitutive relations, Elasto-plastic Drucker-Prager model, Elasto-plastic Mohr-coulomb model, Elasto plastic Cap model and many more. Each of these models comes with its own set of benefits and drawbacks, the nature of which is heavily determined by the specific application in consideration. The most significant negative associated with improved and complex

models is the high number of appropriate parameters, many of which often cannot be obtained using ordinary experiments. This is by far the most problematic aspect of these models. The Cam Clay model (e.g., Schofield and Wroth, 1968), which was established well over half a century ago, was a paradigm-shifting constitutive model for geomaterials. This is due to the fact that the model presented a coherent framework for explaining the consolidation and shear behaviors of unstructured clays, both of which had been explored independently up until that point in time. Unfortunately, with the exception of reformed regularly consolidated clay under the standard axis-symmetric tri-axial compression condition, the Cam clay model is unable to anticipate the soil behavior. A number of proposals for constitutive models to address the shortcomings of the Cam clay model; however, most of these models are either too complicated or can only be used under certain circumstances. In this research, the Mohr coulomb model, Subloading- t_{ij} and the Hardening soil model have been used. A brief description of these models has been discussed.

i. Mohr –Coulomb Model:

Mohr –coulomb is a perfect linear elastic perfectly plastic constitutive law. It involves actually five parameters namely Young’s modulus, Poisson’s ratio, cohesion, angle of friction and angle of dilatancy to express the stress –strain behavior. **Fig. 2.7** shows the stress-strain consideration of Mohr-coulomb model. Because of the simplicity of this model, it’s still been used in many calculations.

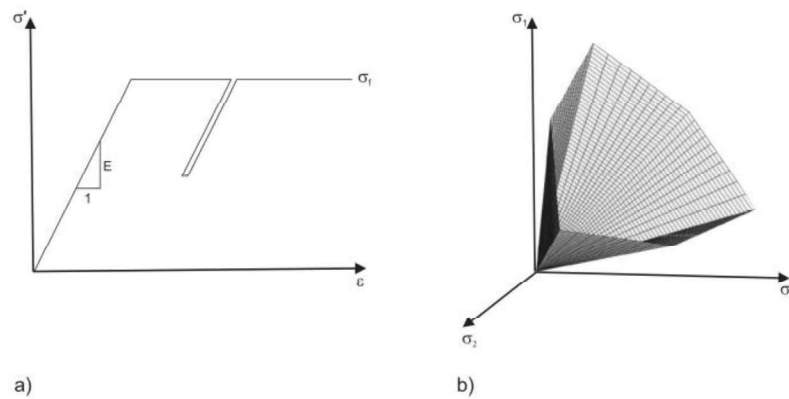


Figure 2.7 Basic ideas of MC model: a) linear elastic perfectly plastic material behavior, b) yield surface in principal stress space with $c'=0$

Even though problems like bearing capacity can be modelled with this law easily, it has some imperfections while simulating the excavation problems like tunneling.

ii. Hardening Soil Model

In hardening soil model, the total strains are calculated using a stress-dependent stiffness, different for both virgin loading and reloading. The plastic strains are calculated by introducing a multi-surface yield criterion. Even though this model represent some parameters similarly to the MC model limiting states of stress are simulated by means of the effective shear parameter cohesion, friction angle and dilatancy angle, the pre failure states of soil behavior are more accurately described by using three input stiffness, the triaxial loading stiffness E_{50} , the oedometer loading stiffness E_{oed} , and the triaxial unloading stiffness E_{ur} . (Schanz et al., 1999) .**Fig 2.8** shows the stress strain consideration for Hardening soil model.

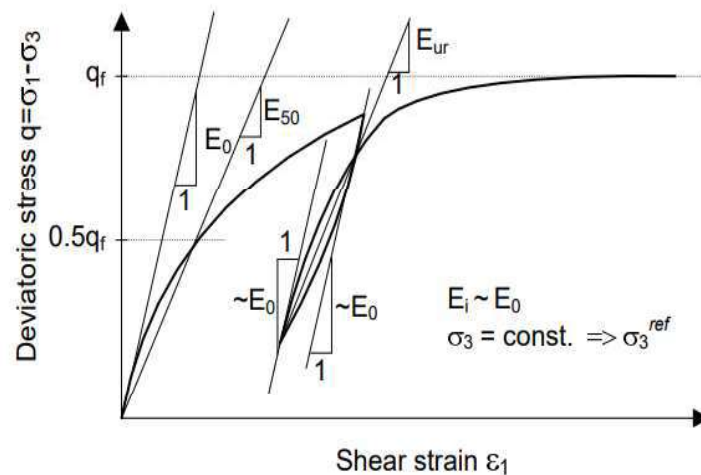


Figure 2.8 Hardening Soil model- common definitions of different moduli on a typical strain-stress curve for soil (Schanz et al., 1999)

iii. Subloading tij Soil Model:

Subloading tij model (Nakai and Hinokio, 2004) is an elastoplastic constitutive model for two dimensional (2D) finite element analysis used in numerical analysis. The Subloading tij model (Nakai and Hinokio, 2004) has the following advantages over other constitutive models:

(1) Subloading t_{ij} model requires only a few unified material parameters.

(2) This model can describe the characteristics of soils which are as follows:

- ✓ Influence of intermediate principal stress on the deformation and strength of soil.
- ✓ Influence of stress path on the direction of plastic flow is considered by splitting the plastic strain increment into two components.
- ✓ Influence of density and/or confining pressure.

Nakai et al. (2011) has presented a simple and unified constitutive model for soils considering some effects such as the influence of density, bonding, time dependent behavior and others in one-dimensional condition which is presented here.

Both elasto-plastic and elastic analysis of soil can be simulated by the subloading t_{ij} model. The soil parameters are required to be assigned in this model in order to define the mechanical behaviors of different soil layers. So, all the required parameters of soil layers are determined, estimated and collected based on laboratory test results, sub-soil analysis results for Chattogram soil. The model parameters are:

λ = Compression index (or slope of virgin loading curve in e -log p' curve at the loosest state)

κ = Swelling index (or slope of unloading- reloading curve in e -log p' curve at the loosest state where, e is void ratio and p' is consolidation pressure)

$R_{CS} = (\sigma_1 / \sigma_3)_{cs(comp.)}$ = Critical state stress ratio.

OCR = Over consolidation Ratio.

N or e_N = Reference void ratio on normally consolidation line at $p=98$ kPa & $q=0$ kPa (or void ratio at mean principal stresses (p) 98 kPa in e -log p' curve)

e_0 = Initial void ratio.

ν = Poisson's ratio.

β = Model parameter responsible for the shape of the yield surface.

a = Model parameter responsible for the influence of density and confining pressure.

2.7 Analysis of the Tunnel Section

To analyze the tunnel construction in soft soil, the analysis has been divided in two distinct parts, they are:

I. Ground Behavior Analysis

In this section, the maximum surface settlement has been calculated using the empirical equation. The results were then further compared with finite element analysis results. Also, the stress strain behavior, effective stress, pore water pressure during and after tunnel construction has been analyzed.

II. Tunnel lining analysis

For using different constitutive model of the soil and considering Case i and Case viii, the tunnel lining behavior has been analyzed as well. Also, the maximum bending moment, shear force and normal force were compared with the Elastic equation method proposed by JSCE (Japan Society of Civil Engineers,2006).

2.7.1 Ground Behavior Analysis

Estimating the surface settlements during shield tunneling is important aspect during construction. Schenck (1968) pointed out 8 causes for surface settlement during shield drive. **Fig. 2.9** shows the schematic diagram of the causes:

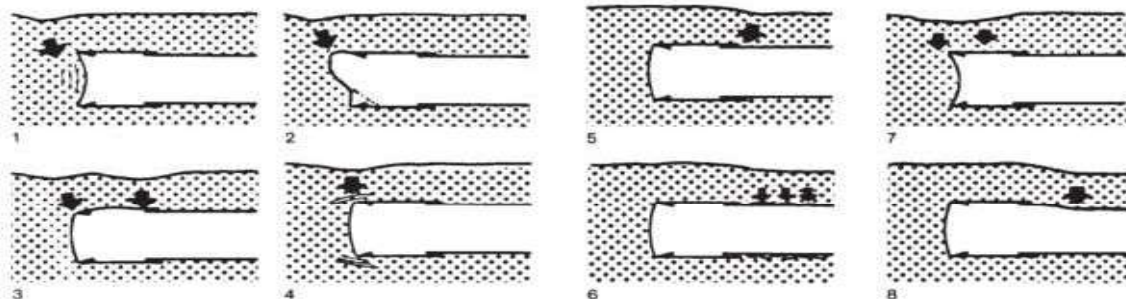


Figure 2.9 Causes of settlement from a shield drive.

The causes are as following:

- i. Relaxation of ground
- ii. Too much removal of ground
- iii. Deformation of shield
- iv. Vibration effect
- v. Ground falling in
- vi. Insufficient filling of annular gap
- vii. Compaction of ground
- viii. Deformation of tunnel lining

The first 4 reasons (i , ii , iii, iv) can be minimized after taking a proper steps while (v) and (vi) can be prevented by early and sufficient grouting. Only (vii) and (viii) causes can be regarded as unavoidable.

The surface settlement is calculated using following methods:

- i. Empirical Method
- ii. Numerical Analysis

2.7.1.1 Empirical Method for Predicting Surface Settlement

This method is based on empirical observations as it is widely used for experience. This method helps to evaluate the shape of the subsidence in absence of a structure (Greenfield condition). Schmidt (1969) and Peck (1969) were the first to show that transverse settlement trough, taking place after the construction of the tunnel. **Fig.2.10** shows the settlement trough due to tunneling:

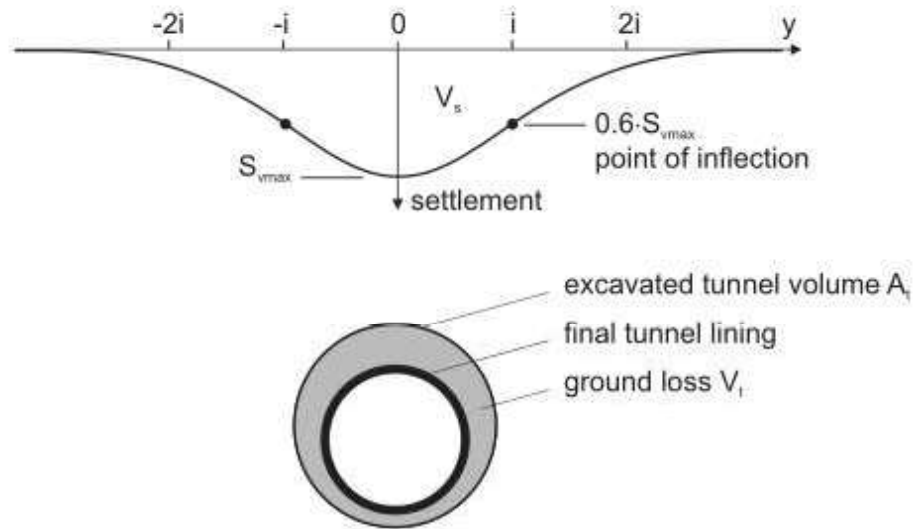


Figure 2.10 Gaussian curve for transverse settlement trough and ground loss V_t (Möller, 2006)

The settlement curve derived from this approach is Gaussian shaped with a maximum settlement value “ S_{max} ” in correspondence of the vertical axis of the tunnel and the area of subsidence equal to the loss of volume V_L (extra volume of the ground excavated with reference to tunnel excavation value). Many Case histories (ATTEWELL & WOODMAN, 1982; New & O’Reilly, 1991) for geotechnical conditions has confirmed the effectiveness of this approach. The procedure is discussed in detail in the next chapter of the thesis.

2.7.1.2 Finite Element Analysis for Predicting Surface Settlement

Finite element analysis for predicting surface settlement has been studied by many researchers. Sharma (2019) used Plaxis 2D based on assessment of sub-surface settlements and impact on pile foundations due to tunneling . Ferrão et. el. (2020) prepared a numerical model in the software ANSYS with the aim to evaluate the surface settlements induced by tunneling. Yuan et. el.(2022) used finite element analysis to establish a three-dimensional numerical model of a double-line tunnel in a weathered mudstone area.

So it is understandable that in finite element analysis, the ground adjacent to the tunnel structure can be analyzed more precisely. For different soil condition ,the ground

will behave differently for different types of civil engineering works. That's where the importance of finite element analysis is lying. Also, using proper constitutive models, the stress strain diagram can be developed, the pore pressure can be analyzed which is almost impossible for empirical methods. In our research, the ground behavior during different stages of the construction has been analyzed.

In this research plastic analysis and consolidation analysis have been carried out. The plastic analysis is elastic plastic deformation analysis.

2.7.2 Tunnel Lining Analysis

2.7.2.1 Definition and purpose of tunnel lining

Tunnel lining is the structural element of tunnel which resist the inward pressure from the surface to secure the tunnel space. Lining is actually a ring structure. It designates systems installed either shortly or considerably after excavation to provide permanent support and durable, maintainable long-term finishes.(Kuesel, King, and Bickel 1996)

Lining can be various types considering the tunneling system, soil properties, and excavation technique and so on. For our research purpose, we have chosen pre cast segmental ring lining which is the most common, flexible quality ensuring lining system used all over the world. The main reason behind choosing this kind of lining systems can be understood in following points (Guglielmetti et al., 2008):

- Continuous support of the excavation with the shield in order to block the development of surface settlements;
- Prevention of water flow into the tunnel by installing a lining which is immediately impermeable;
- Facilitated the maintenance of the TBM's resistance to longitudinal thrust during excavation;
- Provided assistance for the back-up equipment for the TBM;;
- Reduction in the amount of time that must pass before the "completed" tunnel can be handed over to the civil works department

A brief summary about different segment types, material for segment production, joints, water proofing and other basic information has been discussed below:

(i) Segmental lining types:

The types of segments are chosen based on the assembly process inside the tunnel. In **Figure 2.11** , most common types of segments according to ITA (International Tunneling Association) are shown:

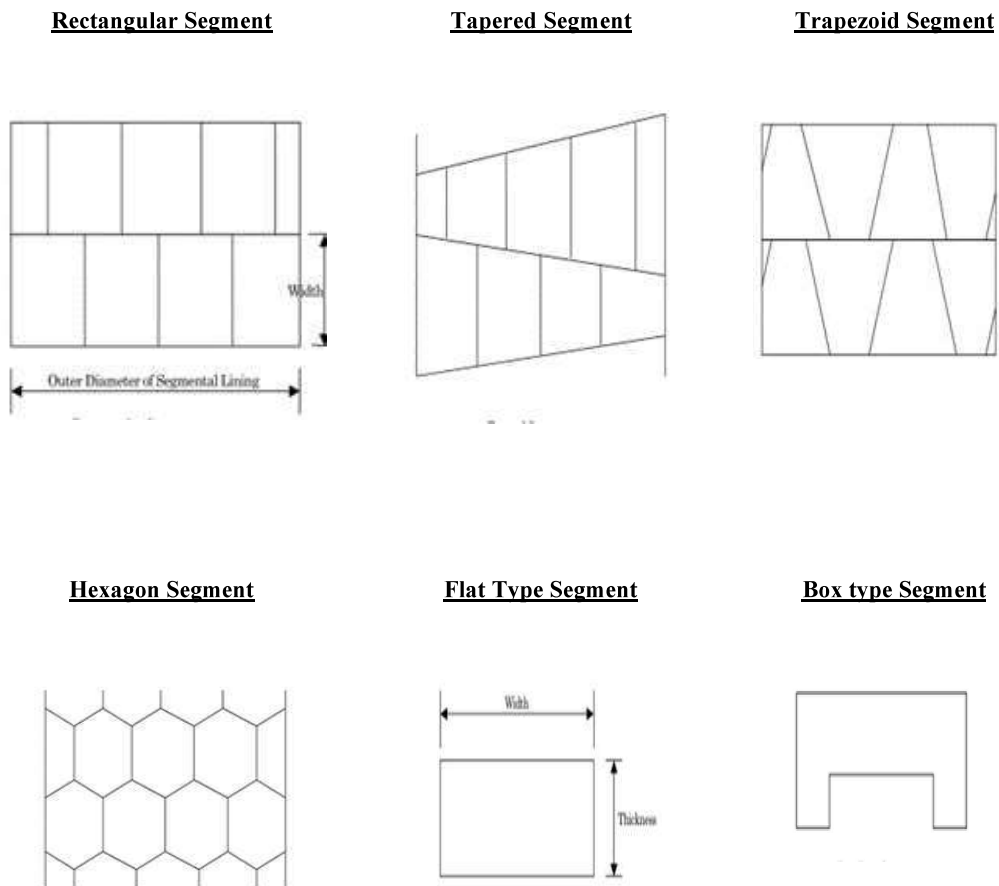


Figure 2.11 Different types of segments

(ii) Materials for Segmental lining types:

Segmental lining consists of two material, concrete and steel reinforcement. There are various standards for choosing the materials and their desired strength for the segment. Steel mould for segment casting, reinforcement arrangement and construction ready precast concrete segments are shown in **Fig. 2.12** .



Figure 2.12 Segmental Lining Construction

While choosing the cement, preference given to additive free rapid hardening cement. For aggregate, maximum dimension of 25-30mm is preferred. Fly ash or fillers (limestone-based materials) can be used as admixtures if the aggregates are lacking fines. Superplasticizers are advice to use for better workability.

(iii) Joints:

To connect the segments with one another, joints are provided in the segmental lining. In the concrete segments, there are basically two types of joints between two segments, they are Longitudinal joints and Circumferential joints. **Figure 2.13** shows the arrangement of these two types of joints.

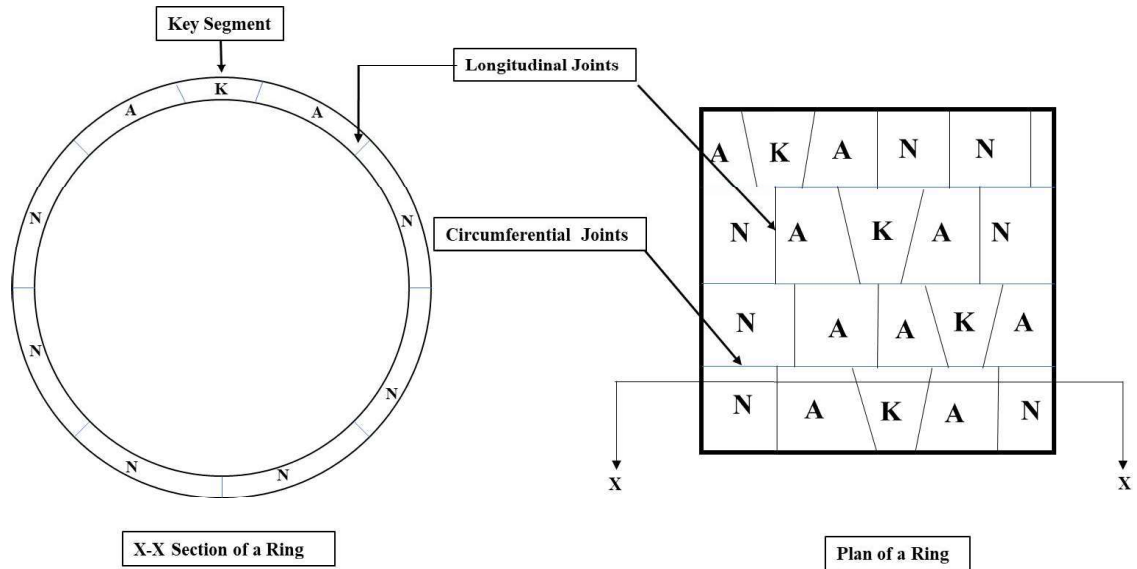


Figure 2.13 Tunnel segment Joints

The rings are built by circumferential joints while the segments are built by longitudinal joints. These joints are further connected with bolts and dowels.

(iv) Waterproofing System

Waterproofing is the most important factor during the tunnel construction. Since the sealing materials are being arranged in pairs in the specific grooves surrounding the segments, they usually operate together effectively. Typically, there are two types of Gaskets:

- a. Compression Gasket
- b. Compression and Swelling Gasket

2.7.2 .2 Tunnel lining analysis methods:

While designing the tunnel lining, it should be designed in such a way it can achieve the ability to maintain the excavated opening of the tunnel. There are numerous methods for tunnel lining design which can specify the loads and deformations in accordance with the geologic and construction conditions and also represent the ground-lining interaction

as well. But there are disparity as well among the researchers which analysis provide the best results at all.

According to International Tunneling Association (ITA, 2000) the member forces have to be computed by using any of the following techniques (ITA, 2000):

- Elastic Equation Method
- Schulze and Duddeck Method
- Muir Wood Model
- Beam-Spring Model
- Finite Element Method or Numerical Analysis.

For this research the main analysis is done using finite element analysis and then the results are further compared with elastic equation method proposed by Japanese Standard for Shield Tunneling (JSCE) Society. A brief overview on these two methods is provided below.

(i) Elastic Equation Method:

The Elastic equation method was proposed by Japanese Standard for Shield Tunneling (JSCE) Society (JSCE, 2006). It can calculate the member forces of circular tunnel without using the computer. The method was first introduced in the year of 1960.

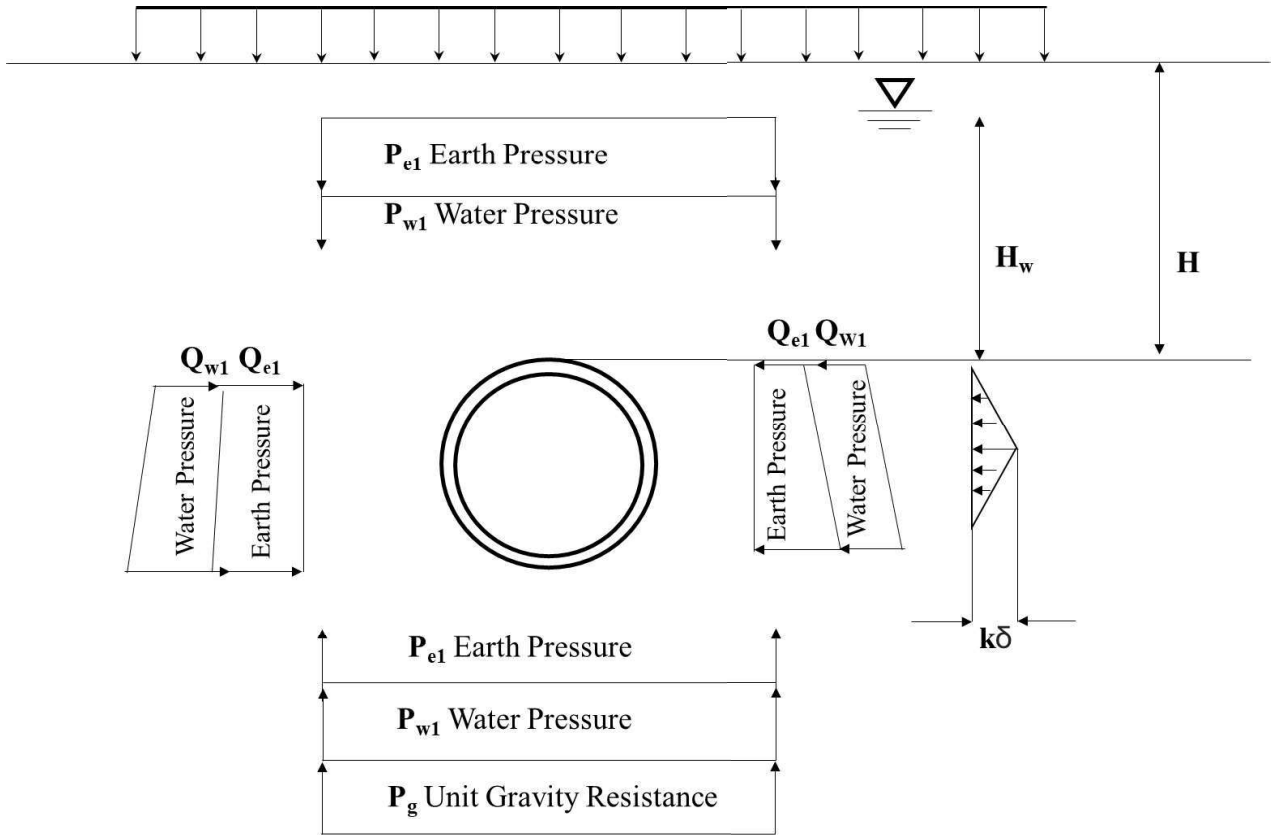


Figure 2.14 Load Distribution model as per JSCE

Detail calculation of these method has been provided in the Appendix section of this thesis book.

In most cases, a segmented ring will be made up of a few different segments that will be joined by bolts or dowels. Because the stiffness of joints is lower than the rigidity of the segment section, the deformation that occurs at these connection joints is greater than the one that occurs in a ring whose rigidity is constant everywhere.. Furthermore, the connections at the segment joints are generally staggered. However, this method assumes that the segmental ring with uniform bending rigidity and cannot represent staggered rigidity. But it has to be mentioned that the solution obtained by this method can be very practical and helpful for checking the results obtained by numerical methods. In addition, the elastic equation approach has benefits over other closed form solutions since it is capable of computing the bending moment, axial forces, and shear forces at any point in the lining. Other closed form solutions do not have this capacity. Other closed form

solutions, on the contrary, are only able to calculate the bending moments and hoop forces at the point when the respective optimum value are reached..

(ii) Finite Element Method:

With the advancement of computer technology, the forces on the structural members on the tunnel lining can be analyzed easily using FEM program like Plaxis. The work process in FEM is same as discussed in the previous sections for ground displacement calculation. In lining analysis, the lining element is divided into finite elements and the surrounding pressure is taken into account for calculation. Some additional loads like grouting pressure, water pressure can be easily applied on the lining materials. In Plaxis 2d, the tunnel lining can be simulated as a plate material or as volume material (Shi et al., 2016).Kavvas et al., (2017) modelled the segments as shell elements.

To model the connections(joints) between the segments is also very important to verify during the lining analysis. In plaxis, the joints can be modelled using the connection feature with different spring stiffness. Xiaochun et al., (2006) analytically studied the influence of segmental joint in Plaxis where the joints were assumed to be fully hinged .

In this research, Mohr-Coulomb, Subloading- t_{ij} and Hardening soil model are used during the lining analysis in Plaxis .The lining material has been simulated using plate material .The joints are modelled with fixed and hinge connection to get a deeper insight about the forces acting on the lining.

2.7.3 Research Gaps

Surface settlement due to tunneling has been studied by many researchers. Case studies for certain types of tunneling has also been studied for many locations. (Wang et al. 2022).But in Bangladesh, Karnaphuli tunnel will be first underground tunnel to be constructed. So an analysis of the ground behaviour due to tunneling would provide a lot of insight for future tunnel construction in Bangladesh. Use of hardening soil model ,which captures the loading reloading behaviour during tunnel excavation can provide great output for Bangladeshi soil. Though it has been used for some surface settlement analysis for

filling soil (Shahin et. al. 2022) ,deep tunnel excavation analysis has not been studied that much.

To understand the actual behaviour of the ground, the comparison of the site monitoring values with the finite element analysis results are very much important for validation which has not been carried out for any tunnel research in Bangladesh. So, there is ample scope to study such ground deformation behaviour using finite element analysis software. Also, too much dependency on Mohr-coulomb model, which is one of the popular and common method for analysis can create severe design faults for the final design. A proper comparison only can identify the limitation of this model. So, to bridge the gap for construction underground tunnel, FEM model of Karnaphuli tunnel with different soil constitutive model can work as a guideline for future tunnel construction activities.

CHAPTER 3: METHODOLOGY

3.1 General

In this chapter, the methodology of the research work is summarized. The surface settlement for the excavation works of the tunnel is calculated using both empirical formula and finite element method. Certain soil parameters are assumed based on available correlations for the Chattogram soil. 2D plane strain surface contraction method is considered for simulating the excavation works. The contraction method has been applied by changing the volume loss parameter in Plaxis.

3.2 Geometry of the Tunnel

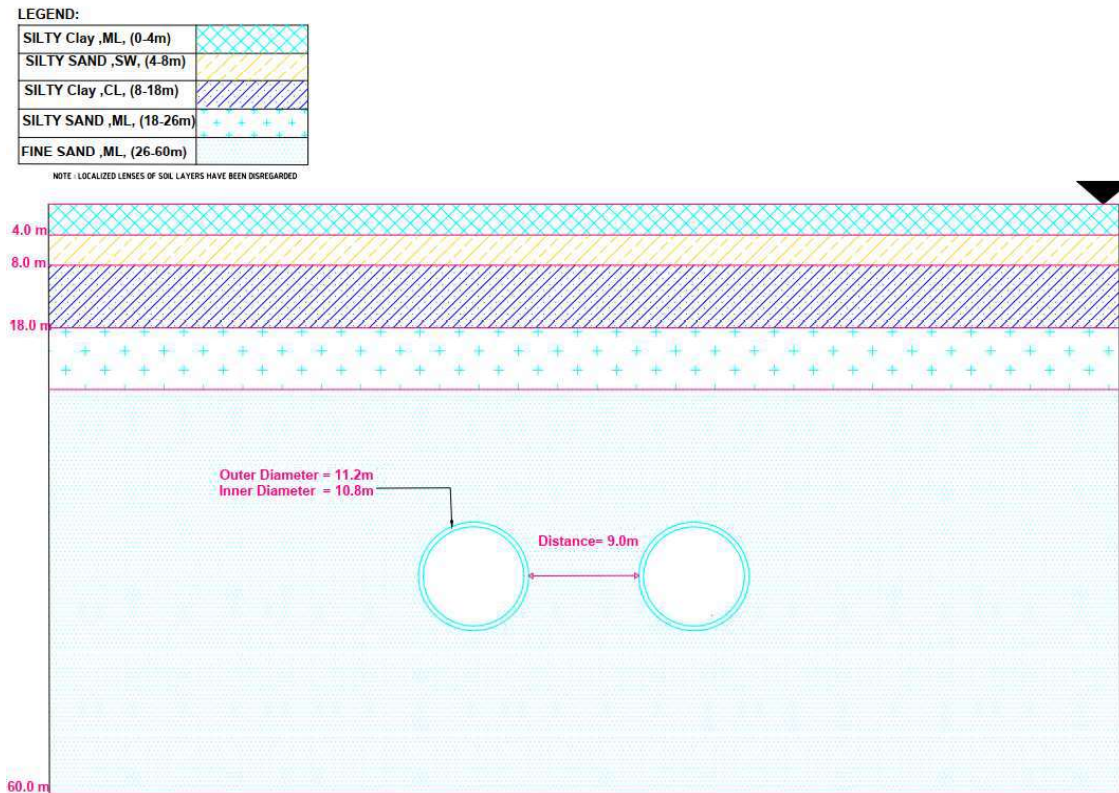


Figure 3.1. Geometry of the tunnel

For the analysis, the **Fig 3.1** shows the section which has been considered for the analysis. The geometrical details of the tunnel properties are shown in the **Table 3.1** below:

Table 3.1. Tunnel Properties

Type	Inner Diameter (m)	Outer Diameter (m)	Distance between tunnel (m)	Segment Type (m)	Segment Thickness (m)	Segment Width (m)
TBM Tunnel	10.8 m	11.2	9	Reinforced Concrete Segment	0.5	2.0

In this research, 2D FEM model has been created with twin tunnel to analyze the ground surface behavior and the respective moments in the lining. Above figure shows the clear dimensions of the proposed model. In Plaxis, the model length is considered 5(Five) times of the diameter of the tunnel on bother sides to ignore the boundary effects during the analysis.

3.3 Sub Soil Investigation and Laboratory Tests

Sub-soil investigation was done for deriving the soil parameters for the analysis. Previous soil report of the Karnaphuli tunnel project has also been used in this research.



Figure 3.2. Soil Sample Collection

About 4 boreholes have been executed at the study area. The soil borings of the selected location have been executed up to 30.0m depth. Each 1.5m of the boring, disturbed samples were collected. Wash boring method is used while conducting the boring works. The SPT(Standard penetration test) test values were tabulated in the field log sheet. This field test was executed according to the ASTM D1586 code. Detail of the sub-soil investigation bore log is provided in the appendix section of the thesis.

After the collection of soil sample, specific laboratory testing has been done which includes grain size analysis, moisture content, liquid limit, plastic limit, direct shear tests etc. A summary of the test procedure is provided below for better understanding:

Table 3.2. Laboratory test summary

Types of Test	Standards
Grain Size Distribution	ASTM C 136; ASTM D 422
Specific Gravity (Gs)	ASTM D 854
Moisture Content(w)	ASTM D 2216
Liquid limit (LL), Plastic Limit (PL), Plasticity Index (PI)	ASTM D 4318
Direct Shear Test	ASTM D 3080
Consolidation Test	ASTM D 2435

3.4 Elementary Analysis for the Tunnel

3.4.1 Empirical Analysis for Predicting Settlement

As it has been mentioned in the previous chapter the empirical solution for surface settlement follows the Gaussian curve, which can be depicted through the following equation.

$$S = S_{\max} e\left(-\frac{x^2}{2i^2}\right) \quad (3.1)$$

Where S= Settlement,

S_{\max} = Maximum Settlement, x = Distance from tunnel centerline

i = distance to the point of inflection on the settlement trough

Where $i = kz$

k = Settlement trough parameter,

z = depth from the ground surface to tunnel spring line.

Typical value of settlement trough parameter **k** (Chapman, Metje, and Stark 2017) is given in **Table 3.3**

Table 3.3. Typical k values

Soil Types	k value
Stiff fissured clay	0.4- 0.5
Glacial deposits	0.5- 0.6
Soft Silty Clay	0.6-0.7
Granular soils above water table	0.2- 0.3

The maximum settlement S_{max} can be defined as

$$S_{max} = \frac{V_L \left(\frac{\pi D^2}{4} \right)}{2.5i} \quad (3.2)$$

Where, V_L = Volume of ground loss during excavation of tunnel,

D = Diameter of the tunnel.

However, the above equation is workable when there is only single tunnel is excavated. O'reilly et al. (1982) suggested using the subsequent formula to calculate the total settlement profile:

$$S = S_{max} \left[e\left(-\frac{x_a^2}{2i^2}\right) + e\left(\frac{(x_a-d)^2}{2i^2}\right) \right] \quad (3.3)$$

where d is the lateral distance between the two tunnel center lines, and x_a is the lateral distance from the center line of the first bored tunnel. This formula presupposes that the tunnels are parallel, have the same diameter, and ignore any interactions between them, meaning that the excavation of the first tunnel has no bearing on the second tunnel's volume loss or settlement trough width.

As these are empirical equation, certain parameters have to be considered based on experience. Generally, the maximum volume loss for shield tunneling is assumed 0.5%. For this research, the trough width parameter k has been assumed 0.5 and the settlement is calculated for the volume loss is considered from 0.5% to 1.0 % for the shield tunneling.

3.4.2 Elastic Equation analysis for Tunnel lining

Elastic Equation analysis of tunnel lining is one of the most common methods for analyzing the lining behavior at the preliminary stage of the design work. In this research, ITA guidelines and JSCE guidelines have been followed for retrieving the most realistic results. These two guidelines are the most common and popular method used around the world.

For tunnel lining analysis, the basic and most important part is to define the loading conditions properly. The loads (JSCE ,2000) are classified as follows in this method:

Table 3.4. Load classification according to JSCE

Classification	Load Type
Primary Loads	Ground Pressure, Water Pressure, Dead Load, Surcharge, Soil Reaction
Secondary Loads	Internal Loads, Construction Loads, Effects of Earthquakes
Special Loads	Impact of nearby activity, effects of shrinkage, effects of neighboring tunnels etc

As the tunnel proposed in this research work located in the greenfield condition, only primary loads are considered (ground pressure, water pressure and dead load of the tunnel). No other secondary or special load is considered in this calculation. These loads are further discussed below:

3.4.2.1 Primary Loads

i. Ground Pressure:

The ground pressure is calculated for both vertical and lateral direction. As the proposed tunnel is a deep tunnel (depth H=35), for this case, the vertical soil pressure calculation formula will be:

$$P_{e1} = P_o + \sum \gamma_i H_i + \sum \gamma_j H_j \quad (3.1)$$

Where ,

P_{e1} = submerged unit weight of the soil.

$\gamma_{i,j}$ = unit weight of different soil layers

$H_{i,j}$ =Height of the soil layers

If the soil layer is situated above the water table, then the dry unit weight should be used. On the other hand, the submerged unit weight should be utilized for any soil layers that are located underneath the water table.

For the determination of lateral earth pressure, after multiplying the vertical earth pressure by the coefficient of lateral pressure($k=0.5$), the results are shown..

ii. Water Pressure:

Water Pressure acting on the tunnel lining shows different characteristics than the original ground due to the change in conditions caused by tunneling. It's very difficult to predict the groundwater conditions as the groundwater level will go a long-term change due to natural or artificial influences. For circular tunnels, setting the groundwater levels higher doesn't always lead to safer design but setting it lower does so. Water pressure is calculated using following formula:

$$P_{w1} = \gamma_w H_w \quad (3.2)$$

Here,

P_{w1} =Water pressure at tunnel crown

γ_w =Unit weight of water

H_w =Depth of water at tunnel crown

For the determination of lateral water pressure, the vertical water pressure has been multiplied with coefficient of lateral pressure ($k=0.5$) .

iii. Dead Load:

The dead load is the vertical load acting along the centroid of the cross section of tunnel. It is calculated in accordance with the following equation for circular tunnel:

$$P_g = \frac{W}{2\pi.R_c}$$

W=Single ring weight

R_c=Radius

As tunnel construction is a complex process, there are variety of loads to be considered such as surcharge load, construction loads (e.g., thrust force) etc. For the ease of computation, most basic loads are considered in the thesis.

3.5 Finite Element Analysis of the Tunnel

3.5.1 Geotechnical and Other Material Parameters for analysis

The study area is consisting of mixed layers of soil. The upper layers of soil are mostly clay type soils where the bottom layers are sandy layer. The alignment of the tunnel mostly faces sandy layers of soil. The ground water table is considered 5.0m below from the existing ground level. The soil layers are assumed drained considering that necessary water removal has been done using pumping or other means. For this research, following basic parameters are followed:

Table 3.5. Basic Soil Properties

Soil	Soil Type	Depth (m)	Coefficient of permeability in x and y direction (m/day)	Soil unit weight above phreatic level, γ_{unsat} (kN/m ³)	Soil unit weight below phreatic level, γ_{sat} (kN/m ³)
Clay	ML	0-4	0.26	16	18.56
Silty Sand	SW	4-8	5.77	17	19.5
Silty Clay	CL	8-18	0.26	16	18.33
Silty Sand	SW	18-26	5.44	17	18.73
Fine Sand	SW	26-60	7.56	17	18.73

Parameters required to run the simulation using sub loading tij and hardening soil model has been calibrated from real life project data. Such soil models were prepared and triaxial test has been simulated in plaxis software. However, the correlations and calibrations result from simulation has been provided in the appendix.

For the finite element analysis, following Mohr-Coulomb, Hardening Soil and Subloading-tij parameters have been considered which have been shown through **Table 3.6** to **Table 3.8** :

Table 3.6. Mohr coulomb Model Properties

Soil Type	Silty Clay	Silty Sand	Silty Clay	Silty Sand	Fine Sand
Cohesion (c) kpa	7	0	7-9	0	0
Friction angle (Φ)	32	29	30	32	37
Poisson's ratio ν	0.28	0.29	0.35	0.3	0.35
Young's modulus (E) kN/m ²	8E+03	30E+03	10.0E+03	40 E+03	80E+03
Dilatancy angle (ψ)	0	0	0	1.1	8

Table 3.7. Hardening Soil Model Properties

Material No.	Clay	2-Silty Sand	3-Silty Clay	4-Silty Sand	5-Fine Sand
Classification USCS	CL	SW	ML	SW	SW
Type of Material Behavior	Undrained(A)	Drained	Undrained(A)	Drained	Drained
Soil unit weight above phreatic level, γ_{unsat}	16	17	16	17	17
Soil unit weight below phreatic level, γ_{sat}	18.53	19.5	18.33	18.73	18.73

Initial void ratio e_0	0.9806	0.6293	1.14	0.6133	0.6270
Cohesive Force, C kpa	5	5.4	12.6	0.1	0.1
Internal Friction, Φ	30	31.1	4.4	34	35.5
Young's Modulus, E50	5250	14.7E+03	6600	22.79E+03	28.0E+03
Young's Modulus, Eoed	8053	14.63E+03	5127	1824E+03	28.0E+03
Young's Modulus, Eur	15.17E03	44.54E+03	22.31E+03	75.0E+03	84.0E+03
Poisson's ratio, ν	0.2	0.2	0.3	0.3	0.2

Table 3.8. Subloading-t_{ij} Model Properties

Material No.	1-Silty Clay	2-Silty Sand	3-Silty Clay	4-Silty Sand	5-Fine Sand
Classification USCS	CL	SW	ML	SW	SW
Type of Material Behavior	Undrained(A)	Drained	Undrained(A)	Drained	Drained
Compression index, λ	0.0567	0.02561	0.35	0.02035	0.011

Swelling index, κ	0.02700	7.57E-03	7.0E-03	3.675E-03	1.5E-03
Critical state stress ratio, R_{cs}	3.5	3	2.17	3.520	3.720
Reference void ratio, N	0.98	0.75	1.14	0.6133	0.6270
Poisson's ratio, ν	0.2	0.2	0.2	0.2	0.2
Model parameter responsible for the shape of the yield surface, β	1.55	1.65	1.7	1.860	1.6
Initial void ratio, e_0	0.98	0.6293	1.14	0.6133	0.6270
Power, p	2	2	2	2	2

Except the soil parameter, the tunnel lining has been designed as plate material in the analysis. To attain realistic results, the TBM has been considered as plate material during construction. The tunnel lining parameters are given below:

Table 3.9. Plate Material Properties

Parameter	Lining	TBM	Unit
Type of Behavior	Elastic; Isotropic	Elastic; Isotropic	
Material Type	Plate	Plate	
Axial Stiffness, EA	1.75E+07	63E+06	kN/m

Bending Stiffness, EI	3.65E+05	472.5E+03	Kn m ² /m
Material Weight, w	12.5	17.7	kn/m ³
Poisson's ratio, ν	0.15	0	

3.5.2 General Layout of the Finite Element Model

The general layout of the analysis for three different models (Mohr-Coulomb, Hardening Soil and Subloading- t_{ij}) has been described below:

- i. **Subsoil Model:** The subsoil model is 60.0m deep and 140.0m wide in Plaxis 2D model. The twin tunnels have been positioned at 35m depth from the existing surface level. The tunnel internal and external diameters are 10.8m and 11.8m respectively where internal center to center distance between twin tunnels is 9.0 m.
- ii. **Mesh and Elements Used:** For 2D analysis in Plaxis, 6 noded triangular elements have been used. The interface between tunnel and soil are 3-node line elements with pair of nodes instead of single nodes.
- iii. **Displacement Boundary:** The displacement boundary conditions are considered as follows:

For 2D model in Plaxis,

- at bottom, both vertical and horizontal displacements are fixed.
- at left edge, the horizontal displacement is fixed but vertical movement is allowed; i.e., vertical displacement is pinned.
- at right edge, the horizontal displacement is fixed but vertical movement is allowed; i.e. vertical displacement is pinned

- iv. **Drainage Boundary:** The drainage boundary is considered for the whole model.

3.5.3 Calculation Phases of the Finite Element Model

The calculation phases are defined as follows in Plaxis 2D program:

- i. Initial Phase**

In initial phase, all the structural (lining) members are deactivated. In Plaxis, this stage calculation type done using K0 procedure. The K0 procedure is provided in the appendix section for reference
- ii. Excavation of the First Tunnel**

In this phase, the plate material, which represents the TBM is activated and inside the tunnel geometry, the soil cluster volume is deactivated (dry condition).
- iii. Contraction of First Tunnel**

The volume loss at site is simulated using the contraction stage. The contraction is applied from 0.5% to 1.0% for the first tunnel.
- iv. Grouting for First Tunnel**

The Grouting pressure is applied at this stage. Grouting is simulated by applying waiter pressure to the surrounding soil.
- v. Activation of First Tunnel lining**

At this stage the first tunnel lining is activated. To simulate the concrete lining, the “Lining” property is assigned to plate material. Also, the negative interfaces are activated as well.
- vi. Excavation of second Tunnel**

The excavation of second tunnel is similar to the first tunnel construction sequence. For the second tunnel, the TBM is simulated by activating the circular plate inside the geometry and “TBM” material has been assigned to the plate material. The soil cluster volume inside the second tunnel geometry is deactivated (dry condition). From this phase to the last phase, the first tunnel lining has been kept activated.
- vii. Contraction of Second Tunnel**

The contraction is applied from 0.5% to 1.0% for the second tunnel.

viii. Grouting for Second Tunnel

The Grouting pressure is applied at this stage. Grouting is simulated by applying soil pressure to the surrounding soil of the second tunnel

ix. Activation of Second Tunnel lining

At this stage the first tunnel lining is activated. To simulate the concrete lining, the “Lining” property is assigned to plate material. Also, the negative interfaces are activated at this stage

x. Consolidation

After the construction of both tunnels, the Consolidation stage is implemented. The consolidation stage will continue until “Minimum water pressure” is achieved.

3.5.4 Forces in Plate Material

The tunnel lining has been characterized using plate elements. Here, the pressure or load on the lining is calculated from the previous material properties of soil. For better understanding of how the lining will behave of in the soft soil, only the primary loads are taken into account. For 2D analysis, two joints have been considered between the tunnel linings to prepare a simple calculation.

Main advantage of using this method is to compare the change in moment while constructing the second tunnel. It gives a lot of insight for taking precautions while constructing in actual site conditions. The FEM boundary condition and other parameters regarding the finite element analysis has been discussed earlier. The moment on the lining changes during this different construction phases.

CHAPTER 4: RESULTS AND DISCUSSIONS

4.1 General

In this chapter, the results obtained throughout the investigation are summarized and discussed. For ground deformation analysis, the results have been arranged in the following manner:

4.1.1 Ground Deformation Analysis

Surface settlement after sequential construction of both tunnels has been determined using 2D finite element analysis. The outcomes were later compared with empirical analysis.

4.1.2 Ground Stress Analysis

Effective stress and excess pore water pressure analysis was done after the construction of both tunnels. Consolidation analysis was carried out at the final stage until the minimum pore pressure was obtained.

4.1.3 Tunnel lining analysis

Axial force, shear force and bending moment for both tunnel lining was reviewed. Analytical and finite element analysis forces were compared.

Additionally, the surface settlement has been studied for varying volume loss conditions (0.5 to 1.0 percent) to ascertain the worst-case scenario during the construction phase.

4.2 Ground deformation and Surface Settlement

Two-dimensional (2D) analysis of the ground settlement has been done using three different constitutive model: Mohr-coulomb, Hardening Soil and Subloading- t_{ij} model.

Comparative graphs have been plotted to summarize the settlement behavior for ease of understanding.

4.2.1 Mohr-Coulomb Model

The settlement comparison is shown for two stages, after the installation of the first tunnel lining and secondly, after the installation of second tunnel lining. **Fig. 4.1** shows the surface settlement curves for different volume loss after installing the first tunnel lining and **Fig. 4.2** shows the settlement after installing the second tunnel lining

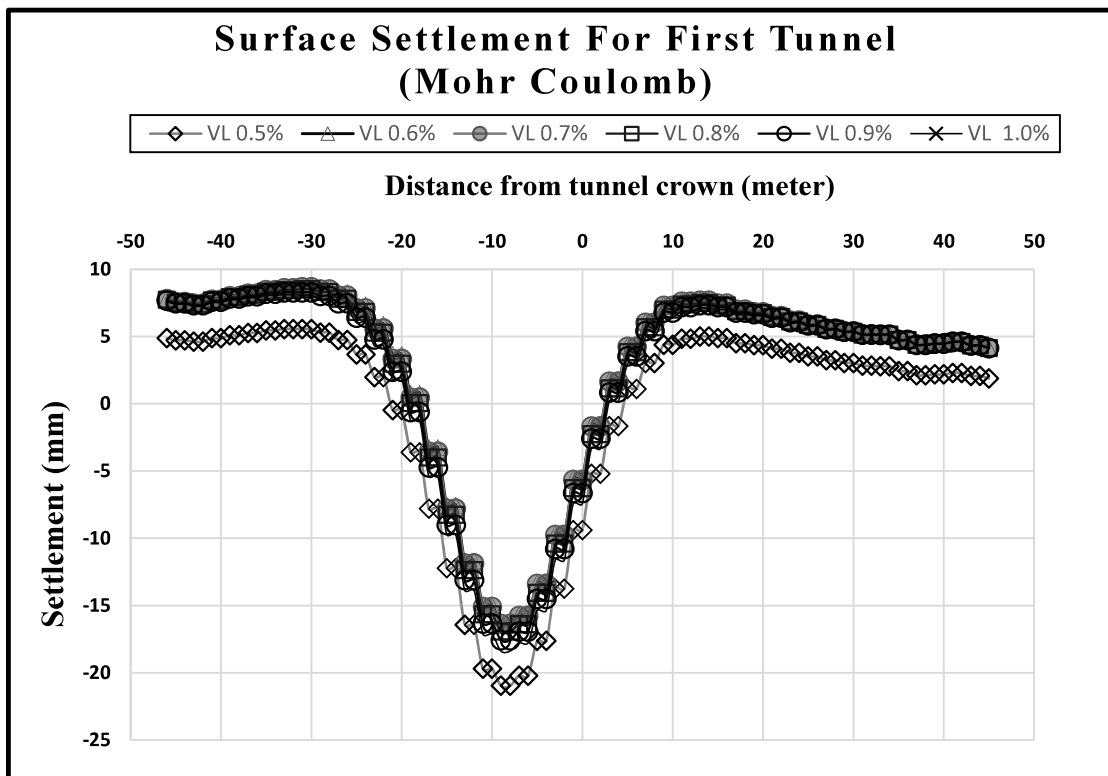


Figure 4.1 Surface Settlement after the construction of first tunnel varying volume loss(Mohr-coulomb model)

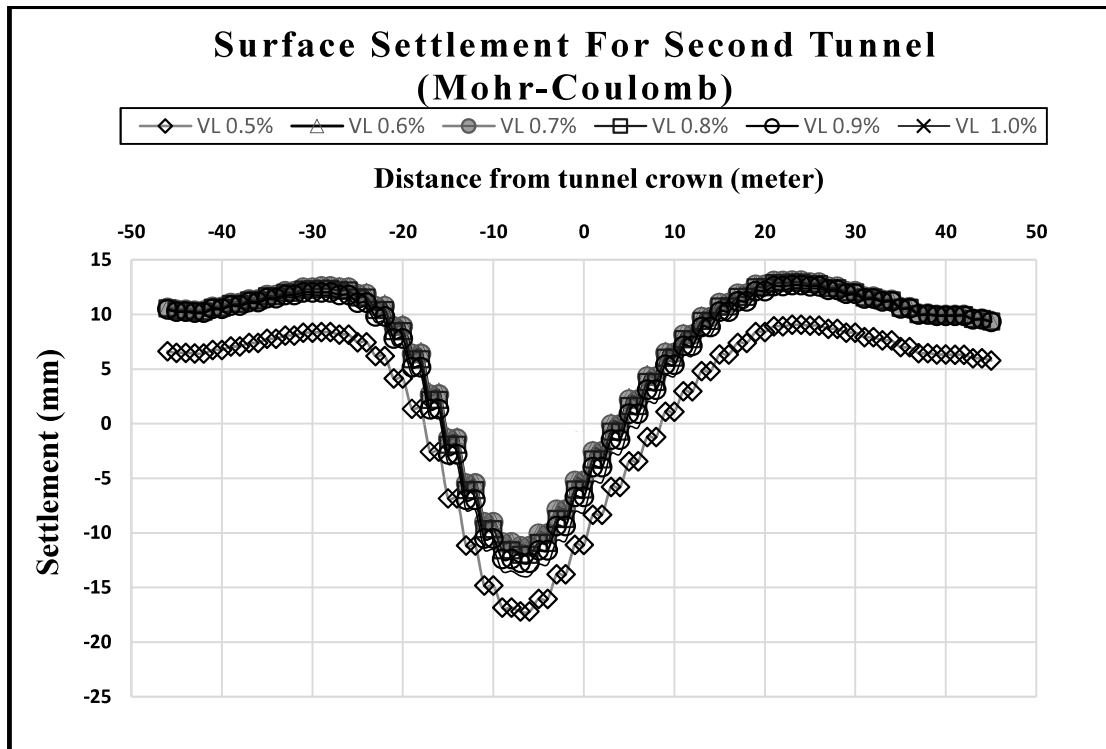


Figure 4.2 Surface Settlement after the construction of second tunnel varying volume loss(Mohr-coulomb Model)

With the increasing value of contraction, the surface settlement increases for the first tunnel lining installation stage. But soil heaving is also observed for the almost all the cases. But the settlement is reduced while installing the second tunnel lining which is not practical or realistic. As the higher value of contraction means excess removal of soil, the settlement should also be higher in respective cases. In Mohr-Coulomb model, it is not possible to capture the loading and unloading behavior, so the analysis is not able to capture the real-life excavation problems.

4.2.2 Hardening Soil Model

The surface settlement for varying volume loss (0.5% to 1.0 %) is also analyzed in hardening soil model. The surface settlement during the first and second tunnel lining installation has been plotted in the graphs and shown in **Fig 4.3** and **Fig 4.4**.

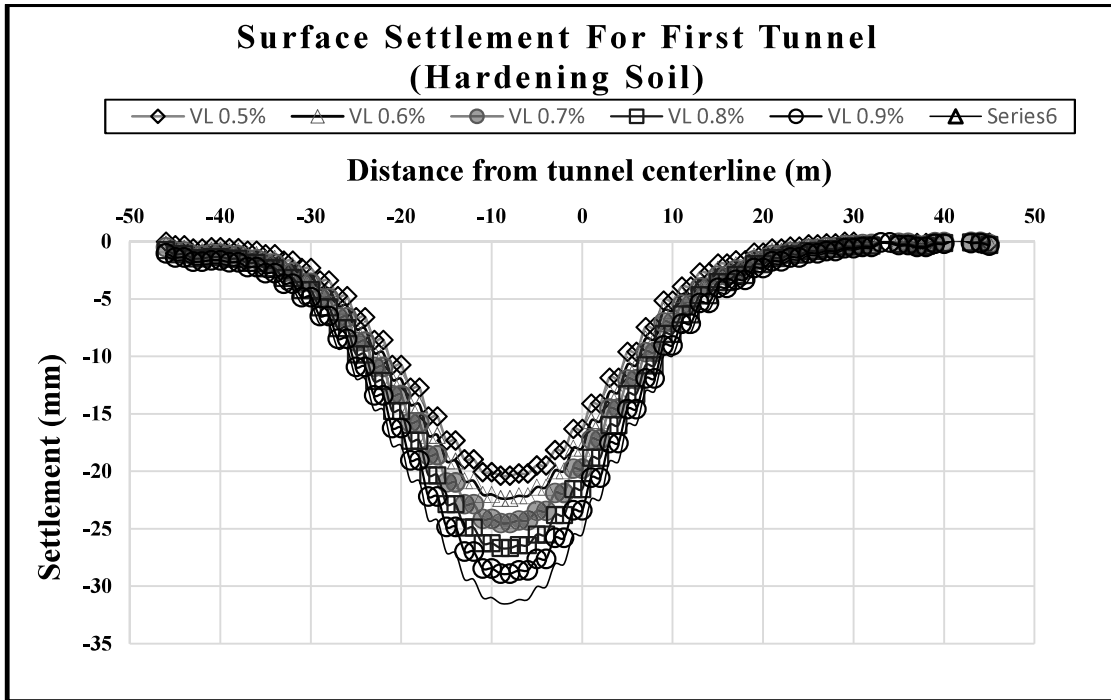


Figure 4.3 Surface Settlement after the construction of second tunnel varying volume loss(Hardening Soil Model)

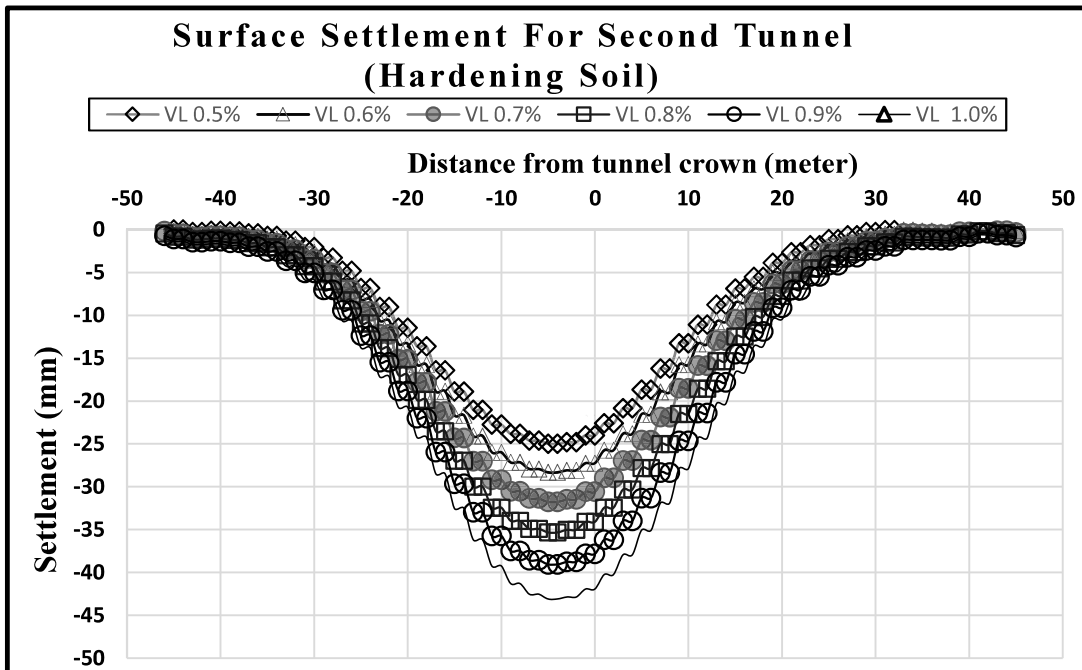


Figure 4.4 Surface Settlement after the construction of second tunnel varying volume loss(Hardening Soil Model)

For both cases (first and second tunnel lining installation), the surface settlement values increase with the increment of contraction values. However, maximum settlement observed after the first tunnel lining installation is 31mm (for 1% volume loss) and for second tunnel lining is 43mm (for 1% volume loss).

4.2.3 Subloading- t_{ij} Model

The surface settlement for varying volume loss (0.5% to 1.0 %) is also analyzed in hardening soil model. The surface settlement during the first and second tunnel lining installation has been plotted in the graphs and shown in **Fig 4.3** and **Fig 4.4**.

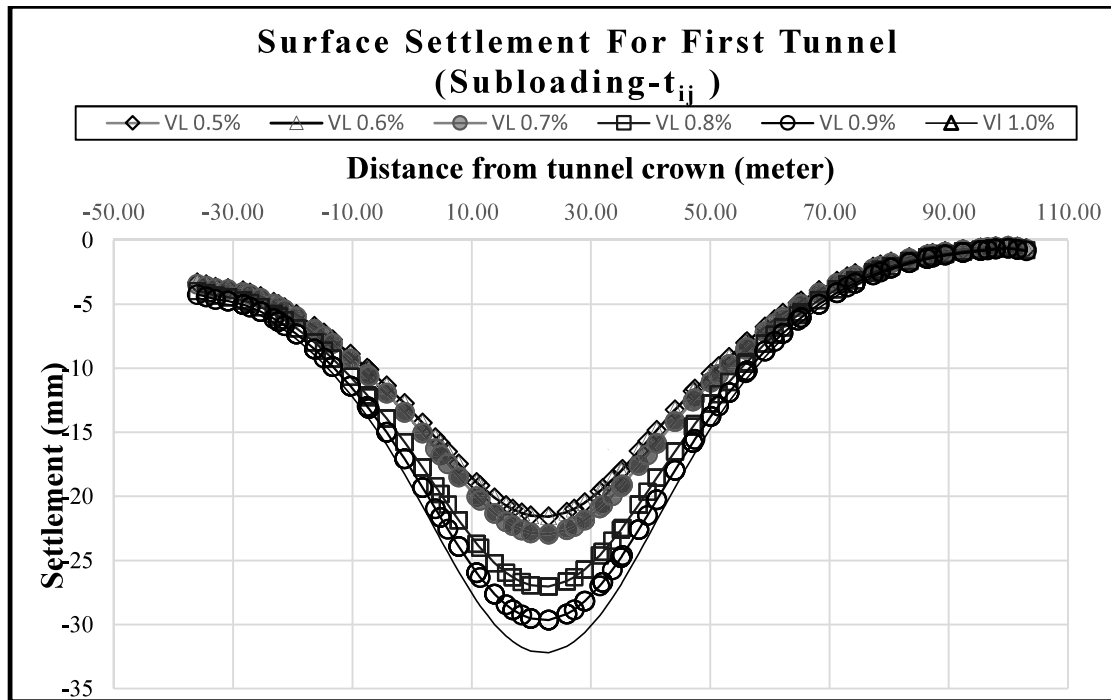


Figure 4.5 Surface Settlement after the construction of second tunnel varying volume loss (Subloading t_{ij} model)

For both cases (first and second tunnel lining installation), the surface settlement values increase with the increment of contraction values. However, maximum settlement observed after the first tunnel lining installation is 32mm (for 1% volume loss) and for second tunnel lining is 57mm (for 1% volume loss).

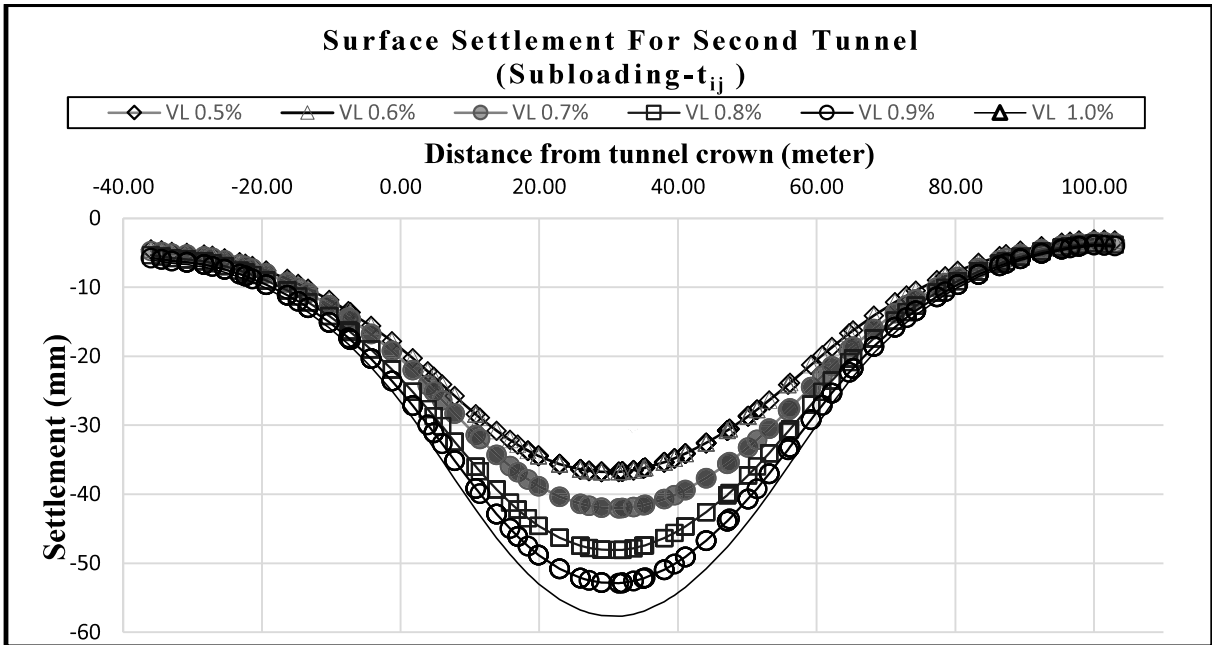


Figure 4.6 Surface Settlement after the construction of second tunnel varying volume loss (Subloading- t_{ij} model)

4.2.4 Settlement Data Comparison

As the volume loss for shield tunnel is assumed 0.5% at site, a comparison graph has been plotted in Fig 4.7 and Fig 4.8.

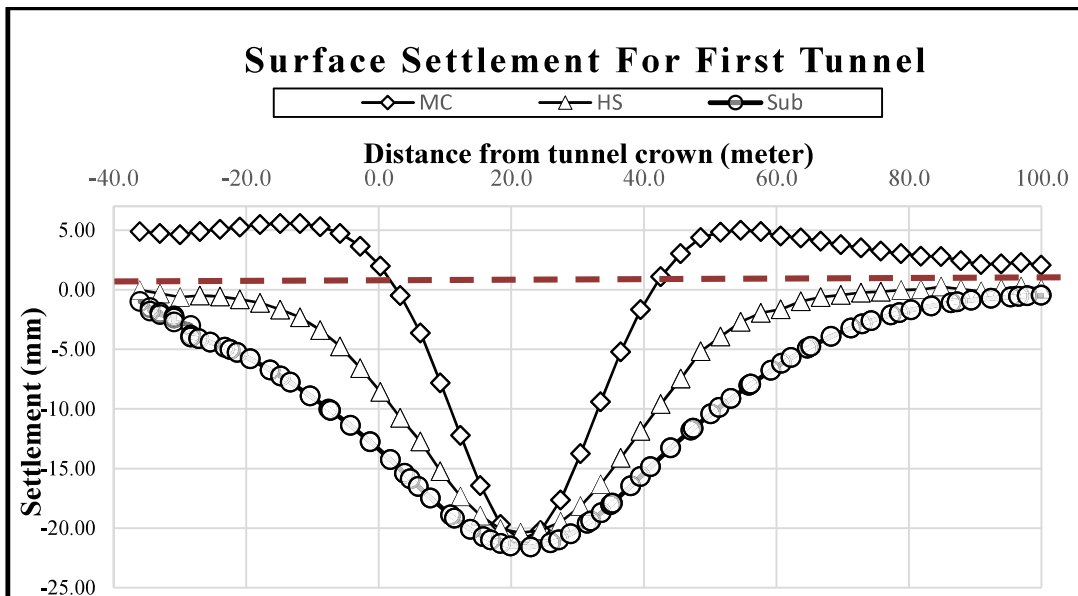


Figure 4.7 Surface Settlement after the construction of first tunnel for 0.5% volume loss

In the **Fig 4.7**, after the first tunnel construction , the maximum settlement is observed for Subloading- t_{ij} model and minimum settlement is observed for Hardening soil model. In Mohr-coulomb model, soil heaving phenomena has been observed.

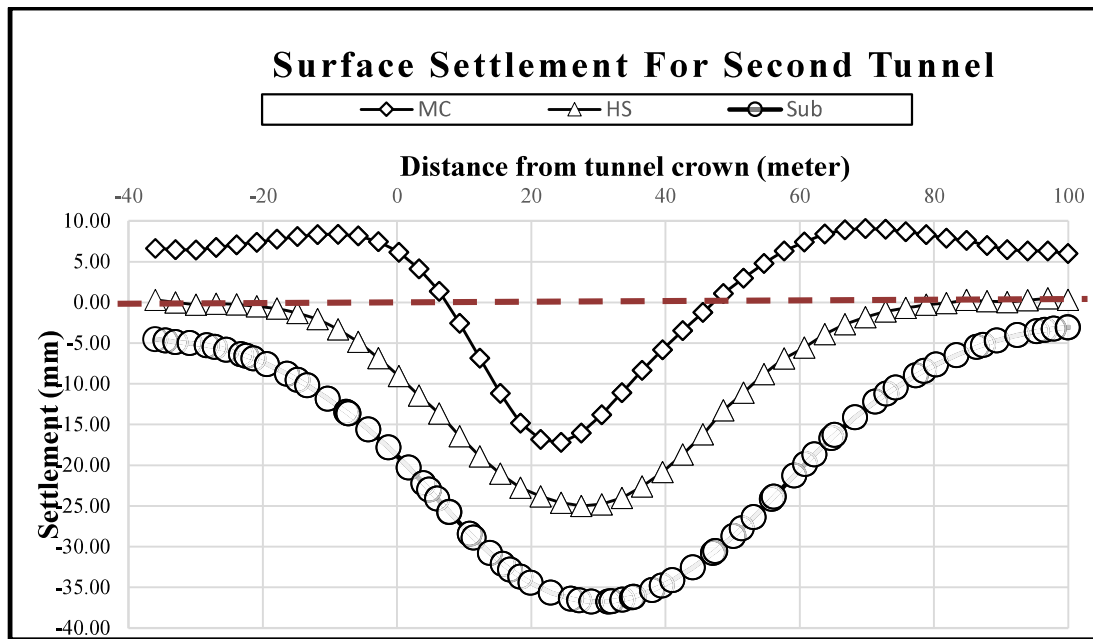


Figure 4.8 Surface Settlement after the construction of second tunnel for 0.5% volume loss

In the **Fig 4.8**, after the second tunnel construction ,the maximum settlement is again observed for Subloading- t_{ij} model and minimum settlement is observed for Hardening soil model. However, in Mohr-coulomb model, the settlement values actually decreased and soil heaving has been observed. To compare the values more properly, a summary of settlement values is provided in **Table 4.1**

Table 4.1. Final Settlement(in mm) for 0.5% Volume loss

Tunnel	MC	HS	Subloading- t_{ij}	Analytical	Field Monitoring
After First Tunnel Construction	-20.97	-20.39	-21.58	-16	-11
After Second Tunnel Construction	-17.20	-24.79	-36.69		-25

In the **Table 4.1**, the negative value is denoting the falling or settlement value of the ground. As it can be seen from the above summary table, the Mohr-coulomb(MC) model settlement values gets reduced after the second tunnel construction which is not a realistic behaviors of the ground. On the other hand, the Subloading- t_{ij} model overestimates the settlement value much higher than the analytical or field monitoring data. The most accurate settlement result is predicted by the Hardening soil model in the analysis. As the slurry shield tunneling method was used in Karnaphuli Tunnel with 0.5% volume loss, the comparison has been shown only this specific volume loss for better understanding of the settlement phenomena. With the increment of volume loss, the surface settlement increases linearly which has been discussed in other graphs.

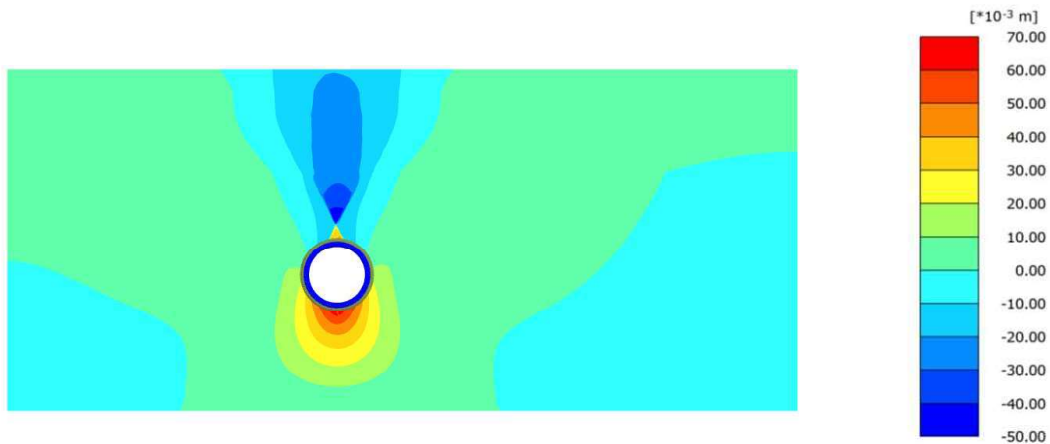
4.3 Ground Stress and Strain Analysis During Tunnel Construction

It can be noticed that, for the contraction and volume loss of 0.5%, the settlement matches with the field monitoring value. The other values of contraction were taken for verification but not included because of the long range of results for all the reasonable values. However, in this section, the contour plot from the fem analysis for different constitutive models has been discussed. The effect of construction sequences can be explained in a much better way through these diagrams.

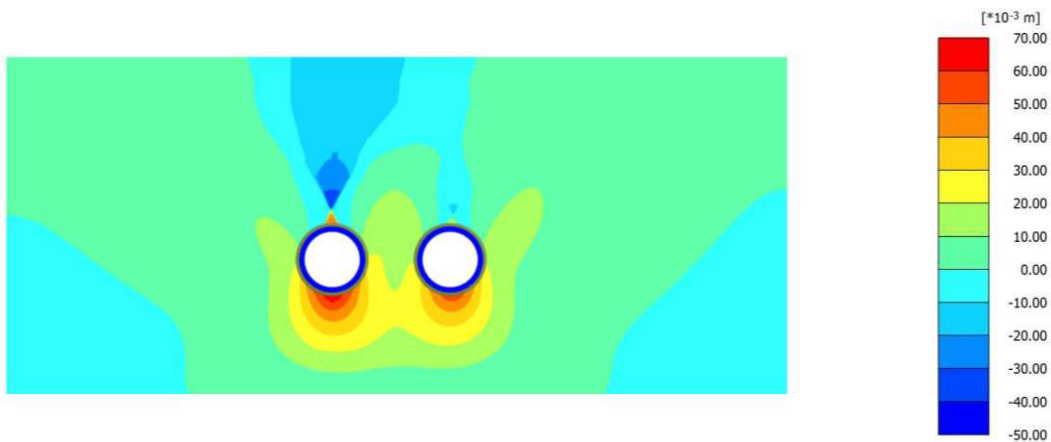
4.3.1 Mohr Coulomb Model

4.3.1.1 Ground Displacement During the Construction

Tunnel excavation disturbs the existing ground condition. The ground behavior changes mostly on the volume loss during the excavation activities. The ground displacement during the tunnel construction has been shown in **Fig 4.9**:



a) After first tunnel lining installation

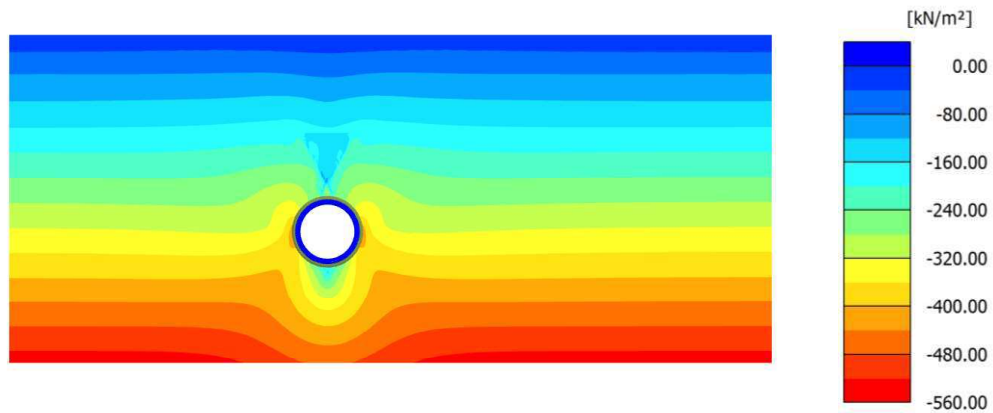


b) After second tunnel lining installation

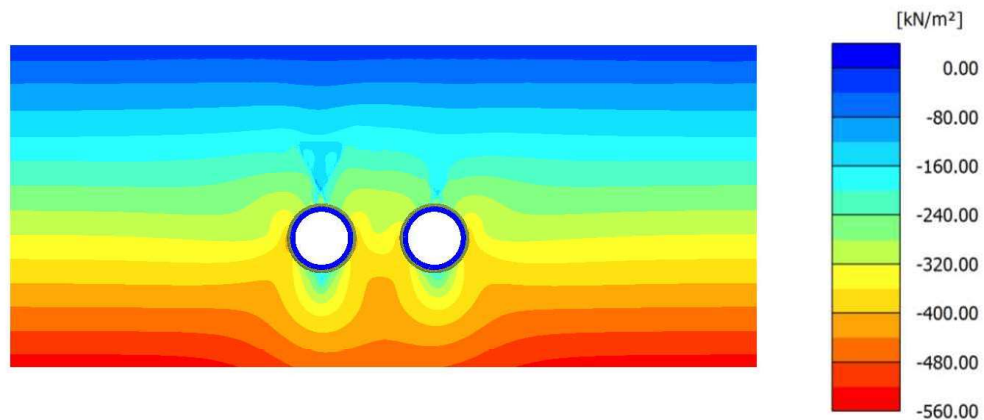
Figure 4.9 Ground Displacement during the construction phases of the tunnel

The maximum surface after the first tunnel construction is observed 26.0mm and after the second tunnel construction it is found 41.0mm. From the above figure it is clearly visible that with the advancement of tunnel excavation works, the surface settlement did not change that much but the bottom of the tunnel had higher displacement.

4.3.1.2 Effective Stress Analysis



a) Effective Stress during the excavation of first tunnel



b) Effective Stress during the excavation of Second tunnel

Figure 4.10. Ground Stress Analysis tunnel Construction(a,b)

The maximum effective stress in the ground after the first tunnel construction is observed 540 kN/m² and after the second tunnel construction it is 541 kN/m². That the distance between the tunnels has remained relatively constant suggests that the tunnel construction can be carried out without much disturbance and no additional grouting or other improvement is required during construction.

4.3.1.3 Excess Pore Pressure During Excavation

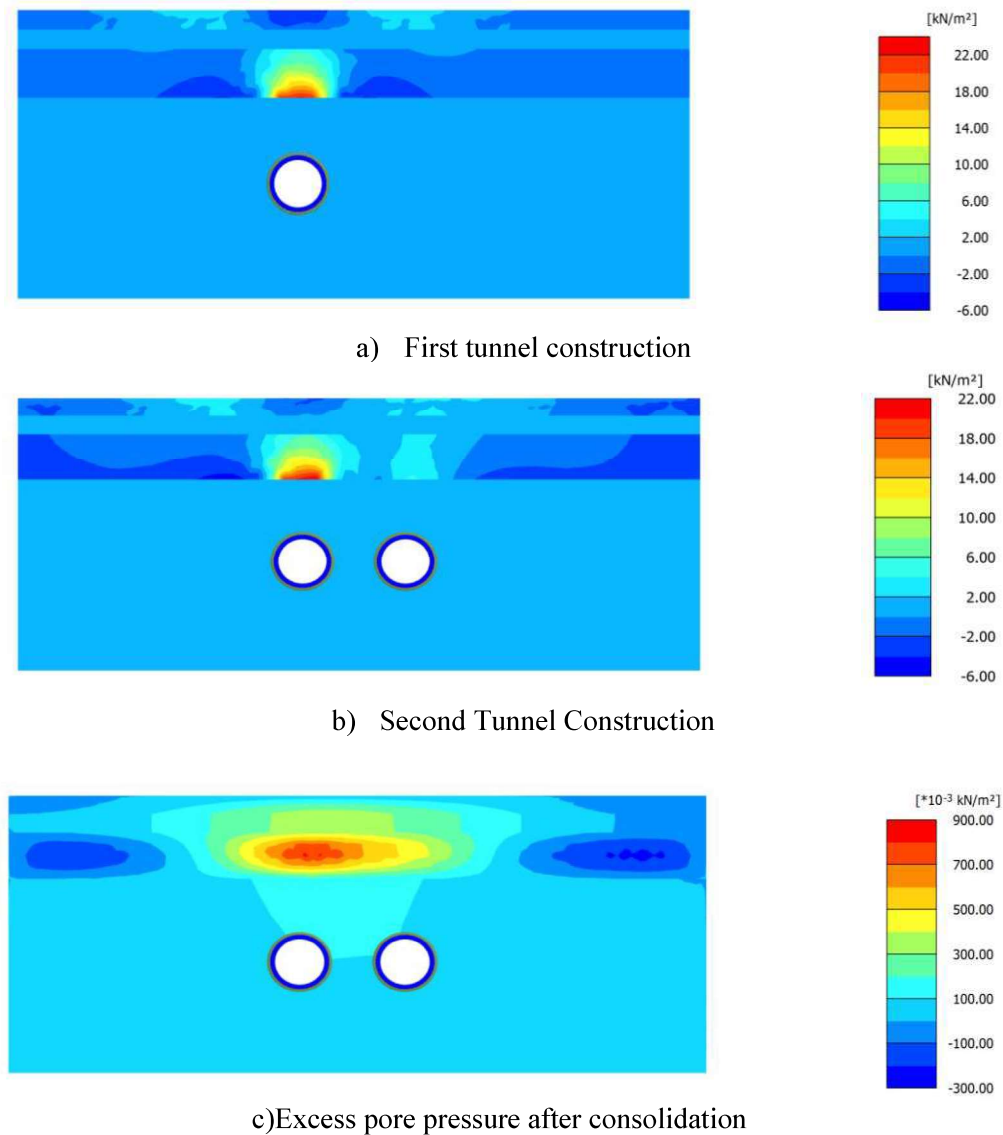
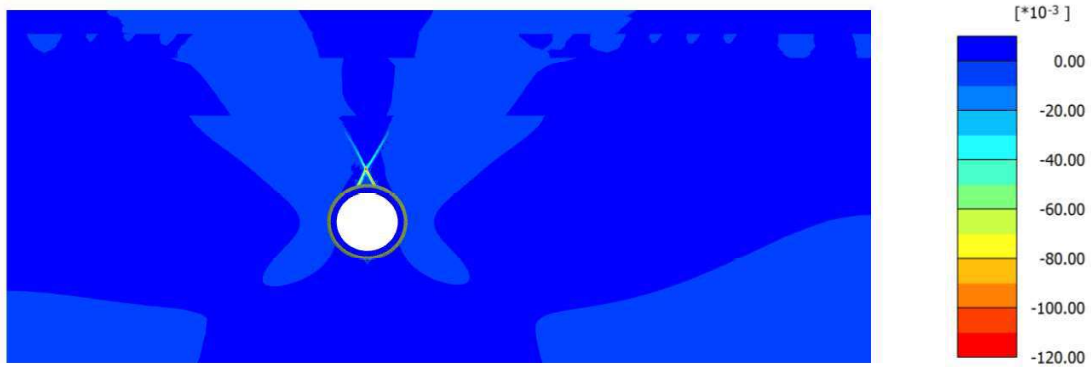


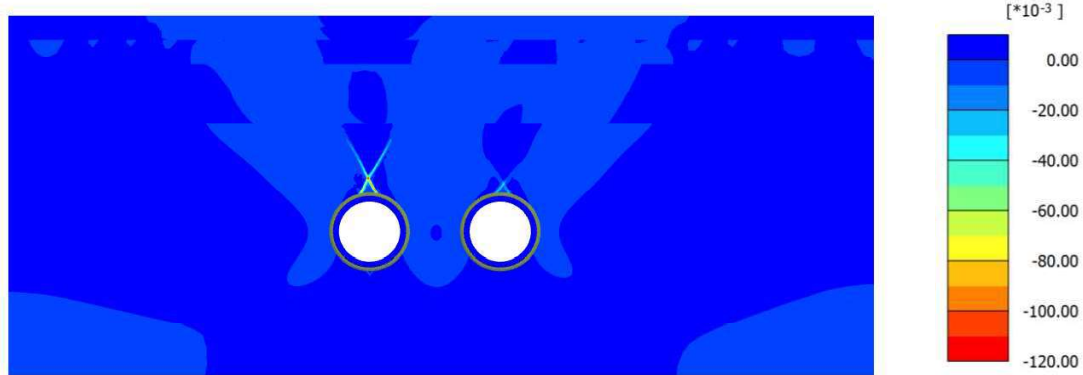
Figure 4.11. Excess pore pressure during tunnel Construction(a,b,c)

From the above figure it is seen that with the pore water pressure mainly generated at the clay layer (undrained condition). The maximum pore water pressure generated after the construction of first tunnel is 22 kN/m^2 and after the second tunnel construction value remains the same. After the consolidation, the excess pore pressure values reduce to almost zero.

4.3.1.4 Total Strain during construction



a) Total strain during the installation of first tunnel lining



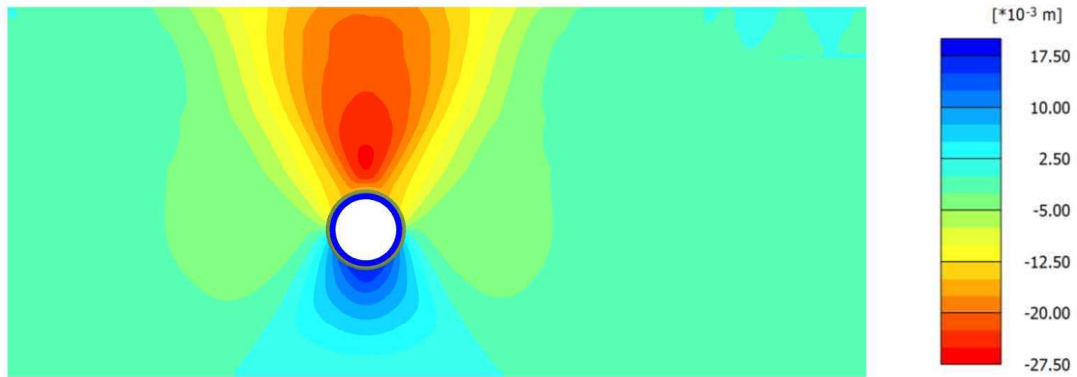
b) Total strain during the installation of second tunnel lining

Figure 4.12. Variation of ground strain during tunnel construction

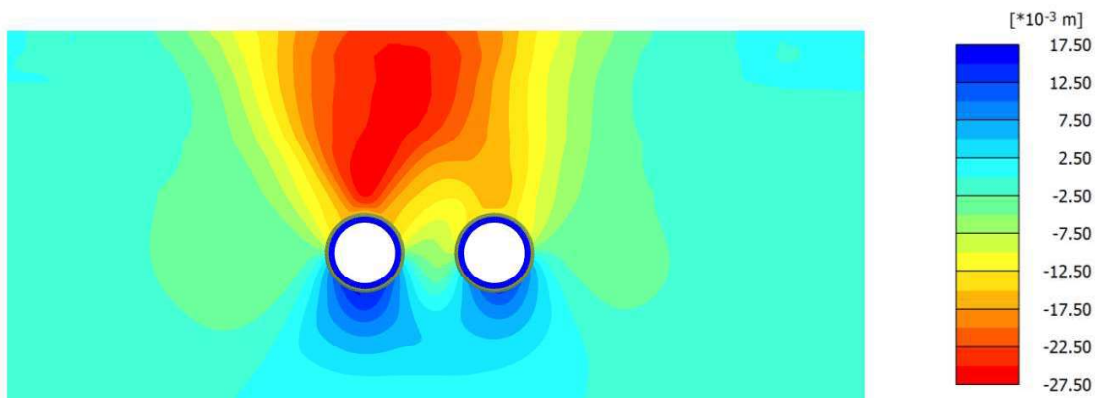
The ground strain value ranges from -0.1194 to $9.827e-3$ during the first tunnel lining installation and for second tunnel lining installation, the value ranges from -0.1196 to $9.5e-3$. However, the variation in ground strain due to tunnel excavation is not significantly visible in the Mohr-coulomb model.

4.3.2 Hardening Soil Model

4.3.2.1 Ground Displacement During the Construction



a) After first tunnel lining installation

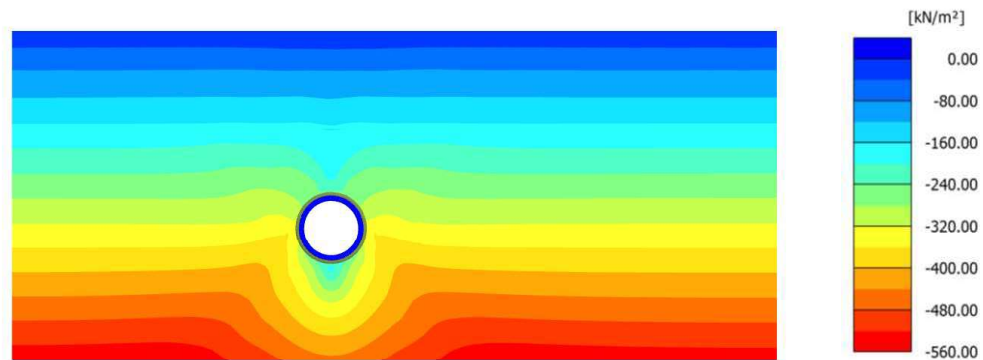


b) After second tunnel lining installation

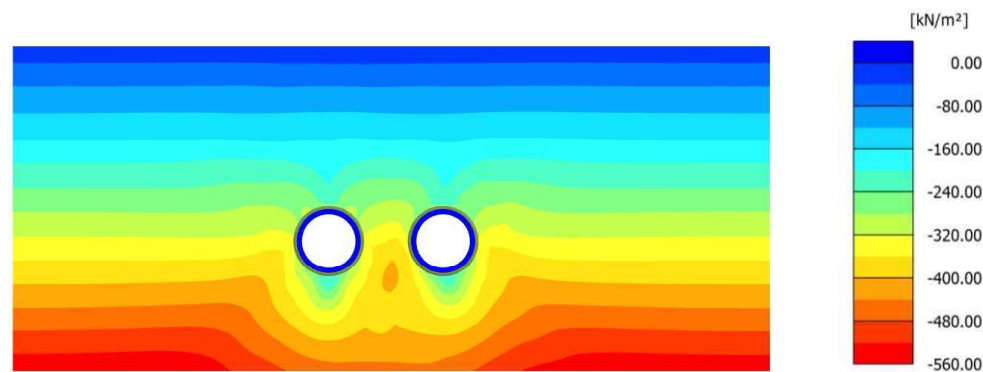
Figure 4.13. Variation of ground strain during tunnel construction

The maximum surface after the first tunnel construction is observed 25.50mm and after the second tunnel construction settlement is found 26.54mm. From the above figure it is clearly visible that with the advancement of tunnel excavation works, the surface settlement increases the area of influence as well have increased to a significant level. However, the maximum deformation occurred right above the tunnel crowns.

4.3.2.2 Effective Stress Analysis



a) Effective Stress during the excavation of first tunnel



b) Effective Stress during the excavation of first tunnel

Figure 4.14. Ground Stress Analysis tunnel Construction(a,b)

The maximum effective stress in the ground after the first tunnel construction is observed 551 kN/m^2 and after the second tunnel construction it is 554 kN/m^2 . According to these numbers, there is a sufficient amount of space between each tunnel for the construction works and no additional grouting or other improvement is required during construction. Also, the stress transfer in the soil due to the arching effect for deep excavation works can be interpreted from the above diagrams. It is apparent that the effective stress generated at the first tunnel crown ranges from 160 kN/m^2 to 220 kN/m^2 and for the second tunnel, the value remains the same. This stress helps the soil to provide the support during excavation works.

4.3.2.2 Excess Pore Pressure During Excavation

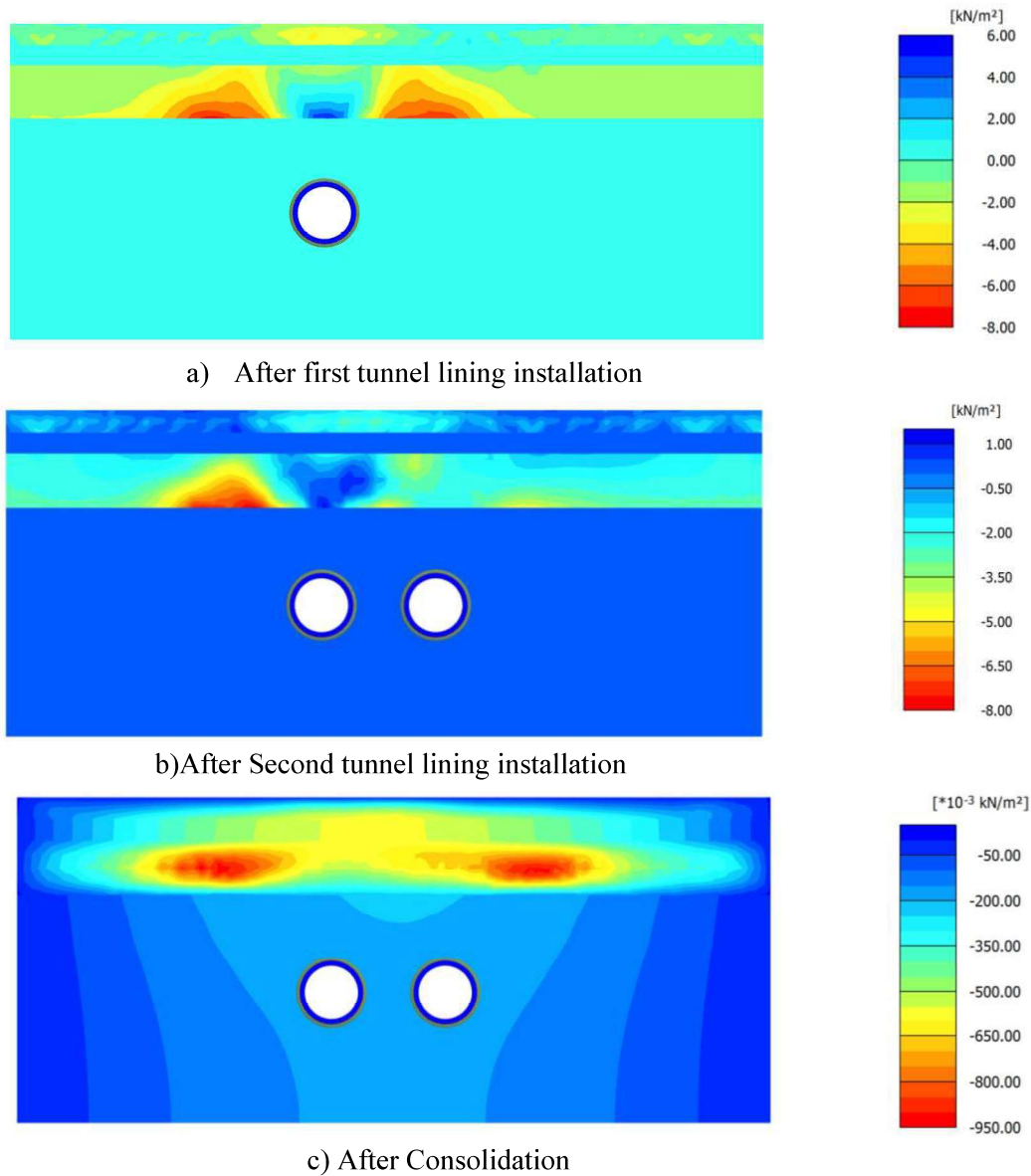


Figure 4.15. Excess pore pressure during tunnel Construction(a,b,c)

From the above figure it is seen that with the pore water pressure mainly generated at the clay layer(undrained condition).The maximum pore water pressure generated after the construction of first tunnel is 7.48 kN/m^2 and after the second tunnel construction value remains the same. After the consolidation, the excess pore pressure values reduces to almost zero.

4.3.2.2 Total Strain during construction

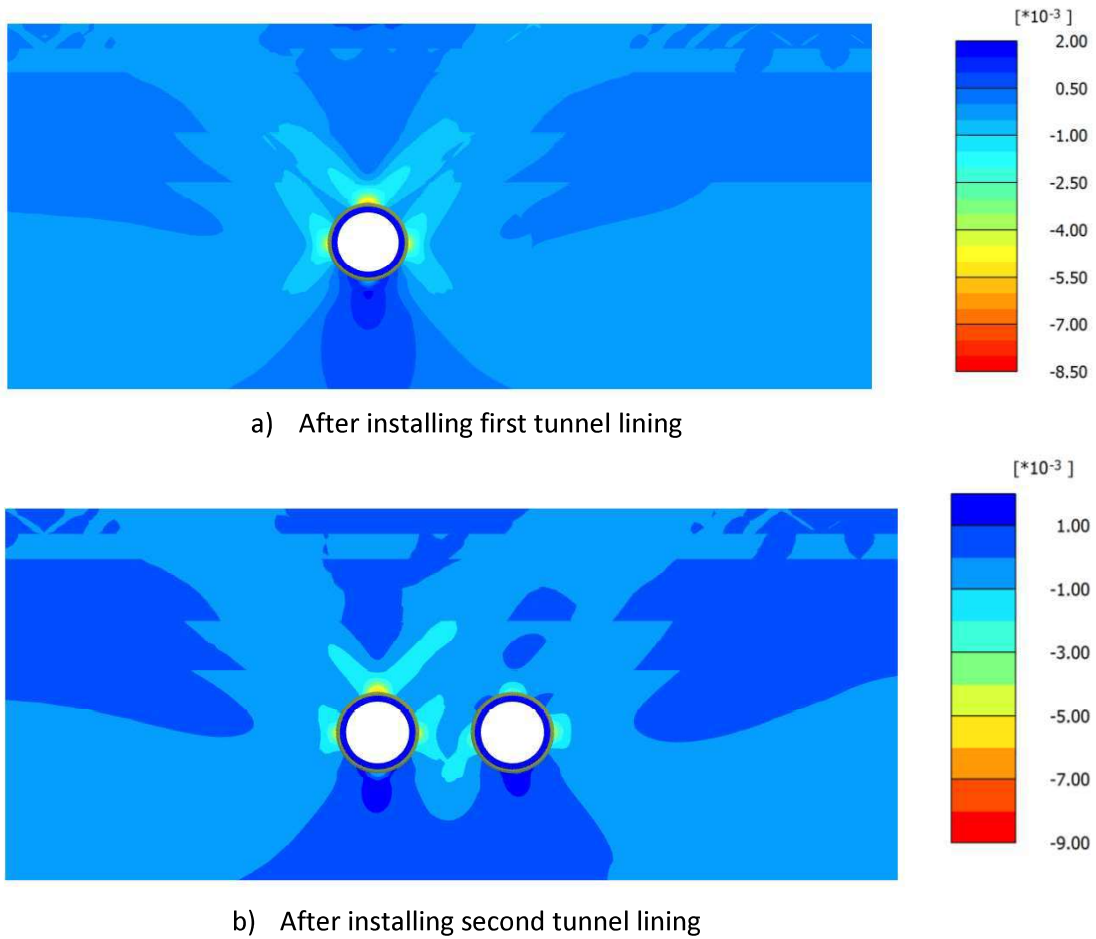
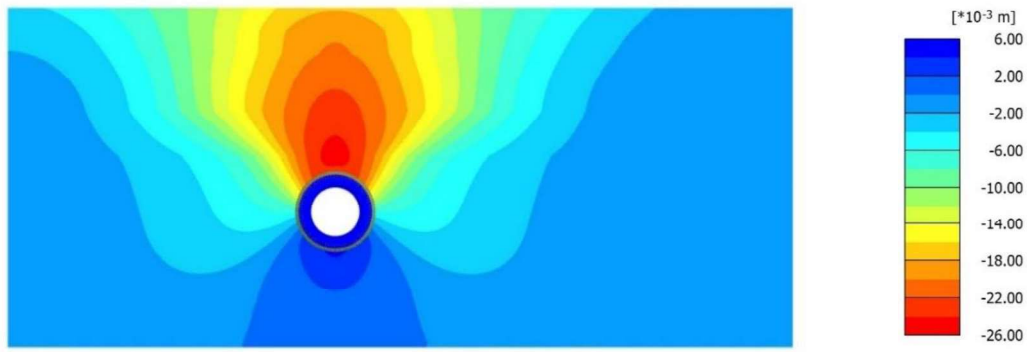


Figure 4.16. Total strains during the construction of the tunnel

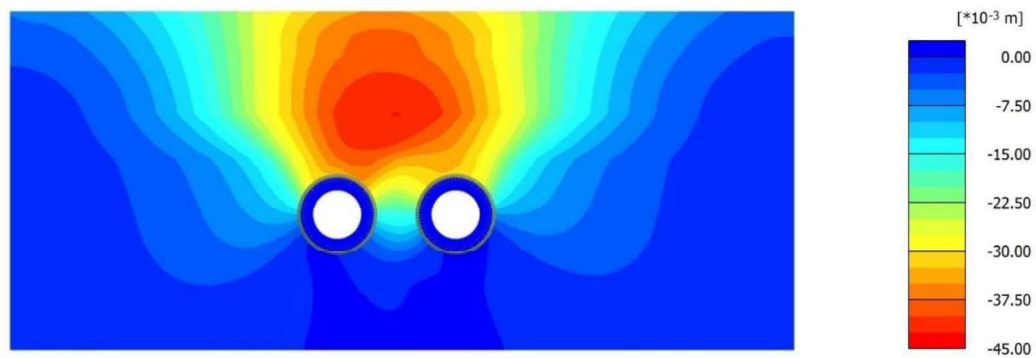
The ground strain value ranges from -8.352×10^{-3} to 1.613×10^{-3} during the first tunnel lining installation and for second tunnel lining installation, the value ranges from -8.6×10^{-3} to 1.536×10^{-3} . The strain value is higher at the tunnel crown both sides of the tunnel lining. The strain generated due to the huge overburden pressure above the tunnel crown which is responsible for the ovalisation of the lining of the following tunnel.

4.3.3 Subloading- t_{ij} Soil Model

4.3.3.1 Ground Displacement During the Construction



a) After first tunnel lining installation

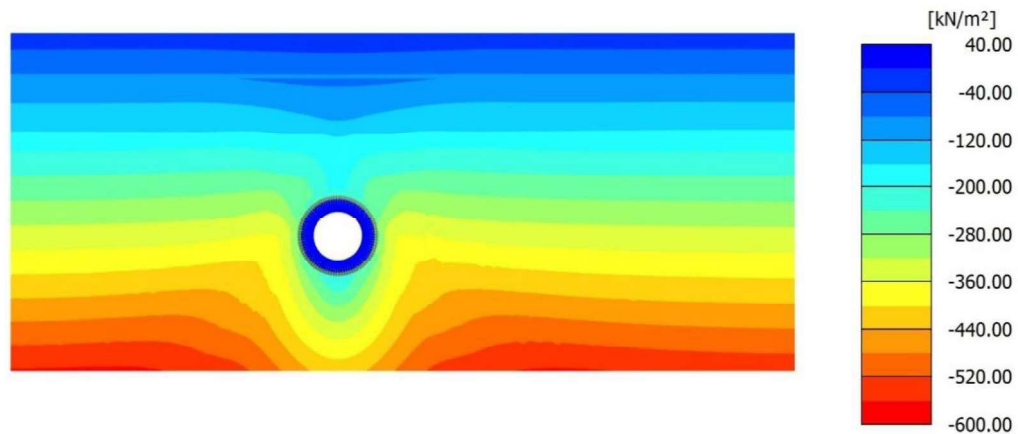


b) After second tunnel lining installation

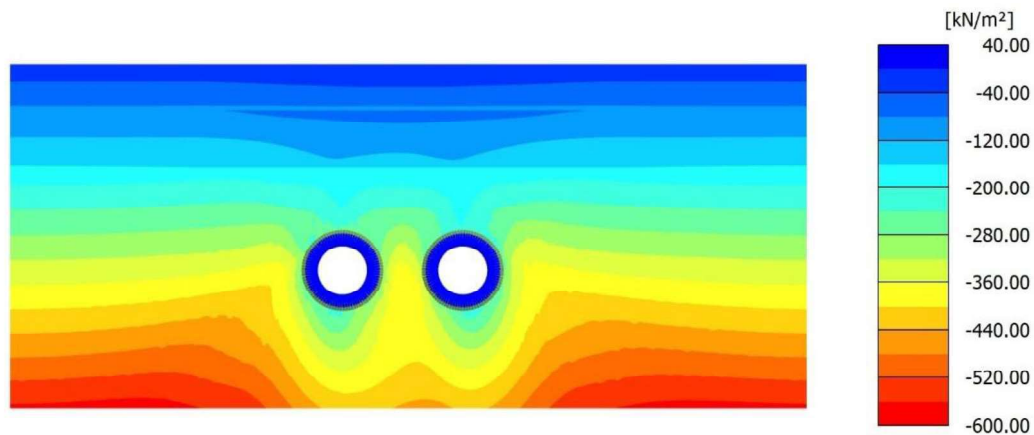
Figure 4.17. Total strains during the construction of the tunnel

The maximum surface after the first tunnel construction is observed 25.14mm and after the second tunnel construction settlement is found 35.5mm. From the above figure it is clearly visible that with the advancement of tunnel excavation works, the surface settlement increases the area of influence as well have increased to a significant level. However, the maximum deformation occurred right above the tunnel crowns.

4.3.2.2 Effective Stress Analysis



a) Effective Stress during the excavation of first tunnel



b) Effective Stress during the excavation of first tunnel

Figure 4.18. Effective stress during tunnel construction

The maximum effective stress in the ground after the first tunnel construction is observed 551 kN/m^2 and after the second tunnel construction it is 554 kN/m^2 . According to these numbers, there is a sufficient amount of space between each tunnel for the construction works and no additional grouting or other improvement is required during construction. Also, the stress transfer in the soil due to the arching effect for deep excavation works can be interpreted from the above diagrams. It is apparent that the effective stress generated at the first tunnel crown ranges from 160 kN/m^2 to 220 kN/m^2 and for the second tunnel, the value remains the same. This stress helps the soil to provide the support during excavation works.

4.3.2.2 Excess Pore Pressure During Excavation

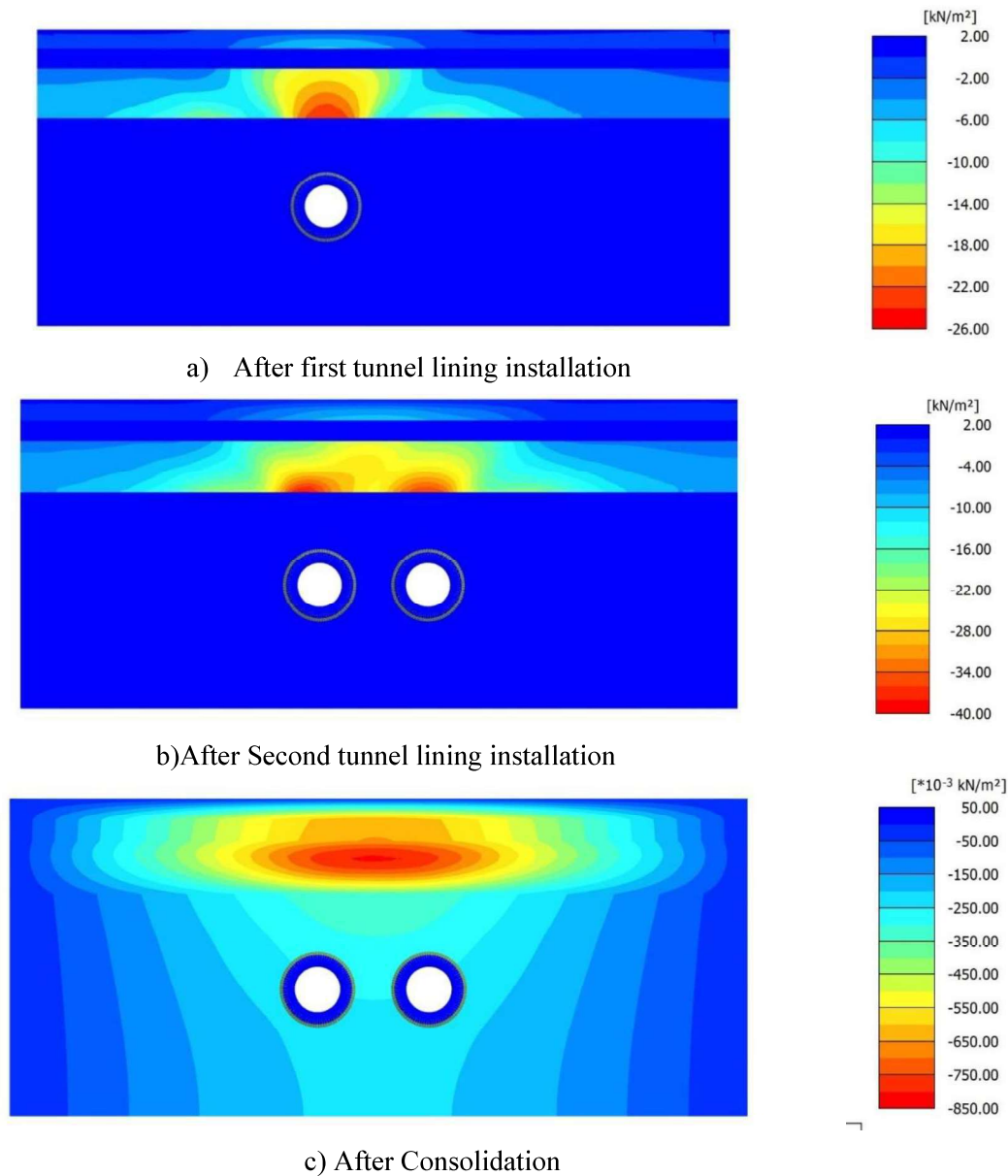


Figure 4.19. Excess pore pressure during tunnel construction

From the above figure it is seen that with the pore water pressure mainly generated at the clay layer (undrained condition). The maximum pore water pressure generated after the construction of first tunnel is 24.0 kN/m^2 and after the second tunnel construction value is 38.61 kN/m^2 , which is higher than the Mohr-Coulomb and hardening soil model. After the consolidation, the excess pore pressure values reduce to almost zero.

4.3.2.2 Total Strain during construction

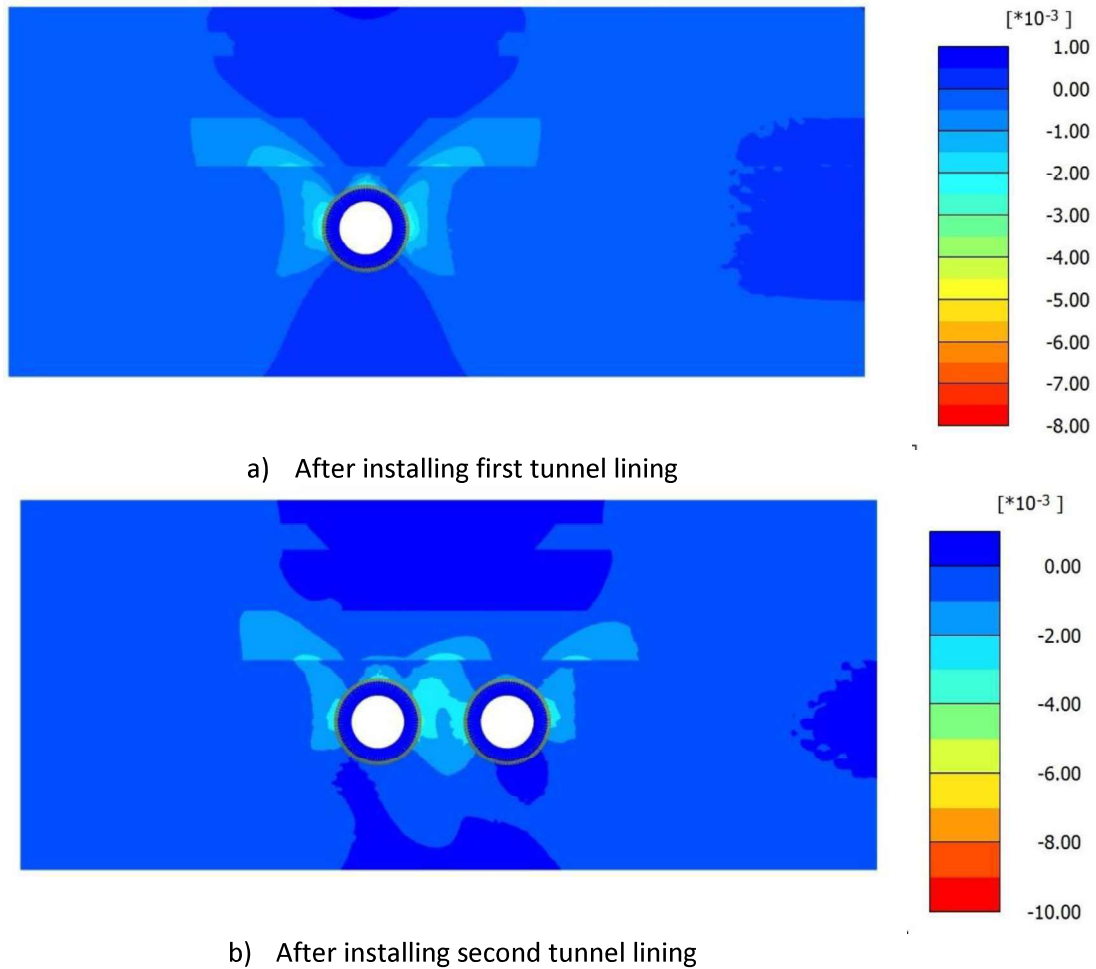


Figure 4.20. Variation of strain during tunnel construction

The ground strain value ranges from -7.618×10^{-3} to 0.5613×10^{-3} during the first tunnel lining installation and for second tunnel lining installation, the value ranges from -9.4×10^{-3} to 0.811×10^{-3} . The strain value is higher at the tunnel crown both sides of the tunnel lining. The strain generated due to the huge overburden pressure above the tunnel crown which is responsible for the ovalisation of the tunnel lining.

4.4 Tunnel Lining Analysis

The tunnel lining forces have been evaluated for the “wish in place” condition. The variation of forces is observed for different soil constitutive model. Maximum bending moment is observed for mohr-coulomb model while hardening soil and subloading -t_{ij} model shows lesser values. Comparative graphs of bending moments, axial forces, shear forces and lining deformations are shown in **Fig 4.21** through **Fig 4.26** from analyses results after first and second tunnel lining installation.

4.4.1 Bending Moment Comparison

4.4.1.1 After first tunnel lining installation

A comparable graph of the bending moment after putting in the first liner for a tunnel shown in **Fig 4.21**. The graph clearly shows that the Mohr-coulomb model has the highest bending moment..

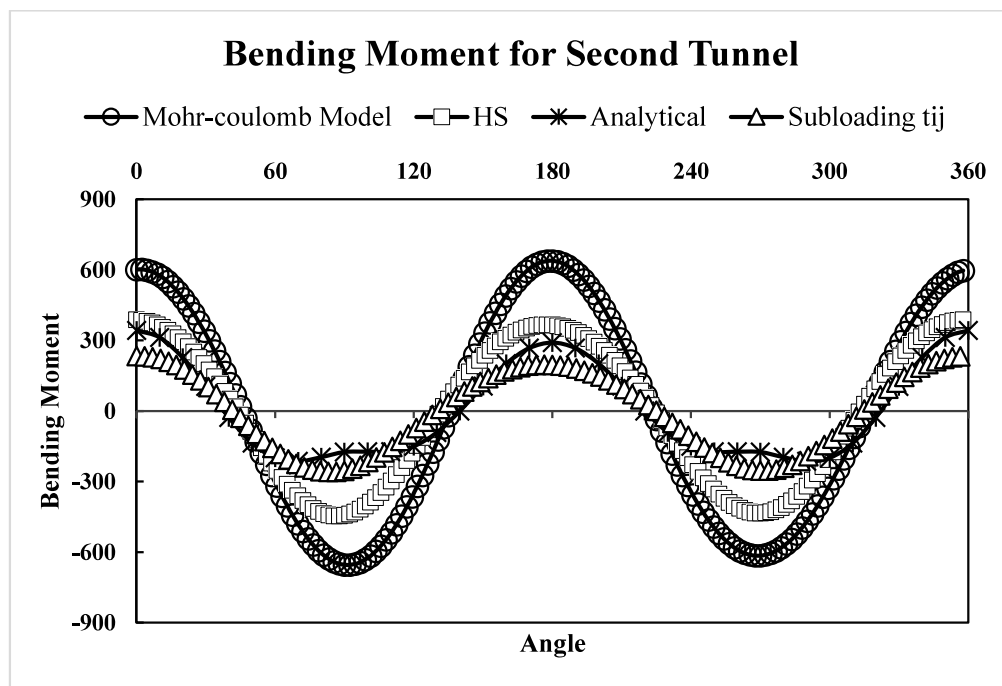


Figure 4.21. Bending Moment Diagram For First Tunnel Lining

Maximum negative moment observed in Mohr-coulomb model is 707 kN/m² and maximum positive moment is found 701 kN/m² . For hardening soil model the maximum

positive moment is observed 419 kN/m^2 and maximum negative moment is observed 410 kN/m^2 . For Subloading t_{ij} model the maximum positive moment is observed 232.46 kN/m^2 and maximum negative moment is observed 228 kN/m^2 . The analytical calculation shows the value maximum positive moment 342.98 kN/m^2 and maximum negative moment 338.98 kN/m^2 .

4.4.1.2 After second tunnel lining installation

Fig 4.22 shows the comparable graph of the bending moment after the installation of second tunnel lining. It is evident from the graph that maximum bending moment is observed for the Mohr-coulomb model.

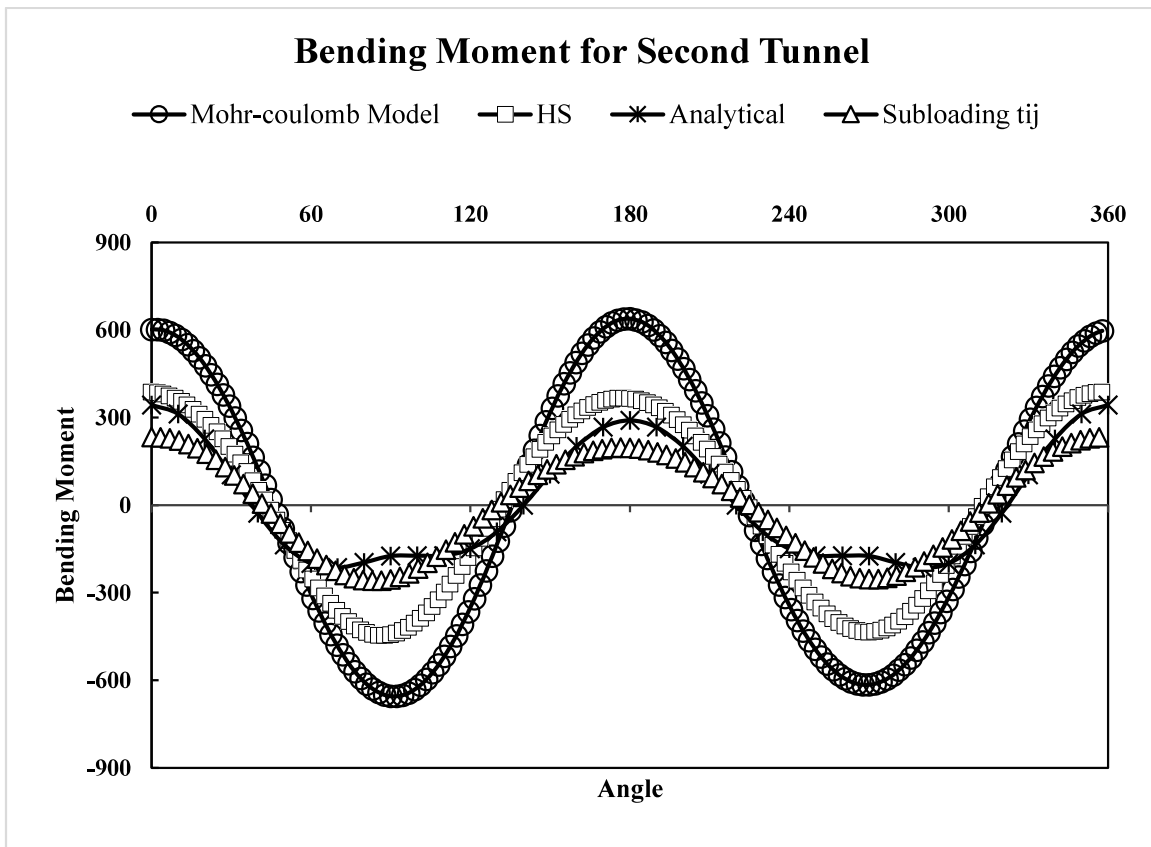


Figure 4.22. Bending Moment Diagram for Second Tunnel Lining

Maximum negative moment observed in Mohr-coulomb model is 638 kN/m^2 and maximum positive moment is found 631 kN/m^2 . For hardening soil model the maximum

positive moment is observed 387 kN/m^2 and maximum negative moment is observed 382 kN/m^2 . For Subloading t_{ij} model the maximum positive moment is observed 234.46 kN/m^2 and maximum negative moment is observed 222 kN/m^2 . The analytical calculation is same for both tunnel. The results shows that the second tunnel experience less bending moments than the first tunnel except Subloading $-t_{ij}$ model. As the ground already experienced variation of stress due to the construction of first tunnel, less stress is experienced during the second tunnel construction.

4.4.2 Shear Force Comparison

4.4.2.1 After first tunnel lining installation

A comparable graph of the shear forces after the installation of first tunnel lining shown in **Fig 4.23**. It is evident from the graph that maximum shear force is observed for the Mohr-coulomb model other than the analytical calculation.

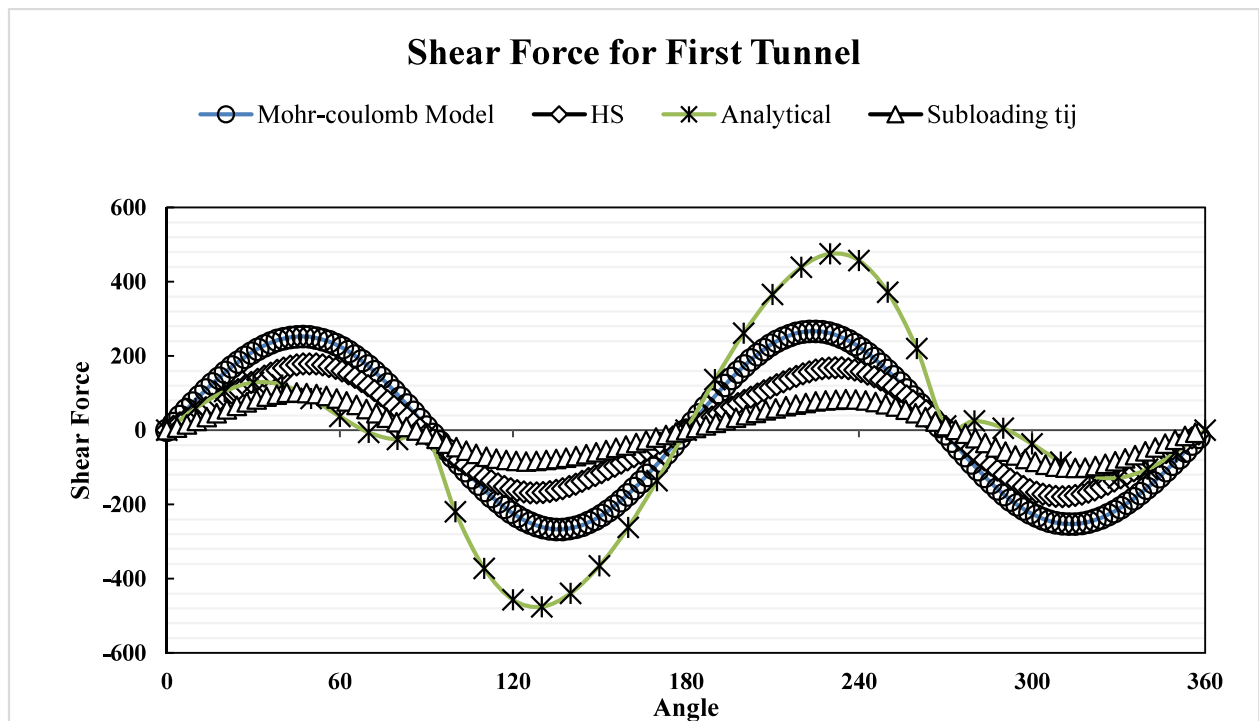


Figure 4.23. Shear forces comparison for First Tunnel Lining

Maximum shear force observed in Mohr-coulomb model is 226.88 kN , for hardening soil model the maximum shear force is observed 179.03 kN and for Subloading-

t_{ij} model the maximum shear force is observed 101.66 kN .The analytical calculation shows the value maximum shear force 475.46 kN .

4.4.2.2 After second tunnel lining installation

Fig 4.24 shows the comparable graph of the shear forces after the installation of second tunnel lining . It is evident from the graph that maximum shear force is observed for the Mohr-coulomb model other than the analytical calculation.

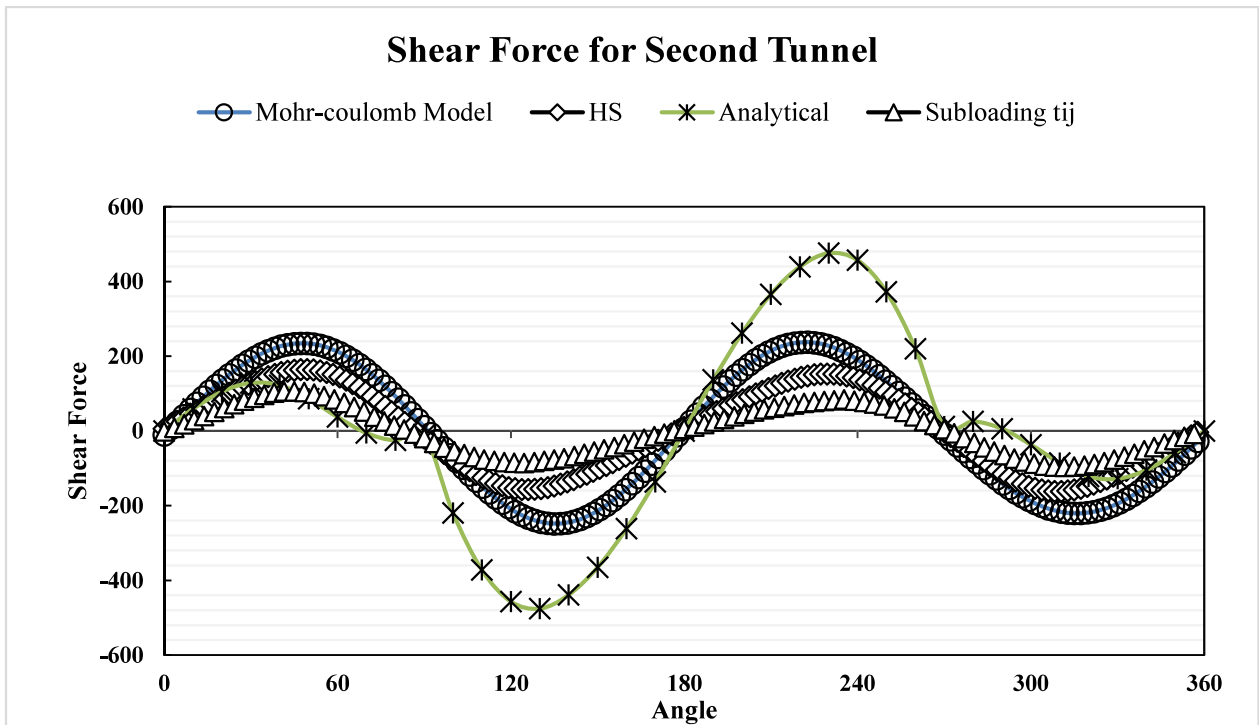


Figure 4.24. Shear Force Comparison for Second Tunnel Lining

The shear forces observed for the second tunnel at the final stage is 287.47 kN for the Mohr-coulomb model, 164.48 kN for the Hardening soil model, 106.21 kN for the Subloading-tij model and 475.46 kN for the Analytical model.

4.4.3 Axial Force Comparison

4.4.3.1 Axial Forces in First Tunnel Lining

A comparable graph of the axial forces after the installation of first tunnel lining shown in **Fig 4.24**. It is evident from the graph that maximum axial force is observed for the Mohr-coulomb model other than the analytical calculation.

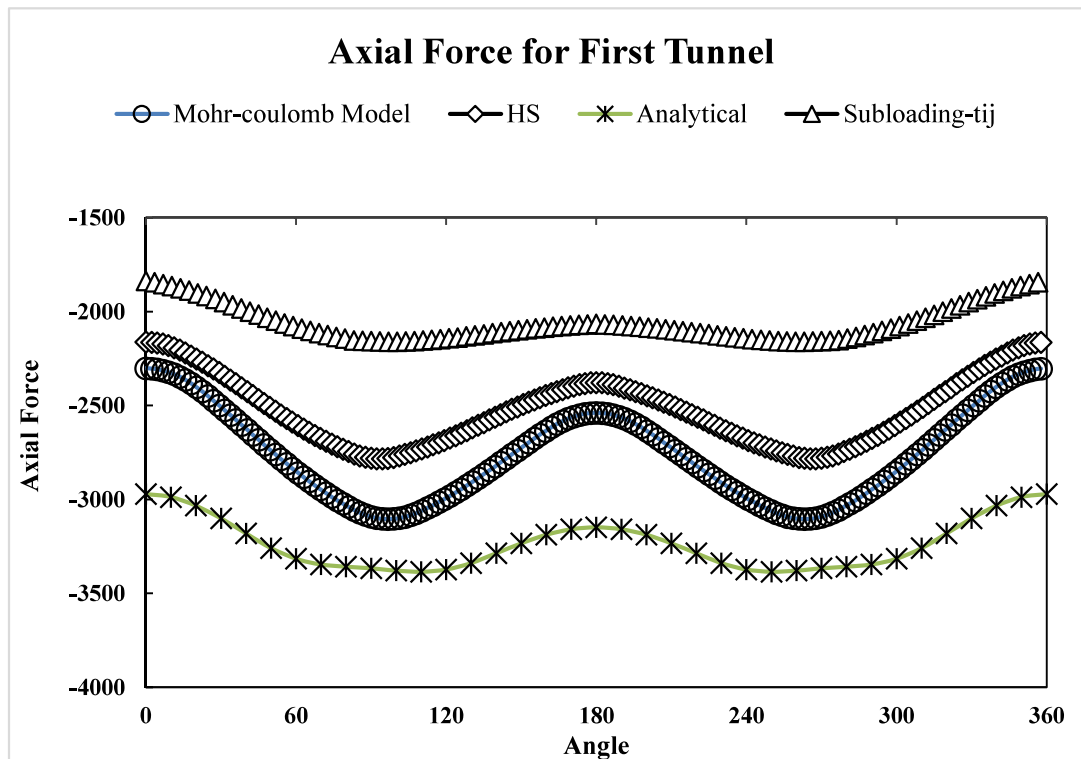


Figure 4.25. Axial forces for Mohr-coulomb model

The axial force of first tunnel lining at the final stage is 3104.73 kN for the Mohr-coulomb model, 2784.21 kN for the Hardening soil model, 2159.99 kN for the Subloading-tij model and 3385.51 kN for the Analytical model.

4.4.3.2 Axial Forces in Second Tunnel Lining

Fig 4.26 shows the comparative axial forces diagram for the analysis. The axial force of second tunnel lining at the final stage is 3091.86 kN for the Mohr-coulomb model, 2787.83 kN for the Hardening soil model, 2175.81 kN for the Subloading-tij model, and 3385.51 kN for the Analytical model.

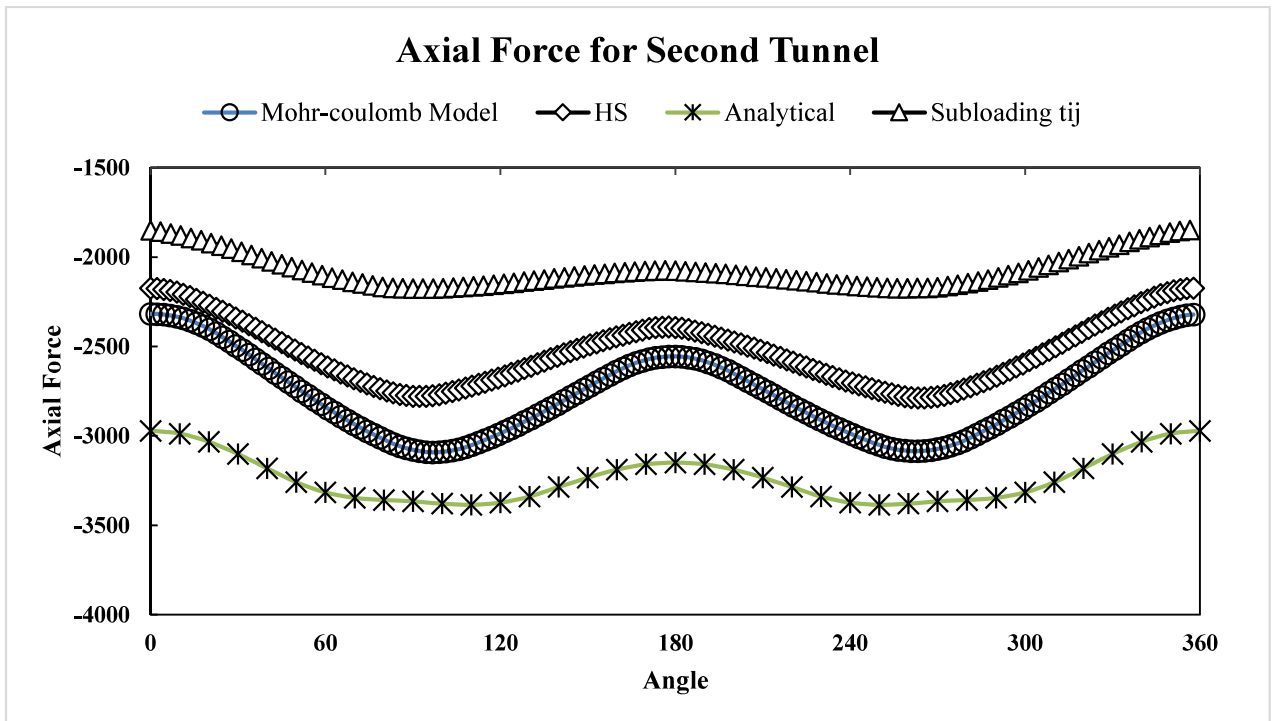


Figure 4.26. Axial forces for Mohr-coulomb model

CHAPTER 5: CONCLUSIONS AND RECOMMENDATIONS

5.1 General

This chapter includes the summary of the research findings based on discussions in **Chapter 4**. Moreover, recommendations and guideline for future work related to this investigation are also proposed in this chapter.

5.2 Conclusions

This research aims at both analytical and finite element approach for a specific section of underground tunnel. Based on the results, the following conclusions are drawn:

1. The maximum surface settlement value was observed for the Mohr-coulomb model while the Hardening Soil as well subloading t_{ij} settlement values were much more conservative and closer to the empirically calculated values. The constant stiffness in the Mohr-coulomb model leads to inappropriate modeling of the settlement trough where in Hardening soil model, the unloading reloading behaviour for the excavation problem is captured. For the subloading $-t_{ij}$ model, the surface settlement profile is similar with empirical profile but the settlement boundary was much bigger than other two constitutive model. For all three models, the maximum settlement occurred at the crown of the tunnel.
2. As the tunnel modelled in this research is a deep tunnel, arching effect of soil is observed for both tunnel in Hardening soil and Subloading t_{ij} model. In the Mohr-coulomb model, the change in stress concentration is very less visible which concludes that, the excavation sequence cannot properly be captured in this model.

3. Soil stress for the circular tunnel changes around the tunnel lining uniformly for all the models. No concentrated stress is actually formed which will provide less complexity during the tunnel design.
4. Earth pressure varies significantly with the advancement of construction sequences. So having large overburden depth like section considered in the research, should be carefully during construction phases as well. Also, with the decrease of volume loss value (less than 0.5%), the settlement values were also decreased.
5. Considering the displacement and forces in the lining, maximum displacement occurred for Subloading- t_{ij} model which justifies the increased settlement values than Hardening soil model. Also, the bending moment is lower in Subloading t_{ij} model for this lining displacement.
6. After the second tunnel is constructed in the model, normal forces in the first tunnel grow noticeably. So, while designing the tunnel lining, the distance between the tunnels, construction sequences and final design moments should be analyzed very carefully.

5.3 Recommendations for Future Work

For the FEM analysis, only 2D options were explored. No additional surcharge or internal loads inside the tunnel were considered. Mainly the model has been checked for SLS condition. Also, some of the soil parameters were calibrated from SPT N-value using empirical correlations. There was a scope to analyze only one section due to the unavailability of the data.

Future works can be planned to study the 3D FEM models using Mohr-coulomb, Hardening Soil and Subloading $-t_{ij}$ model to understand the excavation behaviour in much better way. Also, triaxial tests data of the sample will replicate the actual site condition to

a great extent. For calculating the forces of the lining, other specific parameters for concrete lining (e.g. joint stiffness ,number of segments etc.) has to be considered for more accurate values.

Also, surface settlement monitoring data for different conditions of the tunnel (e.g shallow depth, maximum overburden depth, inclined surface, close proximity tunnel etc.) can be collected and compared with the FEM analysis data to provide more insight into using these three models for Bangladeshi soils.

REFERENCES

- Attewell, P., Woodman, J. (1982), “Predicting the dynamics of ground settlement and its derivatives caused by tunneling in soil”, *Ground Engineering*, 15(8), pp. 13–22.
- Bickel, J. O., Kuesel, T. R., & King, E. H. (1996). “Tunnel Engineering Handbook”, Springer US.
- Chapman, D., Metje, N., & Stark, A. (2017). “Introduction to Tunnel Construction” , Taylor & Francis.
- China Communications Second Highway Survey, Design and Research Institute Co., Ltd. (2016), “ Detailed Investigation Report of Engineering Geology.”
- Duddeck, H., & Erdman, J. (1985), “Structural design models for tunnels in soft soil.” *Underground Space*, Vol. 9, pp. 246–259
- Guglielmetti, V., Grasso, P., Mahtab, A., Xu, S. (2008). “Mechanized Tunnelling in Urban Areas -Design Methodology and Construction Control.” ,CRC Press.
- JSCE. (2006). *Standard Specifications for Tunneling-2006: Shield Tunnel* (3rd ed.).
- Kolymbas, D. (2005). “Tunnelling and Tunnel Mechanics. In Tunnelling and Tunnel Mechanics”, Springer US.
- Mathewson, A. (2006). “The Brunels’ tunnel”, The Brunel Museum.
- Möller, S.(2006), “Tunnel Induced Settlements and Structural Forces in Linings”, PhD Thesis, Stuttgart University
- Neto, F, Kochen, R. (2002). “Safety,rupture and collapse of urban NATM tunnels” (in Portuguese). *4th Symposium on Tunnels in Urban Environment*, Sao Paulo, pp.47–52.
- New, B., & O’Reilly, M. (1991). Tunneling induced ground movements; predicting their magnitude and effects. *4th International Conference on Ground Movements and Structures*, Volume 1, pp. 671-697.

- Nakai, T., Hinokio, M. (2004). "A Simple Elastoplastic Model for Normally and Over Consolidated Soils with Unified Material Parameters." *Soils and Foundations*, 44(2), pp.53–70.
- Nakai, T. (1989). "An Isotropic Hardening Elastoplastic Model for Sand Considering the Stress Path Dependency in Three-Dimensional Stresses." *Soils and Foundations*, 29(1), pp. 119–137.
- Nakai, T. (2007). "Modeling of soil behaviour based on t_{ij} concept". *Proceedings of the 13th Asian Regional Conference on Soil Mechanics and Geotechnical Engineering*, Kolkata, India, Vol. 2, pp. 69–89.
- Nakai, T., & Matsuoka, H. (1986). "A Generalized Elastoplastic Constitutive Model for Clay in Three-Dimensional Stresses." *Soils and Foundations*, 26(3), pp.81–98.
- Nakai, T., & Mihara, Y. (1984). "A New Mechanical Quantity for Soils and its Application to Elastoplastic Constitutive Models". *Soils and Foundations*, 24(2), pp.82–94.
- Nakai, T., Kyokawa, H., Kikumoto, M., Zhang, F. (2009a.). "Elastoplastic modeling of geomaterials considering the influence and density and bonding." *Proceedings of Prediction and Simulation Methods for Geohazard Mitigation*, pp. 367–373.
- Nakai, T., Shahin, H. M., Kikumoto, M., Kyokawa, H., Zhang, F. (2009b). "Simple and unified method for describing various characteristics of geomaterials." *Journal of Applied Mechanics JSCE*, 19, pp. 371-382 (in Japanese).
- Nakai, T., Shahin, H. M. D., Kikumoto, M., Kyokawa, H., Zhang, F., & Farias, M. M. (2011). "A simple and unified three-dimensional model to describe various characteristics of soils". *Soils and Foundations*, 51(6), pp. 1149–1168.
- Obrzud, R. F. (2010). "On the use of the Hardening Soil Small Strain model in geotechnical practice", Numerics in Geotechnics and Structures, Elempress International

Peck, R. (1969). “Deep excavations and tunneling in soft ground.” *Proceedings of the 7th International Conference on Soil Mechanics and Foundation Engineering*, Mexico city, pp. 225–290.

Potts, D. M., & Zdravković, L. (2001), “Finite Element Analysis in Geotechnical Engineering: Volume two – Application ”, Thomas Telford Publishing, Thomas Telford Ltd

Schanz, T., Vermeer, P. A., & Bonnier, P. G. (1999). “The hardening soil model: Formulation and verification. Beyond 2000 in Computational Geotechnics. Ten Years of PLAXIS” *International. Proceedings of the International Symposium*, Amsterdam, March 1999, pp. 281–296.

Smith, D. (2001). “Civil Engineering Heritage: London and the Thames Valley.” Thomas Telford Ltd.

Schmidt, B. (1969). “Settlements and Ground Movement Associated with Tunneling in Soil.” University of Illinois, Urbana.

Shahin, H. M., Nakai, T., Hinokio, M., and Yamaguchi, D. (2004). “3D Effects on Earth Pressure and Displacements during Tunnel Excavations.” *Soils and Foundations*, 44(5), pp. 37–49.

Shahin, H. M, Nakai, T., and Pedroso, D. (2011). “Explicit Integration of Subloading t_{ij} Constitutive Model in FEM Analysis”. *Journal of Geotechnical Engineering*, 1(1), pp. 16–28.

Shahin, Hossain M, Nakai, T., Hinokio, M., Kurimoto, T., and Sada, T. (2004). “Influence of Surface Loads and Construction Sequence on Ground Response Due to Tunnelling”. *Soils and Foundations*, 44(2), 71–84.

Schanz, T., Vermeer, P. A., Bonnier, P. G., & Brinkgreve, R. B. J. (1999). “The hardening soil model: Formulation and verification”, *Beyond 2000 in Computational Geotechnics, International Symposium, Beyond 2000 in Computational Geotechnics*, pp. 281–296.

APPENDIX A : ANALYTICAL CALCULATION

EMPIRICAL SETTLEMENT COMPUTATION SHEET

Volume loss 0.50%

Depth 35.0m

Ground Movements Due to Tunnelling - Tunnel Geometric Inputs

Geometric Inputs

Number of Tunnels

1 Tunnel

2 Tunnels

3 Tunnels

4 Tunnels

Ground movements Considered

Surface Movements Only

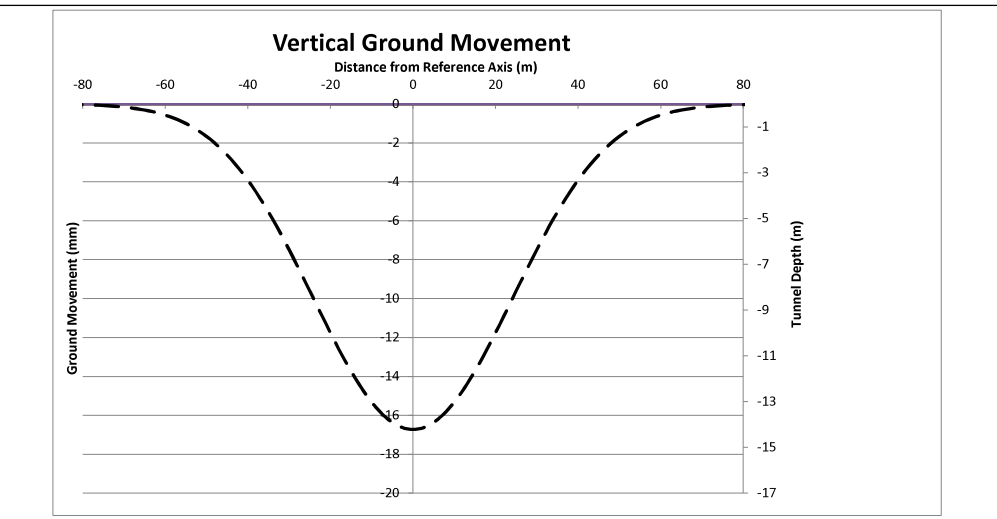
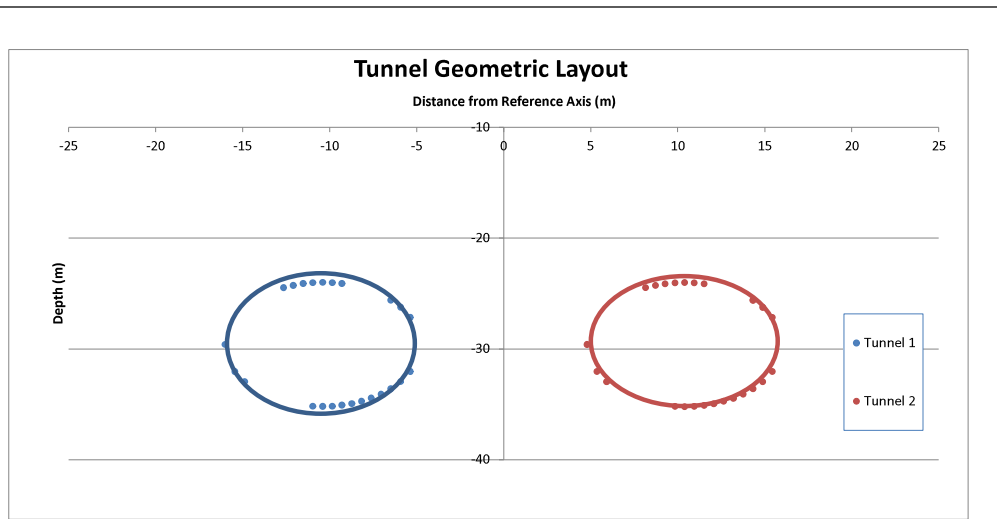
Surface & Subsurface Movements

Tunnel 1

Tunnel 2

Depth to axis (z_1) =	29.6	m
Distance from origin (y_1) =	-10.4	m
Excavation diameter (D_1) =	11.2	m
Face loss (V_{1f}) =	0.5	%
Trough width coefficient (K_1) =	0.7	-

Depth to axis (z_2) =	29.6	m
Distance from origin (y_2) =	10.4	m
Excavation diameter (D_2) =	11.2	m
Face loss (V_{2f}) =	0.5	%
Trough width coefficient (K_2) =	0.7	-



Lining Forces Analytical Calculation

Segment Member Forces Computation by Elastic Equation Method by ISCE (1996, 2006) in ITA (2000)

$\gamma_{conv} =$	25.0	EN/m ³	$t =$	0.55	m	$I_{liming} =$	0.013865	m ⁴ /m	$k_{ball} =$	100000	kN/m ³
$R_c =$	5.9	m	$E_{conv} =$	3.50E+07	kPa	$P =$	549	kPa	at Crown		
$R_1 =$	218	kPa	$P_{w1} =$	331	kPa	$Q =$	440	kPa	at Crown		
$Q_1 =$	109	kPa	$Q_{w1} =$	331	kPa	$Q =$	508	kPa	at Bottom		
$Q_{c1} =$	40	kPa	$Q_{c2} =$	468	kPa	$Q =$	13.75	kPa			

$g = 13.75$ kPa $\dot{Q} = 0.00126506$ m

θ	Moment (EN/m)	Axial (EN/m)	Shear (EN/m)
0	$M_1 = 4777.6725$	$N_1 = 0$	$Q_1 = 0$
0	$M_2 = -8920.1$	$N_2 = 2996$	$Q_2 = 0$
0	$M_3 = -246.5708333$	$N_3 = 125.375$	$Q_3 = 0$
0	$M_4 = -251.0328256$	$N_4 = 265.922144$	$Q_4 = 0$
0	$M_5 = 165.0169368$	$N_5 = -13.53083333$	$Q_5 = 0$
0	$M = 342.98$	$N = 2971.78$	$Q = 0.00$

θ	Moment (EN/m)	Axial (EN/m)	Shear (EN/m)
0.174532925	$M_1 = 4489.543893$	$N_1 = 97.67081601$	$Q_1 = -553.918211$
0.174532925	$M_2 = -3598.177014$	$N_2 = 2517.212102$	$Q_2 = 443.942146$
0.174532925	$M_3 = -235.338383$	$N_3 = 123.4474941$	$Q_3 = 21.76712888$
0.174532925	$M_4 = -800.381766$	$N_4 = 259.9128299$	$Q_4 = 45.8294631$
0.174532925	$M_5 = 158.570641$	$N_5 = -10.8367398$	$Q_5 = -16.29174485$
10	$M = 312.22$	$N = 2987.90$	$Q = -58.67$

θ	Moment (EN/m)	Axial (EN/m)	Shear (EN/m)
0.34906885	$M_1 = 3659.90647$	$N_1 = 378.9027211$	$Q_1 = -1041.026673$
0.34906885	$M_2 = -2933.260777$	$N_2 = 2292.225887$	$Q_2 = 834.383174$
0.34906885	$M_3 = -202.069767$	$N_3 = 117.4711277$	$Q_3 = 42.7504025$
0.34906885	$M_4 = -430.130877$	$N_4 = 248.0069533$	$Q_4 = 90.26675201$
0.34906885	$M_5 = 131.928695$	$N_5 = -3.020112139$	$Q_5 = -31.2345209$
20	$M = 226.44$	$N = 3093.69$	$Q = -104.90$

θ	Moment (EN/m)	Axial (EN/m)	Shear (EN/m)
0.523598776	$M_1 = 2888.88025$	$N_1 = 809.775$	$Q_1 = -1402.571443$
0.523598776	$M_2 = -1914.55$	$N_2 = 1947$	$Q_2 = 1124.100794$
0.523598776	$M_3 = -47.9425$	$N_3 = 167.048826$	$Q_3 = 61.78348$
0.523598776	$M_4 = -315.420752$	$N_4 = 228.545355$	$Q_4 = 131.9012072$
0.523598776	$M_5 = 93.1476584$	$N_5 = 9.25290188$	$Q_5 = -43.5463502$
30	$M = 104.07$	$N = 3101.89$	$Q = -128.27$

θ	Moment (EN/m)	Axial (EN/m)	Shear (EN/m)
0.872646426	$M_1 = -829.6341231$	$N_1 = 1900.781906$	$Q_1 = -1594.9485396$
0.872646426	$M_2 = 664.9162371$	$N_2 = 1072.604665$	$Q_2 = 1278.280463$
0.872646426	$M_3 = 867.2509989$	$N_3 = 72.8687915$	$Q_3 = 86.2887183$
0.872646426	$M_4 = 32.12914121$	$N_4 = 168.21589$	$Q_4 = 200.478683$
0.872646426	$M_5 = -12.47286684$	$N_5 = 45.54102923$	$Q_5 = -55.86865322$
50	$M = -136.53$	$N = 3259.51$	$Q = -85.81$

θ	Moment (EN/m)	Axial (EN/m)	Shear (EN/m)
1.047197551	$M_1 = -388.83825$	$N_1 = 2429.325$	$Q_1 = -1402.571443$
1.047197551	$M_2 = 1914.55$	$N_2 = 649$	$Q_2 = 1124.100794$
1.047197551	$M_3 = 98.62833333$	$N_3 = 50.15$	$Q_3 = 86.862828$
1.047197551	$M_4 = 245.5093333$	$N_4 = 120.6254599$	$Q_4 = 208.9294183$
1.047197551	$M_5 = -69.62696812$	$N_5 = 66.81123005$	$Q_5 = -54.1863382$
60	$M = -199.72$	$N = 3315.91$	$Q = -36.87$

θ	Moment (EN/m)	Axial (EN/m)	Shear (EN/m)
1.221730476	$M_1 = -4659.90047$	$N_1 = 2860.07278$	$Q_1 = -1041.026673$
1.221730476	$M_2 = 2933.260777$	$N_2 = 303.6743128$	$Q_2 = 834.383174$
1.221730476	$M_3 = 183.855199$	$N_3 = 28.02901917$	$Q_3 = 77.6999725$
1.221730476	$M_4 = 480.2277045$	$N_4 = 66.19525455$	$Q_4 = 181.8699672$
1.221730476	$M_5 = 122.0585165$	$N_5 = 88.51124921$	$Q_5 = -46.60403041$
70	$M = -214.50$	$N = 3346.61$	$Q = 5.59$

θ	Moment (EN/m)	Axial (EN/m)	Shear (EN/m)
1.396263402	$M_1 = -4490.548593$	$N_1 = 3141.429184$	$Q_1 = -853.9187231$
1.396263402	$M_2 = 3396.177014$	$N_2 = 78.2397922$	$Q_2 = 443.942146$
1.396263402	$M_3 = 253.388678$	$N_3 = 9.87874625$	$Q_3 = 56.6203078$
1.396263402	$M_4 = 665.3184025$	$N_4 = 19.7484443$	$Q_4 = 111.9672347$
1.396263402	$M_5 = -163.531572$	$N_5 = 100.203162$	$Q_5 = -32.99487503$
80	$M = -196.20$	$N = 3358.53$	$Q = 25.03$

θ	Moment	Axial	Shear
0	342.98	2971.78	0.00
10	312.22	2987.90	-58.67
20	226.44	3033.69	-104.90
30	104.07	3101.89	-128.27
40	-27.51	3181.77	-122.03
50	-136.53	3259.51	-85.81
60	-199.72	3315.91	-36.87
70	-214.50	3346.61	5.59
80	-196.20	3358.53	25.03
90	-174.37	3366.53	11.55
100	-173.07	3379.64	219.95
110	-172.98	3385.51	371.93
120	-149.80	3373.43	456.71
130	-91.24	3339.03	475.46
140	-0.01	3286.74	439.24
150	105.74	3233.41	365.31
160	201.24	3188.86	261.44
170	266.92	3159.50	136.26
180	290.24	3149.27	0.00
190	266.92	3159.50	-136.26
200	201.24	3188.86	-261.44
210	105.74	3233.41	-365.31
220	-0.01	3286.74	-439.24
230	-91.24	3339.03	-475.46
240	-149.80	3373.43	-456.71
250	-172.98	3385.51	-371.93
260	-173.07	3379.64	-219.95
270	-174.37	3366.53	-115.5
280	-196.20	3358.53	-25.03
290	-214.50	3346.61	-5.59
300	-199.72	3315.91	36.87
310	-136.53	3259.51	85.81
320	-27.51	3181.77	122.03
330	104.07	3101.89	128.27
340	226.44	3033.69	104.90
350	312.22	2987.90	58.67
360	342.98	2971.78	0.00

θ	Moment (kN.m)	Axial (kN)	Shear (kN)
0.698131701	M ₁ = 829.841231	N ₁ = 138.318094	Q ₁ = -1594.943996
0.698131701	M ₂ = -666.9162371	N ₂ = 1523.395335	Q ₂ = 1278.280643
0.698131701	M ₃ = -760.0697938	N ₃ = 91.8372834	Q ₃ = 77.06603663
0.698131701	M ₄ = -159.2361545	N ₄ = 202.176299	Q ₄ = 169.6466797
0.698131701	M ₅ = 43.5447495	N ₅ = 26.04731754	Q ₅ = -53.07666683
40	M = -27.51	N = 3181.77	Q = -122.03

θ	Moment (kN.m)	Axial (kN)	Shear (kN)
1.570796327	M ₁ = -477.6725	N ₁ = 329.1	Q ₁ = -1.90410913
1.570796327	M ₂ = 832.1	N ₂ = 9.74121240	Q ₂ = 1.59026113
1.570796327	M ₃ = 295.885	N ₃ = 1.35603745	Q ₃ = 25.075
1.570796327	M ₄ = 666.3723107	N ₄ = 4.39963620	Q ₄ = 4.57217114
1.570796327	M ₅ = -157.2606507	N ₅ = 127.238852	Q ₅ = -13.20833333
90	M = -174.37	N = 3366.53	Q = 11.55

θ	Moment (kN.m)	Axial (kN)	Shear (kN)
2.792528603	M ₁ = 3659.990917	N ₁ = 378.2027231	Q ₁ = 1041.036673
2.792528603	M ₂ = -2933.280777	N ₂ = 2292.323667	Q ₂ = -854.338174
2.792528603	M ₃ = -251.3381434	N ₃ = 236.973425	Q ₃ = -861.871825
2.792528603	M ₄ = -130.131877	N ₄ = 248.605953	Q ₄ = 90.2692301
2.792528603	M ₅ = 156.041484	N ₅ = 32.8323869	Q ₅ = 56.6769068
160	M = 201.24	N = 3188.86	Q = 261.44

θ	Moment (kN.m)	Axial (kN)	Shear (kN)
1.745329252	M ₁ = -4489.543593	N ₁ = 3141.429184	Q ₁ = 553.9187231
1.745329252	M ₂ = 3598.177014	N ₂ = 78.279722	Q ₂ = -443.942146
1.745329252	M ₃ = 302.6980844	N ₃ = 2.219782645	Q ₃ = -12.58903338
1.745329252	M ₄ = 665.3184025	N ₄ = 19.74284443	Q ₄ = 111.9927547
1.745329252	M ₅ = -189.2186804	N ₅ = 137.9735371	Q ₅ = 103.9904284
100	M = -173.07	N = 3379.64	Q = 219.95

θ	Moment (kN.m)	Axial (kN)	Shear (kN)
2.248928028	M ₁ = 829.6341231	N ₁ = 1900.781006	Q ₁ = 1594.945306
2.248928028	M ₂ = 664.9162371	N ₂ = 1072.640665	Q ₂ = -1278.280663
2.248928028	M ₃ = 94.08921215	N ₃ = 93.40329941	Q ₃ = -111.3137176
2.248928028	M ₄ = 32.19214212	N ₄ = 168.21589	Q ₄ = 206.478683
2.248928028	M ₅ = -52.86192309	N ₅ = 104.077958	Q ₅ = 69.6123581
130	M = -91.24	N = 3339.03	Q = 475.46

θ	Moment (kN.m)	Axial (kN)	Shear (kN)
2.96769728	M ₁ = 4489.543593	N ₁ = 97.67881601	Q ₁ = 553.9187231
2.96769728	M ₂ = -1598.177014	N ₂ = 2317.21202	Q ₂ = -443.942146
2.96769728	M ₃ = -120.7483722	N ₃ = 265.658657	Q ₃ = -46.84212038
2.96769728	M ₄ = -500.381766	N ₄ = 259.9128399	Q ₄ = 45.82964631
2.96769728	M ₅ = 196.6792832	N ₅ = 18.54176652	Q ₅ = 27.2921742
170	M = 266.92	N = 3159.50	Q = 136.26

θ	Moment (kN.m)	Axial (kN)	Shear (kN)
1.919862177	M ₁ = -1659.90047	N ₁ = 2860.197278	Q ₁ = 1041.026673
1.919862177	M ₂ = 2933.269777	N ₂ = 303.6784328	Q ₂ = -854.338174
1.919862177	M ₃ = 269.3663812	N ₃ = 18.90246354	Q ₃ = -51.93409725
1.919862177	M ₄ = 430.237045	N ₄ = 66.19252455	Q ₄ = 181.8699762
1.919862177	M ₅ = -162.933869	N ₅ = 136.5329399	Q ₅ = 35.39094286
110	M = -172.98	N = 3385.51	Q = 371.93

θ	Moment (kN.m)	Axial (kN)	Shear (kN)
2.443460953	M ₁ = 829.6341231	N ₁ = 138.318094	Q ₁ = 1594.945306
2.443460953	M ₂ = -664.9162371	N ₂ = 1523.395335	Q ₂ = -1278.280663
2.443460953	M ₃ = -728.0772	N ₃ = 143.596541	Q ₃ = -120.4918066
2.443460953	M ₄ = -159.2361745	N ₄ = 202.176299	Q ₄ = 169.6466797
2.443460953	M ₅ = 21.75292943	N ₅ = 79.25293924	Q ₅ = 734.18232
140	M = -0.01	N = 3286.74	Q = 439.24

θ	Moment (kN.m)	Axial (kN)	Shear (kN)
3.141592654	M ₁ = 4777.6725	N ₁ = 4.861851259	Q ₁ = 3.968381413
3.141592654	M ₂ = -3829.1	N ₂ = 2296	Q ₂ = -1.18092613
3.141592654	M ₃ = -345.1991667	N ₃ = 273.825	Q ₃ = -1.37927114
3.141592654	M ₄ = -524.0382556	N ₄ = 263.9224144	Q ₄ = 0
3.141592654	M ₅ = 210.9906766	N ₅ = 13.5208333	Q ₅ = 2.95879114
180	M = 290.24	N = 3149.27	Q = 0.00

θ	Moment (kN.m)	Axial (kN)	Shear (kN)
2.094395102	M ₁ = -2388.83825	N ₁ = 2429.325	Q ₁ = 1402.571443
2.094395102	M ₂ = 1914.55	N ₂ = 649	Q ₂ = -1124.100974
2.094395102	M ₃ = 197.2566667	N ₃ = 50.15	Q ₃ = -86.8626348
2.094395102	M ₄ = 248.5606633	N ₄ = 126.625459	Q ₄ = 208.9294183
2.094395102	M ₅ = -118.3335386	N ₅ = 124.334458	Q ₅ = 56.1730125
120	M = -149.80	N = 3373.43	Q = 456.71

θ	Moment (kN.m)	Axial (kN)	Shear (kN)
2.617993878	M ₁ = 2388.83825	N ₁ = 809.775	Q ₁ = 1402.571443
2.617993878	M ₂ = -1914.55	N ₂ = 1947	Q ₂ = -1124.100974
2.617993878	M ₃ = -147.9425	N ₃ = 193.881774	Q ₃ = -111.937348
2.617993878	M ₄ = -115.420752	N ₄ = 228.5635155	Q ₄ = 131.9612072
2.617993878	M ₅ = 94.81283288	N ₅ = 54.1883382	Q ₅ = 66.81182665
150	M = 105.74	N = 3233.41	Q = 365.31

APPENDIX B: SETTLEMENT MONITORING POINTS

Figure 1 : The layout picture of Monitoring instrument

